Pacific Northwest
NATIONAL LABORATORY

Proudly Operated by **Battelle** *Since 1965*

Scoping Study of Airlift Circulation Technologies for Supplemental Mixing in Pulse Jet Mixed Vessels

April 2015

PP Schonewill   WC Buchmiller
EJ Berglin   CB Burns
GK Boeringa   MJ Minette

DISCLAIMER

This report was prepared as an account of work sponsored by an agency of the United States Government. Neither the United States Government nor any agency thereof, nor Battelle Memorial Institute, nor any of their employees, makes **any warranty, express or implied, or assumes any legal liability or responsibility for the accuracy, completeness, or usefulness of any information, apparatus, product, or process disclosed, or represents that its use would not infringe privately owned rights**. Reference herein to any specific commercial product, process, or service by trade name, trademark, manufacturer, or otherwise does not necessarily constitute or imply its endorsement, recommendation, or favoring by the United States Government or any agency thereof, or Battelle Memorial Institute. The views and opinions of authors expressed herein do not necessarily state or reflect those of the United States Government or any agency thereof.

Scoping Study of Airlift Circulation Technologies for Supplemental Mixing in Pulse Jet Mixed Vessels

PP Schonewill   WC Buchmiller
EJ Berglin   CB Burns
GK Boeringa   MJ Minette

April 2015

Pacific Northwest National Laboratory
Richland, Washington 99352

Summary

At the request of the U.S. Department of Energy Office of River Protection, Pacific Northwest National Laboratory (PNNL) conducted a scoping study to investigate supplemental technologies for supplying vertical fluid motion and enhanced mixing in Waste Treatment and Immobilization Plant (WTP) vessels designed for high solids processing. The study assumed that the pulse jet mixers adequately mix and shear the bottom portion of a vessel. Given that, the primary function of a supplemental technology should be to provide mixing and shearing in the upper region of a vessel. The objective of the study was to recommend a mixing technology and configuration that could be implemented in the 8-ft test vessel located at Mid-Columbia Engineering (MCE). Several mixing technologies, primarily airlift circulator (ALC) systems, were evaluated in the study, first by reviewing the available literature and then performing tests with a simple Newtonian simulant (water and glass beads). The experimental study was performed in a 90-in. diameter tank with a maximum liquid operating level of ~108 in. The initial testing evaluated the ability of ALC configurations to lift, transport, and distribute solid particles to near-surface locations in the test vessel. This testing established that ALCs generated significant liquid flows (several hundred gallons per minute) at air flow rates of 5 to 20 standard cubic feet per minute (scfm), and solid particles were readily transported up the riser tube at air flow rates as low as ~5 scfm. The principal outcome of the Newtonian testing was that candidate ALC systems were identified and recommended for testing in a non-Newtonian fluid. The candidate ALC system had the following features: a nominally 10-in. riser tube diameter, 5-ft riser tube length, positioned 5 in. off the tank floor, and an air distributor centrally located at the bottom of the riser tube (tube inlet). An alternative technology, a Geyser Hybrid Pump (GHP), was also identified as a possible candidate. Both of the recommended systems were confirmed to be capable of lifting and dispersing very large solid particles up to approximately 6 mm in size.

The non-Newtonian testing was conducted to determine if the recommended ALC configuration from the Newtonian testing was also suitable for mobilizing a Bingham plastic fluid (clay slurry). It was found that mobilizing a yield-stress fluid (initially, the simulant had Bingham parameters of ~22-Pa yield stress and ~34-cP consistency) in the upper region of the vessel required more mixing energy than transporting solid particles in a Newtonian fluid; the 10-in. diameter ALC did not mobilize fluid out to the tank wall in the upper region of the vessel. The GHP was also tested and found to be an improvement over the 10-in. ALC. Some alternatives to the initially recommended ALC were briefly investigated, including testing with a larger diameter ALC and devices that could supply a periodic burst of pressurized air. ALC devices that incorporated pulses of air were demonstrated in proof-of-principle tests to be the most effective in mobilizing the slurry. Interpretation of the non-Newtonian data was complicated by a downward drift in the yield stress that occurred during testing; the data collected suggests that ALC effectiveness (in terms of fluid mobilization) increases as the yield stress decreases. For the 8-ft MCE vessel, the preliminary recommendation is the use of a centrally located, nominally 18-in. diameter ALC with a 5-ft riser tube length. The 18-in. ALC was observed to nearly fully mobilize the top half of the slurry in the test tank, and this might be further improved with simple geometric refinements to the ALC configuration. However, based on promising initial results, it is also recommended that more complete testing of a pulsed air modification to the ALC be conducted.

The scoping study described in this report collected data to confirm the potential utility of the candidate mixing technologies in the WTP but did not conduct any formal design work or explicitly consider implementation of the mixing technologies into the WTP vessels. The testing was conducted

using the PNNL How Do I…? (HDI) general laboratory Quality Assurance program. The PNNL test program was a preliminary demonstration of the efficacy of ALC systems as a potential supplemental mixing system; further development and refinement of the ALC configuration may be required before implementation into the WTP standard high solids vessel design.

Acknowledgements

Acronyms and Abbreviations

ALC	airlift circulator
AOD	air-operated diaphragm
APEL	Applied Process Engineering Laboratory
BM	benchmark
C&W	Cook and Waters (1955)
cfh	cubic feet per hour (as read on rotameter)
cfm	cubic feet per minute (as read on rotameter)
DOE	U.S. Department of Energy
GP	Geyser pump
GHP	Geyser Hybrid Pump
ID	inside diameter
LRB	laboratory record book
MCE	Mid-Columbia Engineering
OBMS	off-bottom motion system
OD	outside diameter
ORP	Office of River Protection
PHi	Pulsed Hydraulics, Inc.
PJM	pulse jet mixer
PNNL	Pacific Northwest National Laboratory
PPM	pulsed plate mixer
PVC	polyvinyl chloride
scfh	standard cubic feet per hour
scfm	standard cubic feet per minute
SHSV	standard high solids vessel
SST	single-shell tank
SP	system performance
WTP	Waste Treatment and Immobilization Plant

Nomenclature

a	adjustment coefficient for standard to actual air flow rate, Equation (4.1)
A_d	area of the downcomer
Ar	Archimedes number, Equation (5.4)
A_r	area of the riser tube
A_t	area of the tank
A_{s1}	area of sieve 1
A_{s2}	area of sieve 2
A_{s3}	area of sieve 3
A_{z1}	area of zone 1
A_{z2}	area of zone 2
A_{z3}	area of zone 3
α	fitting constant, Equation (4.5)
β	fitting constant, Equation (4.5)
c_1	fitting constant, Equation (2.1)
c_2	fitting constant, Equation (2.1)
c_3	fitting constant, Equation (2.1)
d	diameter of a spherical particle
d_a	diameter (OD) of air tube
d_r	diameter (ID) of riser tube
d_t	diameter (ID) of tank
ε_r	gas hold-up (volume fraction) in riser
ε_d	gas hold-up (volume fraction) in downcomer
f_{ij}	mass fraction of particle color j collected after segment i
F_{kj}	mass fraction of particle color j in layer k
g	gravitational acceleration
h	a height (depth) below the simulant surface
h_{ad}	height (submerged depth) of the air distributor where air is injected
h_D	gas-liquid dispersion height
h_r	height (length) of riser tube
h_s	height of fluid surface in tank
h_t	height of tank
K	fitting coefficient, Equation (4.6)
K_B	frictional loss coefficient at the bottom of the riser tube
l	characteristic dimension of a particle
L_c	characteristic geometric parameter (or ratio), Equation (2.1)
m_{ij}	mass of particle color j collected after segment i

m_{oj}	original mass of particle color j loaded into tank
M_{kj}	mass of particle color j collected in layer k
μ	viscosity of the liquid/carrier fluid
N	total number of segments
P_{ad}	hydrostatic pressure at the submerged depth of the air distributor
P_{atm}	atmospheric pressure
P_h	hydrostatic pressure at height h below the simulant surface
P_{rot}	pressure at the rotameter
P_{std}	pressure at standard conditions
$Q_{air,avg}$	actual air flow rate averaged (integrated) over the height of the riser tube
$Q_{air,h}$	actual air flow rate at height h below the simulant surface
$Q_{air,rot}$	observed air flow rate read from a rotameter
$Q_{air,std}$	volumetric air flow rate at standard conditions
Q_{liquid}	liquid (gas-free simulant) flow rate at the riser tube outlet
R	radius of the tank
R_0	radius of a particle
Re_r	Reynolds number, as defined in Equation (5.2)
ρ_L	density of the liquid, gas-free
ρ_S	density of the solid particle
ρ_{sim}	density of the simulant, gas-free
$\Delta\rho$	difference in density between the liquid and a solid particle
s_b	off-bottom separation distance (distance of riser tube bottom above tank bottom)
s_r	riser separation distance (distance of air distributor above bottom of riser tube)
s_s	riser submersion (distance of top of riser tube below fluid surface)
t	transit time of tracer
T_h	temperature of air at depth h
T_{rot}	temperature at the rotameter
T_{std}	temperature at standard conditions
τ_0 or τ_y	Bingham yield stress of the fluid
$\langle U \rangle$	average velocity measured by the velocity probe
U^*_{gr}	height averaged superficial gas velocity in the riser
U_{lr}	liquid velocity in the riser
U_r	relative velocity of fluid from a particle frame of reference, Equation (5.1)
V	net particle velocity
v_T	terminal settling velocity
Y	yield gravity number, Equation (6.1)
Y_g	yield-stress parameter, Equation (6.2)

Contents

Figures

Tables

1.0 Introduction

At the request of the U.S. Department of Energy (DOE) Office of River Protection (ORP), Pacific Northwest National Laboratory (PNNL) conducted a scoping study to investigate technologies for supplying vertical fluid motion and enhanced mixing in Waste Treatment and Immobilization Plant (WTP) vessels designed for processing high solids waste streams. The mixing technologies that were evaluated in the study are intended to supplement the pulse jet mixers (PJMs) that are already planned for use in the WTP vessels. Any evaluated technologies need to be able to operate within the restrictions of the current or future standard high solids vessel (SHSV) design, i.e., have the following general features:

- Ability to withstand a harsh radiological and chemical environment

- Require minimal or no maintenance

- No moving/mechanical parts

- Robust operating principle (will reliably function for full plant life of >30 years)

- Do not negatively impact other engineering systems planned for use

At the outset of the study, an airlift circulator (ALC) was identified as a good candidate that could potentially satisfy these criteria, and it was the focus of the study described herein. For this reason, the test program was generically referred to as the ALC test program, even though it was not strictly limited to the consideration and study of ALC systems. An ALC system consists, in general, of a confined region in a process vessel into which air is injected locally to induce a density-gradient driven circulating flow. Significant vertical (or upwelling) velocity can be generated with air flow rates of less than 20 standard cubic feet per minute (scfm). Conceptually, an ALC is a sheathed or jacketed sparger, but the resultant flow is fundamentally different. A sparger produces a flow that entrains fluid in proximity to the air bubbles as they migrate upward, whereas the ALC generates a bulk recirculation flow that pulls fluid into the bottom of the confined region and ejects it out the top. The potential benefits of an ALC over an array of spargers, which is a different supplemental mixing system proposed for the SHSV, are reduced air usage and fewer aerosols generated in the vessel headspace during operation.

As described in the initial test plan governing the work (Minette 2014[1]), the ALC test program was designated as a scoping study with the following main objective:

PNNL to evaluate features of an airlift circulation system by conducting reviews of prior work and conducting scoping tests for their potential inclusion during Standard High Solids Vessel Testing (SHSVT) and provide recommendations in the form of a letter to ORP.

The literature survey, descriptions of equipment, test data, and system recommendations disseminated in this report satisfy the objective of the test plan. Even though the test plan refers to a specific technology (the ALC), other mixing approaches (all air-driven) were considered during the study, including simple modifications to a "typical" ALC system. Technologies that were considered distinct from an ALC were compared to the performance of an ALC system with a similar geometric

---

[1] Minette, MJ. 2014. *Test Plan for Airlift System Design Feature Evaluations*, Rev. 0.0, ORP-Scoping-01, Pacific Northwest National Laboratory, Richland, WA.

configuration, meaning that the system was centrally located in the tank and had a similar discharge location (if appropriate for the technology).

To accomplish the main objective of the test program, the ALC systems were assessed in two different types of simulants: a Newtonian (water + solid particles) and non-Newtonian (clay slurry) fluid. The non-Newtonian testing, which was not included in the original scope of the study, was added to the test program after successful demonstration of ALC systems during Newtonian testing. Testing in each simulant had a common interest in measuring liquid (gas-free simulant[1]) velocity (from which a flow rate could be estimated) as a function of air flow rate. These measurements were made because the liquid velocity is a quantity that may be useful for scaling up to larger vessels and data from the technical literature was available for comparison.

Aside from the velocity measurements, the evaluation of each simulant was focused on a different aspect of a system's mixing performance. Testing in the Newtonian fluid was concerned with the ability of a supplemental mixing system to lift and transport solid particles from the bottom of the tank to the top of the fluid (surface). This ability is complementary to the function of the PJMs in the WTP, which are expected to suspend solid particles off the tank bottom. Paired with an ALC (or similar) capable of transporting solids to the waste surface and outward to the vessel walls, the WTP vessel should be well-mixed with respect to the distribution of solids in the tank.

Testing using a non-Newtonian fluid was not performed with any settling solid particles present, as the primary emphasis shifted to demonstrating that the supplemental mixing system provides adequate shear or agitation in the fluid. The presence of shear (or fluid motion) in the simulant is expected to correlate with the ability of the system to (a) minimize the presence of dead zones (unmoving fluid) in the vessel and (b) release potentially hazardous gas that is generated in the slurry while waste resides in WTP vessels. In past PNNL studies with PJMs in non-Newtonian fluids, a cavern of mobilized fluid was formed in a (lower) portion of the vessel (see the summary in Bamberger et al. 2005). Above the cavern the fluid was observed to be quiescent. Thus, of particular interest was to test if the ALC system could shear/mobilize the fluid in the upper part of the vessel. Assuming that the PJMs provide adequate shear in the lower part of the vessel, these functions would again be complementary with respect to mobilizing waste for the purpose of gas release.

The rest of this report consists of four major parts. First, in Section 2.0, there is a brief discussion of supporting information in the technical literature for the various supplemental mixing technologies that were investigated (with a focus on ALC or ALC-like systems). Second, the experimental systems, test materials, and completed test matrix are described in Section 3.0. Third, the test data is presented, which includes measurements in Newtonian and non-Newtonian simulants (Sections 4.0 through 6.0). Finally, in Sections 7.0 and 8.0, the results of the study are summarized and a system is recommended for further study or investigation based on the preliminary testing.

---

[1] Sheared non-Newtonian slurry simulant is technically a fluid, not a liquid. However, to readily distinguish the flow of gas-free Newtonian and non-Newtonian simulants (e.g., water and clay slurry, respectively) from the flow of air, which is also a fluid, both types of simulants are referred to as "liquids" throughout this report.

2.0   Background and Literature Survey

There are many variations on the fundamental operating principle of an ALC system, which has alternatively been referred to as a gas-lift circulator, an air-injection circulator, or an airlift reactor.[1] A similar principle is also used in airlift pumping. Generally, airlift pumping is used when the fluid needs to be lifted above the fluid surface or out of a vessel, whereas ALCs are submerged below the surface to create fluid motion in the vessel contents (or in some instances, level with the fluid surface). An ALC system uses a submerged riser tube (or duct) inside a vessel into which air[2] is injected, usually continuously, near the bottom. The injected air reduces the density of the fluid locally and creates a driving force due to the weight (density) of the bulk fluid that is above it and outside of the confined space. This driving force causes the less dense fluid to move upwards through the submerged tube, where it is discharged at the top. Denser fluid moves to replace the fluid migrating up the tube, which creates a circulation pattern in the vessel. The performance of the ALC can depend on several factors, specifically the air flow rate and distribution method, the geometry of the system, and the fluid and its properties.

There is a distinction in prior work discussed in the literature between an external loop ALC and an internal loop ALC (see Figure 2.1 for representations of these ALC variants). They operate on the same principle but the geometries are different, and this leads to different performance for the same operating parameters (e.g., fluid properties, air flow rate). In this report, only ALCs in the internal loop configuration with concentric cylinders were investigated. It is recommended that application of data or results from other configurations to the concentric cylinder geometry be performed with caution.
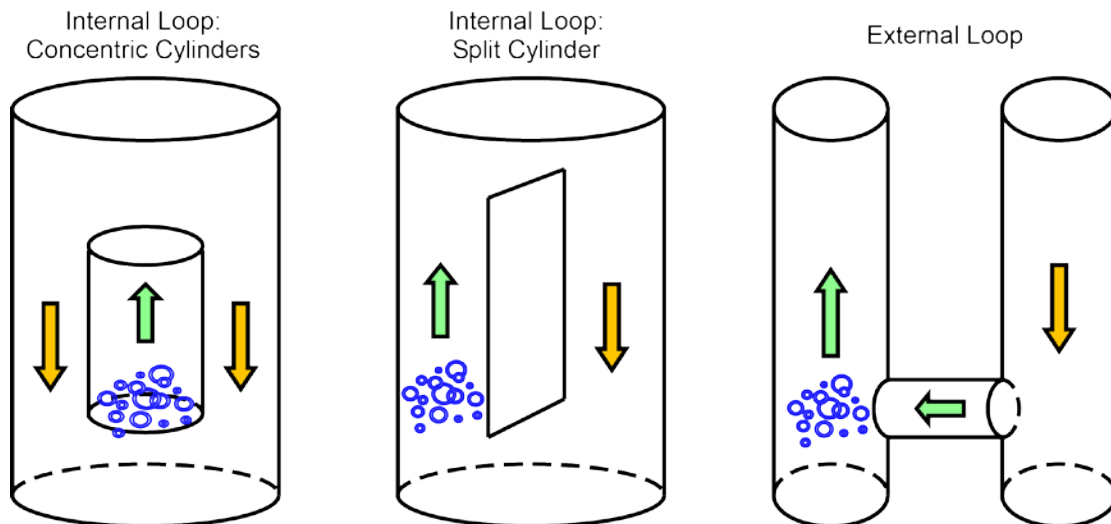
Figure 2.1. Diagrams of Various Airlift Circulator Geometries. The blue bubbles indicate a typical injection location for the air and the arrows indicate the direction of liquid flow.

---

[1] A vessel containing an ALC is similar to a bubble column reactor or sparged vessel but should not be confused with these technologies, as they generally do not have an internal submerged riser tube and depend solely on the gas bubbles to generate fluid motion (or mixing). In fact, part of the motivation for consideration of ALC systems (or similar) is to investigate alternatives to using spargers in the WTP high solids vessels.

[2] The gas is typically air but could be any non-condensable, insoluble inert gas.

The ALC concept was specifically assessed for its application to large radioactive waste tanks several decades ago by Cook and Waters (1955). Cook and Waters (1955) contains some of the earliest published ALC performance data, some of which was selected as a benchmark for the scoping studies described later in this report. They concluded that the ALC system offered "an economic and effective means for achieving mild liquid agitation in large tanks." This was followed later by the work of Dunn and Van Slyke (1964), who evaluated an ALC that was a prototype of the systems installed in the Hanford AX waste tanks, a set of single-shell tanks (SSTs). They obtained large liquid flow rates (up to 5000 gpm) with modest air flow rates (~10 scfm) in a 30-in. inside diameter (ID) riser tube. The ALCs were also installed in four of the Hanford tank farm double-shell tanks. The use and impact of ALCs on retrieval processes in the Hanford tank farm are discussed briefly in several other sources, such as Whyatt et al. (1996), Serne et al. (1996), and Daymo (1997). Daymo (1997) notes that although ALC systems were employed in both Hanford and Savannah River waste storage tanks, experience had shown they generally were not effective at suspending sludge (see Waters 1994). Other analyses suggest a similar conclusion, namely that ALCs can only accommodate very low solids loadings in the waste sludge and may not generate significant flows (Stewart et al. 2005). This is in contrast to results from numerical models of ALCs (also in Stewart et al. 2005), which suggest significant flows are achievable. Other anecdotal mentions are made regarding ALCs in Hanford SSTs, such as in Washenfelder et al. (2010), which describes the "choppy" surface in tank SX-110 when its ALCs were in operation. The observed "choppiness" suggests the ALC was mobilizing an appreciable amount of waste slurry in the tank. Juxtaposed to this observation is photographic evidence of saltcake waste crystallizing and growing "lollipops" inside and on top of ALC installations in waste tanks (see Ballou 1994 or Krieg et al. 1990).[1] Given the disagreement in the literature regarding the efficacy of ALCs in tank waste, there is significant uncertainty in expected ALC performance within a nuclear waste environment.

ALC (or similar) systems have also been used extensively in other industries, such as mining, petrochemicals, wastewater, and biotechnology. The use of ALC systems in the mining industry is of particular interest because they are typically concerned with mobilizing slurries of dense particles (e.g., gold, uranium, zinc, copper) with high solids content (>40 wt%). These slurries are bounding with respect to the solids loading in the WTP high solids process vessels, which will likely not exceed 20-wt% solids. The geometry in which the ALC is deployed is known as a Pachuca tank (see Lamont 1958 or Sorensen 1985 for simple mathematical models of Pachuca tanks). Pachuca tanks differ from the WTP process vessel geometry because the bottom of the tank is conical (versus an elliptical bottom), but the ALC system operates using the same principle. Studies have been performed to assess an optimum design, suggesting that the ratio of the riser tube to the tank diameter should be ~0.1 (Mehrotra and Shekhar 2000, 2001; Rodriguez et al. 2007). The Pachuca tank design was also tested for use as a digester tank for dissolving nuclear fuel particles as described in Lewis (1986). The tests included very large (stainless steel powders and particles up to 5000 μm) and very dense particles (tungsten). In the digester tank testing, the air distribution system in the riser tube was optimized to obtain >90% suspension of the solids in the tank. Thus, the results from ALC system use in the mining industry indicate they are capable of providing sufficient energy to suspend solids at upper tank elevations. This functionality would complement PJM operation in the WTP vessels.

---

[1] It is not clear from these sources if the ALCs accumulated these saltcake formations while the ALCs were actively operating or while they were inactive. ALCs have also been routinely used to concentrate liquid waste in the same tanks as part of in-tank solidification units.

ALCs in wastewater or environmental remediation processes are typically used for relatively low flow rate exchange in a reactor or wastewater pond, as the purpose of the ALC is to aerate the fluid or deliver constituents to cell cultures. There is a wide array of examples over the last several decades to illustrate the diverse applications of the technology; see Salser and Mock (1973), Tobajas et al. (1999), and Arbib et al. (2013). A detailed review of airlift use and effectiveness in the wastewater treatment industry is available in Cozma and Gavrilescu (2012).

Vessels containing ALCs are also commonly used in the biotechnology industry to enhance mixing and aeration. The uses of ALCs in the biotechnology industry are similar to their uses in the wastewater industry (and there is significant overlap between the two areas). In these applications the amount of solids in the vessel is generally low (a few percent) relative to the WTP high solids vessels. Typical bioreactors with ALCs have a much larger ratio of riser tube diameter to tank diameter, so the downward flow that returns to the bottom of the vessel occurs in a thin annular region called a downcomer. The merits of using airlifts for bioreactors are discussed in Merchuk (1990) and Chisti and Moo-Young (1987). Examples of relevant studies in bioreactors can be found in Merchuk et al. (1998), Luo and Al-Dahhan (2008), Margaritis and Sheppard (1981), and Gumery et al. (2009).

Merchuk et al. (1998) studied the effect of air distribution (sparger) geometry on mixing in a bioreactor and found that the sparger geometry and pore size was important at low gas velocities, but at high gas velocity had almost no effect.[1] The mixing study by Luo and Al-Dahhan (2008) concluded that though the bulk of the flow in a bioreactor with an ALC is approximately like plug flow, some unmixed regions still may exist (depending on air flow rate and geometry). The review of Gumery et al. (2009) focuses on mixing induced by ALCs in bioreactors, though the review is thorough enough to be applicable to other vessels. A second recent detailed review with a couple of well-presented reactor examples is available in a book chapter authored by Martinez and Silva (2013). Both reviews discuss the impact of geometric parameters, gas flow rate, properties of the fluid, and sparger design as important contributors to ALC performance.

Consensus on what leads to effective (or efficient) performance is challenging to summarize, as there are many variants on the general operating principle and not a consolidated set of design equations. The flow generated by an ALC system is multiphase and often three-phase (a liquid containing solids being injected with air), making simple expression of the physics complex. For some examples of the complexity involved in describing the vertical multiphase flow and its various regimes, see Taitel et al. (1980), McQuillian and Whalley (1985), Zabaras et al. (1986), and Miller and Cain (1986). There are also many studies available on the hydrodynamics of the ALC system (or similar) and the effect of parameter choices on mixing performance. The studies typically are empirical and generate correlations that could be used to predict mixing performance in other airlift mixed vessels. However, many of the correlations were developed in specific geometries and fluid systems; they likely cannot be extrapolated to other systems. Some examples of these are found in Bello et al. (1984), Blazej et al. (2004), Chisti et al. (1988), Heijnen et al. (1997), Kennard and Janekeh (1991), Kojima et al. (1999), Lu et al. (1994), Merchuk (1986), Miron et al. (2004), Russell et al. (1994), Schlotelburg et al. (1999), Siegel et al. (1986), and Wachi et al. (1991). In all the studies referenced, the flow generated by the ALC system and the efficiency of its mixing performance were susceptible to changes in geometry and the relative amounts of

---

[1] This is one example of a study of the effect of the air distributor/sparger geometry on ALC performance. In general the literature is unclear on the effect of the air distributor on ALC performance—in many cases, it depends on what one defines as "significant."

gas (the air input into the ALC), liquid, and solid. Attempts have been made to characterize the airlift vessel with a more fundamental approach. For example, in Merchuk and Berzin (1995) the energy dissipation in the ALC system is modeled, and from that model a global shear rate is estimated. However, estimation of the global shear rate using the Merchuk and Berzin model requires knowledge of multiple pressures in the system, which is typically not information that is readily available.

The empirical studies are numerous and varied, but they all focus on trying to describe hydrodynamic conditions in the riser and the downcomer (the portion of the vessel outside of the riser where the flow, generally, is primarily orientated vertically down). Gas hold-up correlations, which purport to correlate the fraction of gas retained in the fluid of the riser and downcomer, do not indicate by themselves how the ALC performs as a mixing device in a tank. Of more relevance are correlations for liquid velocity in the riser tube.[1] The studies differ in some aspects but they agree that the liquid velocity in the riser has the general form

$$U_{lr} \sim c_1 (L_c)^{c_2} \left(U_{gr}^* \right)^{c_3} \tag{2.1}$$

where U_{lr} is the liquid velocity in the riser, L_c is a characteristic geometric parameter (or geometric ratio), U_{gr}^* is the height-averaged superficial gas velocity in the riser, and c_1, c_2, and c_3 are empirically derived constants. The constants c_1 and c_2 vary depending on the fluid and geometry, but in all studies $0.3 \leq c_3 \leq 0.5$. Note that c_1 typically has dimensions, whereas the other two constants are always dimensionless. For experimental data collected using Newtonian fluids, all fluid physical properties are usually incorporated into the constant c_3 (in the form of a dimensionless group). The notable exception to the relationship given in Equation (2.1) is found in Chisti et al. (1988), where an energy balance method was used to solve for U_{lr}, yielding the expression

$$U_{lr} = \left[\frac{2 g h_D (\varepsilon_r - \varepsilon_d)}{K_B \left(\frac{A_r}{A_d} \right)^2 \frac{1}{(1 - \varepsilon_d)^2}} \right]^{0.5} \tag{2.2}$$

where g is gravitational acceleration, h_D is the gas-liquid dispersion height, ε is the gas hold-up (gas volume fraction), A is the cross-sectional area, and K_B is the friction loss coefficient at the bottom of the riser tube. The subscripts r and d refer to the riser and downcomer, respectively. Equation (2.2) does not contain any adjustable parameters and can be used provided that gas hold-up, h_D, and K_B can be estimated. The ability to predict U_{lr} is important for ALC assessments. One method that could be used to scale up mixing techniques is matching power per unit volume, and the power can be calculated from the kinetic energy, i.e., kinetic energy $\propto U_{lr}^2$.

Of more specific interest to the application of an ALC in WTP process vessels is the ability of the mixing technology to be used at several operating levels. One approach to operating at multiple fluid levels is to use a properly engineered multi-stage ALC. A multi-stage ALC has one or more intermediate outlets for some of the moving fluid in the riser tube to discharge at more than one elevation. Some recent examples of studies conducted with multi-stage ALCs are found in Li et al. (2009) and Yu et al.

---

[1] There are also many correlations for mixing time or mass transfer coefficients, but these correlations are of more interest for chemical reactions. Mixing, or more specifically mixing energy, is the quantity of principal interest in the WTP vessels; liquid velocity is a useful proxy for mixing energy.

(2009, 2010). These studies demonstrate that the concept of a multi-stage ALC is feasible, but the fluid did not contain significant solid particles, so the effect of having multiple stages on mixing fluids with solids is not clearly known. Cook and Waters (1955) tested both a riser tube with slots and a two-stage riser tube but found that the loss of flow was significant and did not pursue the development of a multi-stage ALC any further. One alternative to a multi-stage ALC would be to adjust the mixing energy in the vessel that the ALC provides by some other means, such as adjusting the air flow rate as the surface level in the vessel changes.

The ALC also needs to be able to perform reliably when the fluid is non-Newtonian, which will be common in some WTP process vessels. Examples of work with non-Newtonian fluids are much more limited in the literature and usually focus on power law fluids (in contrast with yield stress fluids, which are expected in WTP vessels). Some examples are presented in Chisti and Moo-Young (1988), Cerri et al. (2008), Gavrilescu and Tudose (1998), Jin et al. (2006), Kawase and Moo-Young (1986a, 1986b), Sun et al. (2006), and Velan and Ramanujam (1992). Kawase and Moo-Young (1986) observed that the riser tube diameter did not appear to have any effect on the gas hold-up, but the effect on liquid mixing (and mass transfer) was not clear when non-Newtonian fluids were used. Conversely, Velan and Ramanujam (1986) concluded that an optimum riser diameter to tank diameter of ~0.44 existed when non-Newtonian fluids were being used in their test system. There are a few correlations (see Gavrilescu and Tudose 1998 or Jin et al. 2006 for example) relating U_{lr} to the non-Newtonian data collected in these studies, and they are similar in form to Equation (2.1). Extra terms are added to account for the fluid properties, such as apparent viscosity or solids concentration. However, the prediction and scale-up of non-Newtonian fluids in these systems remains relatively uncertain as the parameter space examined in these studies is narrow.

The work of Jin et al. (2006) and Sun et al. (2006) are most representative of the kinds of material that would be processed in the WTP. Jin et al. (2006) conducted experiments using a non-Newtonian fluid with sludge solids and demonstrated that the velocity and gas hold-up decrease with increased sludge loading. Sun et al. (2006) tested a Newtonian fluid with silica sands, comparing a bubble column with no riser tube to a concentric cylinder ALC. The ALC was found to be more stable in performance to changing solids concentration and was found to have more uniform distributions of solids concentration and gas holdup than the bubble column once a minimum air flow rate was reached. Based on what is available in the literature, it was considered likely that ALC data would need to be collected using non-Newtonian fluids in order to support refinements to the WTP SHSV design.

Alternative air-driven systems were also considered during this scoping study. For example, commercially available airlift pumps (one example being Geyser pumps[1]) that create an upwelling flow in the tank center using a similar principle to an ALC were considered a candidate mixing technology that may accomplish supplemental mixing functions. Studies have been conducted using a parallel-plate- or plate-sparger device that introduces large, periodic air bubbles that are forced to spread beneath plates before they release and form large circulation patterns. The device was successfully demonstrated in PNNL studies described in Powell and Hymas (1996), Powell (1997), and Whyatt and Hymas (1997) with waste simulants. Air bubbles alone can also drive significant flows, as fluid motion has even been demonstrated to occur using only an airline and a bubble screen at large depths (~200 m) in ocean water (see Liang and Peng 2005). Using injected air bubbles to generate local flow and mixing is the function of spargers considered for use in the WTP vessels, a topic that has been studied extensively (see Poloski et al. 2005; Russell et al. 2005; and Kurath et al. 2009).

---

[1] http://www.geyser-pump.com/

Airlift pumps are similar to ALCs and thus much of the previously cited literature is applicable. They have also been studied extensively on their own and have a wide-range of applications in various process industries. The principle of operation is very similar to ALC systems; consequently, much of the previously cited literature is also applicable. Many references are available on the topic including Morrison et al. (1987), Zenz (1993), Khalil et al. (1999), Samaras and Margaris (2005), and Kassab et al. (2007, 2009). These references are all in agreement that the flow regime in which the airlift pump operates affects performance, and it is usually beneficial to operate the pump such that the flow can be classified as slug flow. This is the regime that commercially available pumps such as a Geyser pump operate in, and the Geyser pump has demonstrated an ability to mobilize heavy solids effectively (Kondo et al. 2008). Thus, the Geyser pump was considered to be a readily available airlift pump that was important to compare against a more traditional ALC system.

Because the literature describing various studies of airlift technologies is very extensive, the references discussed in this section should not be considered a comprehensive survey of the state of the art. However, a many articles were reviewed to ascertain that ALC technologies are well established in many process industries and offer a potentially effective supplemental mixing technology for WTP high solids vessels. The next section of the report presents a brief discussion of the nomenclature, followed by a description of the PNNL test stand and the mixing systems that were tested during the scoping study.

3.0   Test Equipment, Materials and Matrix

In this section, test stand equipment and simulant materials are described. In Section 3.1, the basic nomenclature and terminology used in the rest of the report is introduced. Section 3.2 describes the test stand and auxiliary equipment, followed by a description of the simulants used in testing (Section 3.3). Finally, Section 3.4 summarizes the test configurations that were used, i.e., the test matrix of the study.

3.1   Nomenclature and Terminology

As mentioned in the previous section, the literature on ALC systems (or similar systems) is expansive. Many authors use different nomenclature or terminology when referring to airlift geometry or operation. To maintain consistency during testing and reporting of the results, the nomenclature for the PNNL test stand was specified prior to the start of operations. A general diagram with the nomenclature used in the PNNL testing is given in Figure 3.1. The geometric parameters in Figure 3.1 are defined in Table 3.1 for reference. Several of the parameters were varied during the ALC program testing, but the vessel dimensions were fixed, with a d_t of 90 in. and an h_t of 121.6 in.
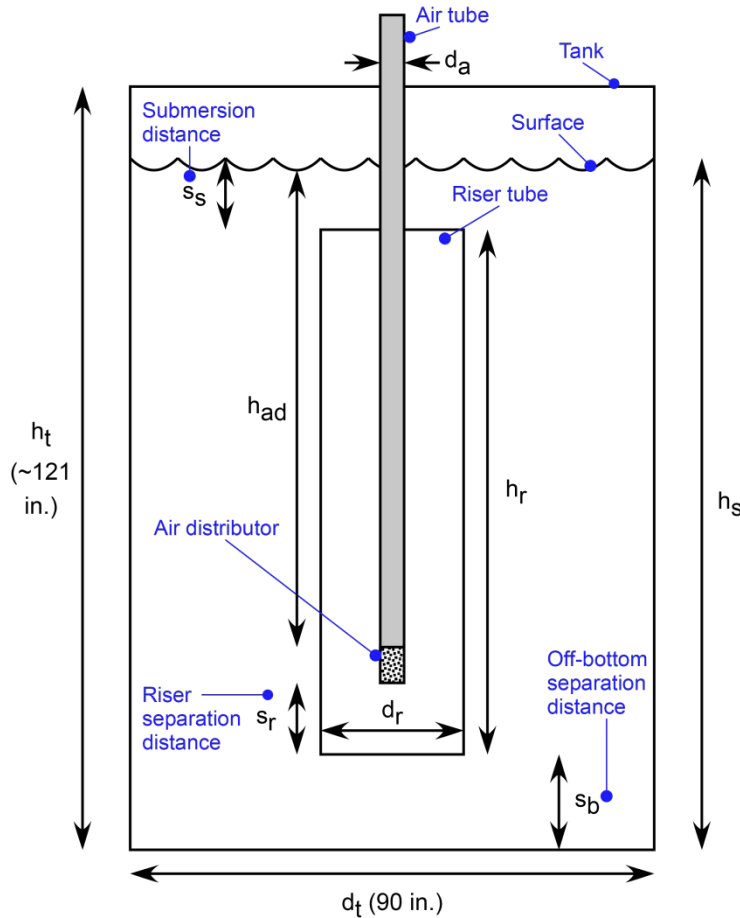
Figure 3.1. Representative System Schematic Showing Nomenclature and Parameters for Airlift Circulator Scoping Tests (not to scale).

Table 3.1. Description of the ALC System Parameters.

Symbol	Name/Description
d_a	Diameter (OD) of air tube
d_r	Diameter (ID) of riser tube
d_t	Diameter (ID) of tank
h_{ad}	Height (depth) of air distributor
h_r	Height (length) of riser tube
h_s	Height of fluid surface in tank
h_t	Height of tank
s_b	Off-bottom separation distance (distance of riser tube bottom above tank bottom)
s_r	Riser separation distance (distance of air distributor above bottom of riser tube)
s_s	Submersion distance (distance of top of riser tube below fluid surface)

Not all of the elements in Figure 3.1 were present exactly as shown, as the diagram is generalized in order to communicate the implemented nomenclature. One example is the position of the air tube, which was not typically installed in the annulus of the riser tube. Another is the riser tube itself: some of the mixing devices tested had a more complex geometry than an open cylinder, e.g., the Geyser pump. The specific configurations that were tested are described more precisely in Section 3.4.

Other elements of the ALC mixing system that were discussed for evaluation (but were not formally tested) include a diverter and an aerosol mitigation device. A diverter is a physical structure placed underneath the riser tube on the tank bottom, with a pyramidal or similar geometry. The diverter would be installed to accomplish two functions: (1) restrict the collection of solid particles directly underneath the ALC tube at the tank bottom-center, and (2) direct bottom-sweeping flow upwards into the riser tube (flow that would be created by PJMs in the WTP process vessel). Because significant quantities of solids were not used in testing and the bottom-mixing was not prototypic (no PJMs were present), a diverter was not installed during any formal PNNL tests.

The use of an aerosol mitigation device was considered in the event that aerosol generation at the fluid surface was observed to be significant and require dampening. The concept for dampening aerosol in the PNNL testing was a physical obstruction of the upward flow from the riser, such as a deflector plate near the fluid surface. Obstructing the flow was not desirable unless aerosol was observed in significant quantities, as it would likely also reduce the mixing energy input into the fluid by the ALC. During testing, aerosol was observed in the headspace (particularly during non-Newtonian testing), but the PNNL test tank had an open geometry that was not well-suited for aerosol quantification without substantial modifications. A single, centrally located ALC is presumed to produce fewer aerosols than an array of spargers due to a projected reduction in the quantity of air required (and only having a single air column breaking the liquid surface). Nevertheless, the quantity of aerosol generated in PNNL ALC testing relative to the current amounts expected during WTP vessel operation was not assessed.[1]

---

[1] More precisely, the amounts expected to be generated by other potential supplemental mixing technologies (for example, spargers) that may be used in the WTP vessels. Aerosol generation is a concern and is a technical gap that likely needs to be addressed in the future.

3.2 Test Equipment

The experimental study of supplemental mixing performance was performed with a readily configurable test stand in order to remain flexible during the testing. The flexibility of the test equipment provided the ability to respond to test results and quickly evaluate changes to a system or implement alternative measures of performance. The test stand was located in the Applied Process Engineering Laboratory (APEL) high bay, i.e., APEL/184 and APEL/186. The major components of the test stand were as follows:

- Flat-bottom polyethylene tank that served as the test vessel. It was originally used as a feed vessel in pilot scale testing of a near-tank treatment system, which is described in Schonewill et al. (2011). It had nominal dimensions of $h_t = 121.6$ in. and $d_t = 90$ in. The tank was surrounded by scaffolding at the 7-ft (84-in.) level for staff to conduct test operations.

- Gantry crane with a 2-ton electronic hoist and two manual 1-ton hoists used to maneuver equipment into and out of the tank.

- Air-driven mixing system being tested, such as an ALC with a riser tube and an air distribution line. All mixing systems were installed so that the system or the support structure holding the system rested on the floor of the vessel.

- System to provide off-bottom motion (also called the OBMS, for off-bottom motion system). The motion was generated by recirculating fluid from the upper portion of the test vessel with a pump and reintroducing this fluid through a series of nozzles near the floor of the tank. This system was only used during the Newtonian testing.

- Building air, which was the motive agent for the majority of the equipment in use.

- Instruments or measuring devices, e.g.,

  - pressure gauges for monitoring air supply pressures to equipment;

  - variable-area flowmeters (rotameters) for metering and measuring air flow;

  - velocity meters for in-tank measurements;

  - video/still cameras for recording in-tank and surface observations;

  - balances for weighing simulant and particles collected;

  - thermocouple and reader for monitoring simulant temperature;

  - laser distance finder for monitoring level during non-Newtonian testing; and

  - timing devices (typically cell phone clocks/timers/stopwatches).

The pressure gauges, rotameters, balances, thermocouple (and reader), and laser distance finder were all standard off-the-shelf instruments and are not described in more detail in this section. The video cameras and velocity meters are described further in this section. Other equipment was used to conduct some (but typically not all) of the tests. When additional equipment was used that is important to understanding a particular set of tests, it is described in the context of the tests for which it was used.

The PNNL test stand was composed of equipment and materials that were selected for maximum flexibility during testing. As the ALC system was assessed, changes needed to be implemented quickly

and easily to narrow down the ALC configurations that would satisfy the objective. Thus, many of the elements of the test stand were developed from materials on hand or readily available parts and materials. Representative images and diagrams of the equipment and materials discussed in this section, along with other supplementary information on the experiments, are provided in Appendix A.

The tank had an internal diameter of 90 in., and a maximum working height of approximately 108 in.[1] Two significant modifications were made to the tank. First, a large section in the middle of the top was cut out to permit loading of the ALC systems and other equipment in and out of the tank. In general, the Gantry crane stationed over the tank was used to lift or move an ALC system, whereas other items (hoses, poles, brooms, cameras, etc.) were moved around by hand. In addition to the large middle cut-out, six approximately 8-in. holes and two approximately 4-in. holes were cut out through the top near the outside wall of the tank to permit easier access for activities such as sampling or positioning cameras. The other major modification was to place bulkhead fittings in the tank. Two 2-in. bulkheads were added at around the 6-ft and 3-ft levels and were used as inlets for flow to a 2-in. air-operated diaphragm (AOD) pump. Four 3/4-in. bulkheads were placed 90° apart around the bottom of the tank (~2 in. from the tank bottom) with a ball valve on the outside. These bulkheads were used to deliver the flow from the AOD pump through nozzles. The initial nozzles were drilled out 3/4-in. polyvinyl chloride (PVC) caps. The AOD, recirculation inlet line (drawn through one of the 2-in. bulkhead fittings), and the 3/4-in. nozzles made up the OBMS as it was initially devised. In typical operation of the OBMS, the AOD was driven by air pressures of up to 50 psi. Subsequent modifications to the OBMS are discussed in Section 5.1.

The riser tube and air tube apparatus comprise the ALC system. In this testing, two types of ALC systems were constructed. A basic diagram of the two types is given in Figure 3.2. Type 1 was an approximately 10-in. ID white PVC tube, cut into sections so that the tube length could be altered in increments of 1 ft between 1 and 8 ft. The modular sections were sealed with heavy-duty tape. The Type 1 air tube was a 1.5-in. ID PVC pipe that ran through the center of the riser tube, creating an annulus between the tube and the riser wall, and terminated in a threaded connection to which various engineered air distributors (e.g., a sieve plate, see Section 4.1) could be attached (or the tube could be left open). Thus, a fraction of the cross-sectional area of the Type 1 riser tube was taken up by the air tube.

The initial Type 2 riser tube was also approximately 10-in. ID, but was a thinner-walled clear acrylic tube. The clear tube was also cut into modular sections and sealed with tape as in the Type 1 ALC. The exterior of the tube was marked in 1-ft increments. The air tube was a 1-in. Schedule 40 PVC pipe and it was affixed on the outside of the riser tube. At the bottom of the riser tube, the air tube had two elbows and terminated in a PVC cap with holes drilled in the top acting as the air distributor. Thus, in contrast with the Type 1 system, the Type 2 air tube did not reduce the cross-sectional area of the tube, with the exception of the very bottom. The clear acrylic riser tube also permitted real-time visualization of the multiphase flow during operation.

In the non-Newtonian testing, Type 2 riser configurations were also tested with a nominally 18-in. ID tube that had a single air tube configured as shown in Figure 3.2 and a modified configuration where a second air tube of identical size and geometric configuration was added right next to the existing air tube (a configuration called SP-05p). The SP-05p configuration is discussed in more detail later in this section.

---

[1] This is in contrast to the maximum height of the tank, which was earlier stated to be 121.6 in. The maximum working height was lower due to the portions of the tank that had been cut out to enable access.
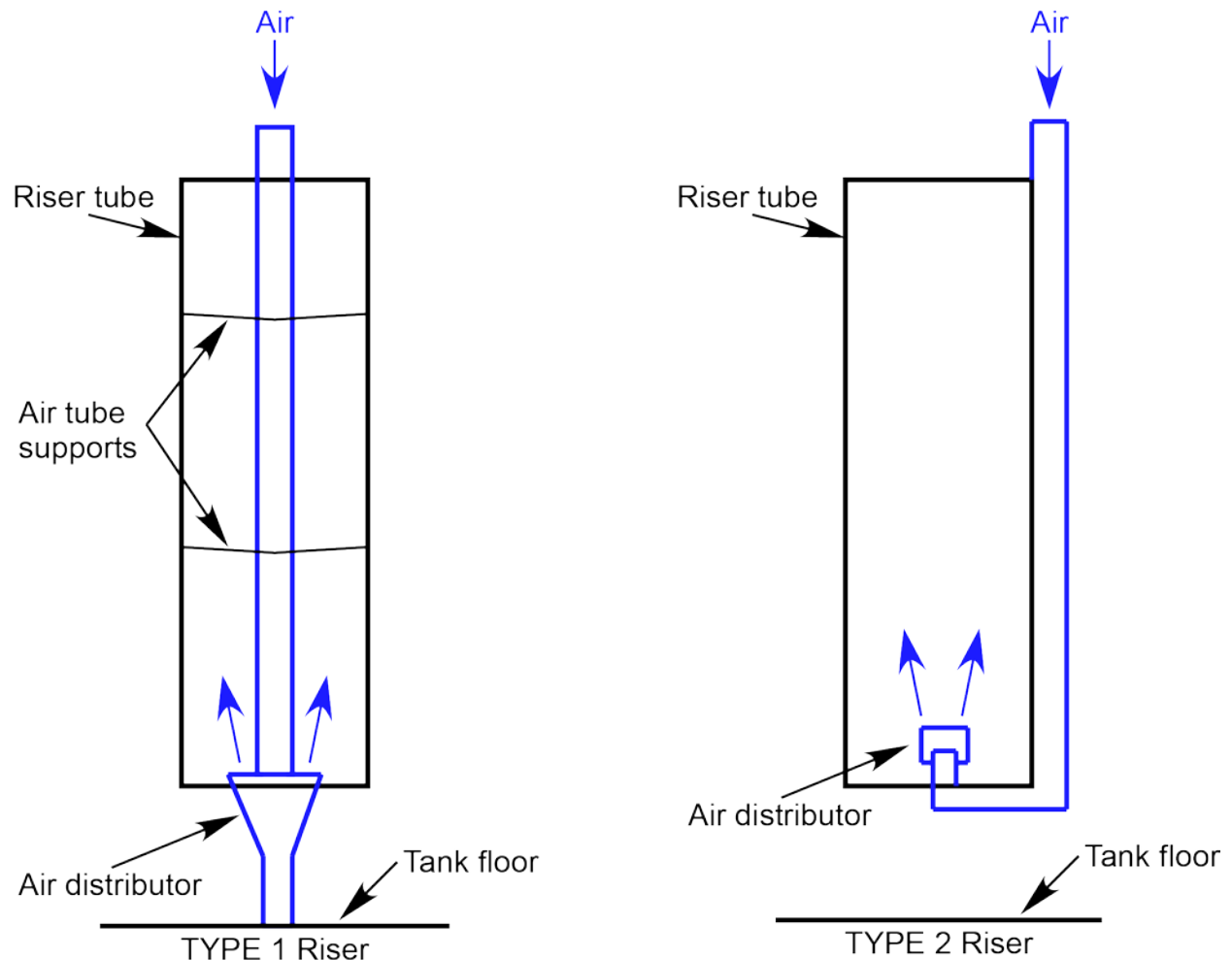
Figure 3.2. Diagram of the Two Riser Types Used in the PNNL Test Stand. The air tube and components are indicated in blue. Riser tube support structure (identical in both cases) is not shown for clarity.

Both riser types were held in place by mounting them on an adjustable Unistrut frame with a lifting ring. The tubes were secured using holes drilled in the riser tube and fastened with screws. The Type 1 air tube was braced by fins (air tube supports in Figure 3.2) inside the riser tube to keep it rigid. The fins were long screws present at two elevations as shown in the figure. The fins were not expected to alter the flow field appreciably, as they negligibly reduced the cross-sectional area in these two locations. The Type 2 air tube was strapped to the riser tube directly to hold it in place during testing. The air tubes were connected via hoses to the building air supply, with the flow controlled using a Dwyer rotameter (or later, a series of Dwyer rotameters in a manifold). Pressure gauges were used to monitor the building and supply pressures. The maximum supply pressure was ~100 psi (subject to other building pressure demands), with the supply air typically regulated down to the pressure required to achieve the desired air flows, typically 20 to 40 psi in most usage scenarios.

In addition to these riser tube and air apparatus configurations (referred to as a "traditional" ALC), three other air-driven mixing devices were used in testing. One was used in both Newtonian and non-Newtonian testing. It is a commercially available air-driven pump called the Geyser Hybrid Pump (GHP). The GHP is an airlift pump that also has a pulse mode. It required two air tubes to be operated

but no additional structural support (it was weighted with a concrete doughnut so it could rest on the floor of the tank). The riser tube of the GHP was made of PVC tube that was approximately 6-in. ID on the suction side and terminated in a flanged discharge that had a ~4-in. ID. The flanged end accommodated the addition of riser tube extensions (also ~4-in. ID clear PVC pipe) as needed. The suction side had a larger cross-section to accommodate a U-shaped chamber that created pulsations when running in pulse mode. A manufacturer's diagram of the GHP is shown in Figure 3.3. Note that the clean-out ports and the air supply for "Airlift Pump Mode 2" were optional features and were not part of the unit PNNL used in testing.
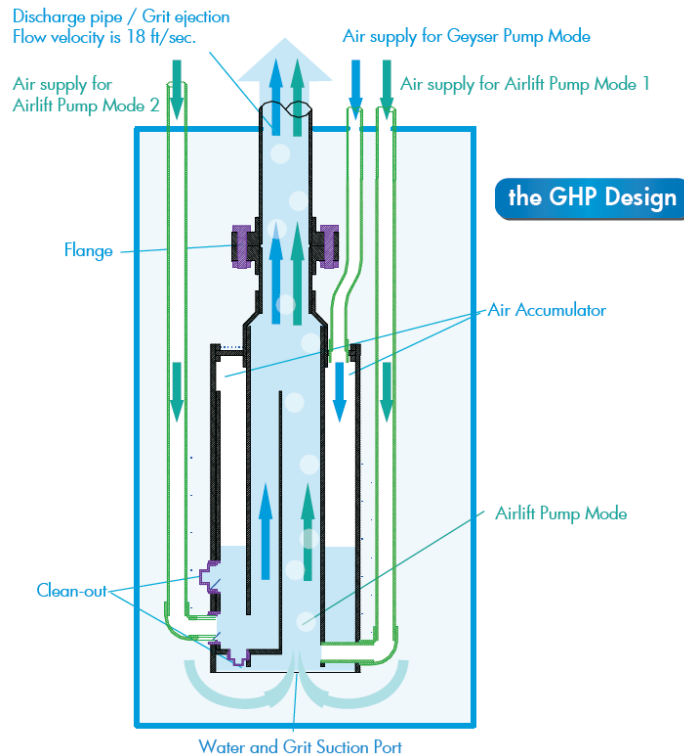
Figure 3.3. Diagram of GHP Pump Provided by Geyser Pump Tech LLC. Note: The PNNL unit did not include clean-out ports or the air supply for "Airlift Pump Mode 2."

The GHP can be operated as a traditional ALC by using only the open air tube that terminates into the side of the riser near the bottom (air supply for "Airlift Pump Mode 1"), in a pulsed mode by using another (air supply for "Geyser Pump Mode") air tube, or in a hybrid mode by operating both air tubes at once. In hybrid mode, the "Airlift Pump Mode 1" air tube runs continuously to create a constant up flow; this is supplemented by the second ("Geyser Pump Mode") air tube that periodically fills a holding chamber ("Air Accumulator") and then releases a larger volume of air, i.e., a pulse. The volume of air is released once fluid is displaced down to the bottom of the U-shaped accumulator leg seen on the left side of Figure 3.3. The frequency of the pulse is determined by the air flow rate to the second air tube, but the chamber volume was fixed (~1 ft^3 at the air supply pressure, typically 20 to 40 psi). For simplicity, the air supply lines for "Airlift Pump Mode 1" and "Geyser Pump Mode" are referred to as the airlift and pulsed air lines, respectively. The pulsed mode (not investigated in this report) is conducted by running only the second air tube.

The other two mixing devices were tested briefly in non-Newtonian fluid only. One device was a pulsed-air apparatus made by Pulsed Hydraulics, Inc. (PHi).[1] The apparatus has a single air tube that terminates in a pair of ~8-in. diameter parallel plates (referred to as a forming plate, pictured in Figure 3.4a). The plates are 3/16-in. thick and separated by a gap of 3/8-in. The top plate is connected to the 1-in. air tube; the air is periodically input to the forming plate via a control box (see Figure 3.4b). The control box has a valve and control system that injects approximately 2 to 4 ft^3 of pressurized air (per the manufacturer literature at 50 psi) every time the control valve actuates. The air pressure at the control valve was typically set to ~80 psi. The user selects the frequency of the pulse, which can be designated at "Low" (pulse every 30 s), "Medium" (pulse every 15 s), and "High" (pulse every 10 s). In the PNNL test stand, the forming plate rested on the tank bottom in the center with radial support legs to keep the plate in place during testing. This configuration is also referred to in this document as the pulsed plate mixer (PPM).

(a) Forming plate of pulsed-air PHi mixer   (b) Control box of pulsed-air PHi mixer

Figure 3.4. Images of Pulsed-Air Mixer Components Manufactured by PHi: (a) forming plate and (b) control box.

The other device was a simple modification to the ALC system and given the configuration name SP-05p. The "p" stands for "pulse." In this configuration, a second, identically configured air tube was added to an existing ALC system (Type 2 riser), such that the second air tube injected air right next to the first tube at the same elevation. The second air tube was operated using the PHi mixer control box pictured in Figure 3.4b, in the same manner as it was operated for the PPM but without the forming plate. This modification provided an ALC that had a continuous flow generated by the first air tube augmented by a pulsed flow generated by the second air tube. The two air lines were controlled independently and could be run separately.

Video cameras were used to monitor and observe the flow dynamics in the tank. In-situ video was collected using GoPro HERO3+ cameras that were placed in waterproof housings and capable of wireless transmission to an iPad.[2] These cameras were mounted to poles or other implements and positioned in

---

[1] See www.phiwater.com.

[2] In practice, real-time monitoring using the iPad was not successful as the wireless signal could not penetrate through several feet of water. It was, however, helpful for positioning the cameras prior to starting test operations.

the tank to view phenomena of interest during the Newtonian testing. Pictures were also taken to document static states in the tank as needed, since the water was optically clear during the Newtonian testing. Video camera use during non-Newtonian testing was restricted to taking videos of surface mixing, as the fluid was too opaque to permit visualization *in situ*.

   The velocity meters used during testing were a commercially available propeller-style velocity instrument (either the General Tools Flowatch® FW450[1] or, later in testing, the same flow meter with the FW 450-50 water impeller accessory). A close-up image of one of the propellers used is shown in Figure 3.5. It could be installed either at the riser tube outlet, which is the default standard, or other locations in the tank, with instantaneous velocity measurements output to a display unit that was capable of averaging the data over user-specified periods. The propeller device is usually used to measure velocities in water, whereas it was used in the PNNL test stand to measure both multiphase water-air (Newtonian) and clay slurry-air (non-Newtonian) flow. Thus, the instrument data that was measured was anticipated to be an approximation of the true velocities of the liquid phase. The inaccuracies in the data due to the two-phase flow would be particularly acute when the flow abruptly alternates between gas and liquid flow (more likely at higher air flow rates when the riser tube contains slug flow). It was also found that the propellers wore down or became damaged during measurements at high velocity, especially in the non-Newtonian fluid. This is likely due to wear on the bearings, which are subject to degradation with time (or stress during use). However, because all velocity data was measured with the same device and subject to similar inaccuracies, comparison of data sets between configurations tested by PNNL indicated relative differences in system hydrodynamics.

Figure 3.5. Representative Image of General Tools Flowatch Propeller Instrument Used to Estimate Velocities During PNNL Testing.

---

[1] For additional information see: http://www.generaltools.com/FW450--Flow-Watch_p_1278.html.

3.3   Simulant Materials

Simulant materials for both the Newtonian and non-Newtonian testing are described in this section. Air, which was input to the system and became incorporated in the simulant being tested as part of the operation of the air-driven mixing devices, was used from the building supply as-is and assumed to be dry (not humidified) air with the standard components ratios of oxygen, nitrogen, argon, carbon dioxide, etc. This assumption is supported by the configuration of the building air supply, which contained filters for removing water and oil as well as a refrigerated dryer to deliver air at a negative dew point.

3.3.1   Newtonian Simulant

The simulant materials during the Newtonian testing were limited to the following:

- Process water, i.e., the carrier fluid. This water was used in quantities of up to ~3000 gal to fill the test tank.

- Mt Hood 480, a biocide used in trace amounts ($\leq$ 75 ppm) to eliminate biological growth.

- "Green" Deco beads acquired from Ceroglass; the particles were soda-lime glass with a base coating of silver and a colored (green) surface coating. The particle diameters ranged between 500 and 750 µm. See Figure 3.6 for an image of these beads.

- Pea gravel: generic material on hand that was heterogeneous in size, nominally 6 mm in largest dimension, and non-spherical.

The green beads had a density of 2.5 kg/L and the pea gravel had a nominal bulk density of ~1.8 kg/L.[1] Clear glass beads (Potters Mil 13, 45 to 90 µm, density of 2.5 kg/L) and "Fuchsia" Deco beads (Ceroglass coated soda-lime glass particles, 200 to 300 µm, density of 2.5 kg/L) were also available but were not used to collect data.
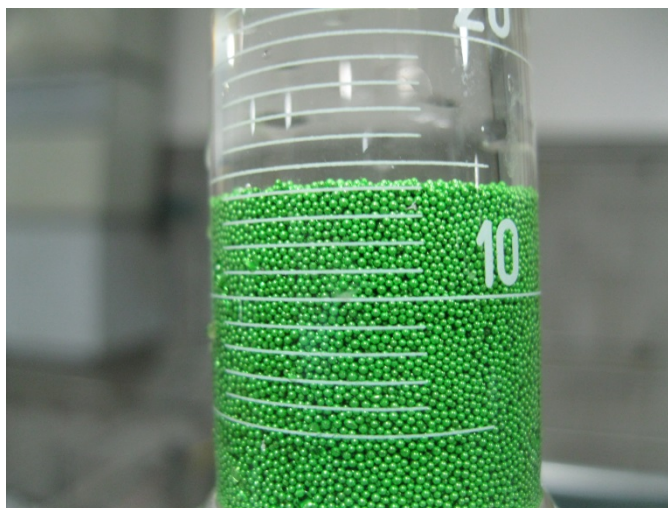
Figure 3.6. Image of Green Beads Used in Particle Transport Experiments.

---

[1] Pea gravel bulk density: http://www.aqua-calc.com/page/density-table/substance/gravel-coma-and-blank-pea. Gravel particle density was not precisely known but is expected to be approximately 2.7 kg/L.

The largest amount of solid particles used in Newtonian testing was 5.46 kg (~12 lb) of the green Deco beads, which is a solids concentration of around 0.05 wt% when the tank contained 105.5 in. of water (a typical fill level). The implication of this low concentration is that solids loadings typical of WTP vessels (up to 20 wt%) were not tested. Note that for the remainder of this document, the green Deco beads are simply referred to as green beads.

The pea gravel (pictured in Figure 3.7) was used in only small amounts in proof-of-principle experiments. Though the green beads are on the upper end of the size range for particles expected in the WTP vessels, pea gravel was considered a bounding case[1] and a good test of the ALC's ability to lift particles to the top of the vessel. The total pea gravel inventory did not exceed 2 lb, and the gravel was usually removed from the tank immediately after use.

Figure 3.7. Detail of Pea Gravel Used in Particle Transport Experiments.

3.3.2 Non-Newtonian Simulant

The non-Newtonian fluid used in the testing was clay slurry composed of kaolin and bentonite solids in water.[2] The kaolin and bentonite solids were targeted to be present in a 4:1 (80:20) kaolin:bentonite mass ratio and a total solids content sufficient to give the slurry nominal rheological properties of 30 Pa (Bingham yield stress) and 30 cP (Bingham consistency). The 30 Pa/30 cP Bingham parameters were chosen as a target because they are the upper design limit parameters for the WTP vessels. A Bingham fluid does not move until the material is yielded, i.e., the local shear stress exceeds the yield stress. Once it begins to move, it flows like a Newtonian fluid with an apparent viscosity that is dependent on the shear rate and about equal to the Bingham consistency at shear rates greater than approximately 100 s^{-1}.

---

[1] Pea gravel is likely bounding for particle size, but not for particle density. However, given the fluid (water) and the size of pea gravel (as large as 6 mm) versus the expected size (<100 μm) of some of the densest particles in the WTP vessels, i.e., plutonium oxides (density = 11.5 kg/L), pea gravel is likely to be bounding (or nearly so). This was confirmed by calculating the expected terminal velocity of a single particle in water, which is an order of magnitude greater for a pea gravel particle of density 2.7 kg/L than it is for a 100 μm plutonium oxide particle.

[2] Kaolin used was EPK kaolin from Edgar Minerals, Inc. and the bentonite was Big Horn bentonite from Wyo-Ben Inc.

The clay slurry was made in 10 batches of approximately 300 gal each, spread over 11 totes. Once the slurry batch had been sufficiently blended, each tote was sub-sampled to measure the solids content of the slurry using a Mettler Toledo Halogen Moisture Analyzer (Model No. NR83), and the measured data was averaged to estimate the bulk solids content. The average total solids was found to be 33.4 wt% (79.8 wt% kaolin and 20.2 wt% bentonite), with the balance being water and a small amount (75 ppm) of biocide. Based on these mass concentrations, the bulk density of the slurry was estimated to be 1.259 kg/L (g/mL).

Bingham parameters of slurry samples were determined from rheograms obtained in the 0- to 1000-s^{-1} shear rate range using a HAAKE RS600 rheometer with a Z41 concentric cylinder geometry. All measurements were conducted at 25 °C and data was processed using the software accompanying the rheometer (HAAKE RheoWin, version 4.41). The rheology was measured on samples from all 11 totes, and the bulk average parameters were a yield stress of 22 Pa and a consistency of 34 cP. The individual sample measurements of Bingham parameter values are presented in Table 3.2 along with the averages. Note that the yield stress spanned a range of 16.3 to 27.2 Pa and the consistency varied from 29.5 to 38.5 cP for the 11 samples. The variation in the Bingham parameters is weakly correlated with the differences in solids content (also shown in Table 3.2). The table also shows two averages, one with all 11 totes and the other with Tote 8 excluded. Tote 8 is excluded because it was not loaded into the tank originally and was not part of the slurry that was tested. In later loads, a portion of Tote 8 was used as make-up slurry since there was always some material lost during testing and transfers.

Table 3.2. Physical Property Measurements from Tote Samples of the Clay Slurry.

Simulant Tote	Solids Content (wt% solids)	Yield Stress (Pa)	Consistency (mPa·s or cP)
		Note: parameters from 250-800 s^{-1}, down ramp	
Tote 1	32.7	16.3	29.5
Tote 2	33.3	19.3	30.3
Tote 3	33.4	17.1	29.5
Tote 4	33.7	27.2	37.7
Tote 5	33.4	25.7	35.4
Tote 6	33.5	24.8	35.0
Tote 7	33.5	24.0	35.6
Tote 8	33.5	21.6	32.8
Tote 9	33.5	22.8	34.3
Tote 10	33.0	19.5	31.3
Tote 11	34.0	19.6	38.5
Average	**33.4**	**21.6**	**33.6**
Average (excluding Tote 8)	**33.4**	**21.6**	**33.7**

During non-Newtonian testing, tracer or seed particles were used in the clay slurry to characterize the regions of the slurry that were being moved (or not moved) by the ALC system. The tracer particles were plastic Airsoft pellets of various colors (see Figure 3.8 for a close-up of yellow pellets). The pellets were nominally 6 mm in diameter and weighed nominally 0.12 g per pellet (found to vary from 0.11 to 0.13 g depending on the particle), with the exception of the red pellets, which had a nominal weight of 0.15 g. By the end of testing, 12 distinctly colored pellets had been used. The colors, as-measured average weights, and estimated average densities of these pellets are given in Table 3.3. The densities were

calculated assuming that all particles were spherical and had a diameter of 5.89 mm, which was the average dimension based on 18 measurements of various particles with a digital caliper. The standard deviation of these measurements was 0.03 mm, so the same value was used for particles of all colors. In the discussion of the non-Newtonian testing, specific sets of pellets will typically be referred to as particles modified by the appropriate color, i.e., the yellow particles.

The approximate density (with the exception of the red particles) of these particles was lower than the density of the clay slurry. However, they were not positively buoyant enough to yield the clay slurry and migrate vertically. This was tested before the particles were loaded into the tank by placing them in a small volume of slurry and leaving them overnight. They were found in the same vertical location the next day. The 6-mm (1/4-in.) particle size was such that they would not pass through a no.-4 sieve or Y-strainer screen, and these were the typical methods for particle recovery.
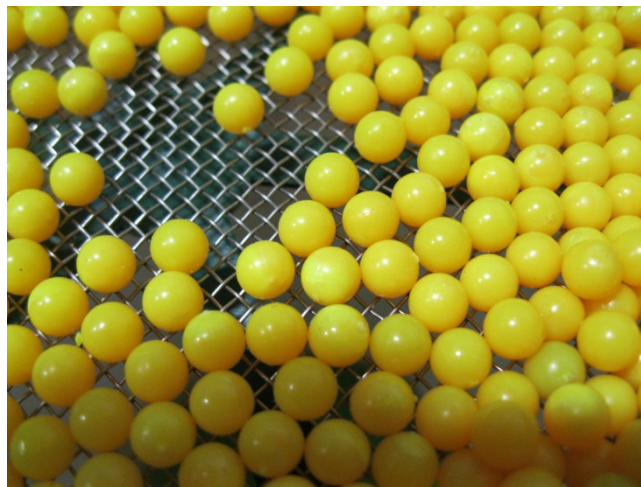
Figure 3.8. Image of Yellow Plastic Airsoft Pellets Used as Tracer Particles.

Table 3.3. Airsoft Pellets Used in PNNL Non-Newtonian Testing.

Pellet Color	Average Pellet Mass (g)	Average Pellet Density (kg/L or g/mL)
Yellow	0.118	1.101
Brown	0.119	1.108
Green	0.131	1.225
White	0.112	1.046
Red	0.149	1.397
Orange	0.117	1.091
Blue	0.114	1.062
Grey	0.118	1.105
Translucent Red	0.111	1.040
Translucent Green	0.111	1.037
Translucent Orange	0.112	1.045
Bright Orange	0.114	1.067

3.4   Test Matrix and System Configurations

The types of ALC tests that were conducted in the PNNL test tank are summarized in Table 3.4. Each "Test Series" shown in Table 3.4 represents a system configuration and encompasses a series of measurements, some of which were conducted only in Newtonian (water with solids) or non-Newtonian fluid (clay slurry with tracer particles). A few configurations were tested in both Newtonian and non-Newtonian fluids. The Test Series is an identifier that will be repeatedly used to refer to the configuration in later sections of this report.

The measurements made during a test often included flow rates, visualization of particle/solid transport, characterization of solids mixing, collection of video data, tracer particle recovery, and/or other miscellaneous methods of data collection. The specific measurements made for each configuration are discussed in later sections. Note that the order of the configurations shown in Table 3.4 is not the order in which they were tested.

Table 3.4. System Configuration (As-Measured) Used during ALC Testing in PNNL Test Stand.

Test Series	Test Configuration				Simulant
BM-01	*Riser tube Type 1* d_r = 9 7/8 in. s_r = ~0 in.	h_r = 83 15/16 in. s_b = 13 in.	*Sieve plate air distributor* d_a = 1 13/16 in. s_s = 8 1/4 in.	h_s = 105 3/4 in.	Newtonian (but no solids)
BM-02	*Riser tube Type 1* d_r = 9 7/8 in. s_r = ~0 in.	h_r = 83 15/16 in. s_b = 13 in.	*Open tube air distributor* d_a = 1 13/16 in. s_s = 8 3/8 in.	h_s = 105 5/8 in.	
SP-01	*Riser tube Type 2* d_r = 10 3/8 in. s_r = 3 in.	h_r = 85 1/4 in. s_b = 10 in.	*PVC cap air distributor* d_a = 1.315 in.[a] s_s = 10 1/8 in.	h_s = 105 1/2 in.	Newtonian
SP-02	*Riser tube Type 2* d_r = 10 3/8 in. s_r = 3 in.	h_r = 85 1/4 in. s_b = 5 in.	*PVC cap air distributor* d_a = 1.315 in.[a] s_s = 15 1/4 in.	h_s = 105 1/2 in.	
SP-03	*Riser tube Type 2* d_r = 10 3/8 in. s_r = 3 in.	h_r = 60 1/8 in. s_b = 5 1/8 in.	*PVC cap air distributor* d_a = 1.315 in.[a] s_s = 40 1/8 in.	h_s = 105 3/8 in.	Newtonian
SP-03	*Riser tube Type 2* d_r = 10 3/8 in. s_r = 2 1/8 in.[c]	h_r = 60 1/8 in. s_b = 5 1/8 in.	*PVC cap or open air distributor* d_a = 1.315 in.[a] s_s = 30 7/8 in.	h_s = ~96 in.[b]	Non-Newtonian
SP-04	*Riser tube Type 2* d_r = 10 3/8 in. s_r = 3 in.	h_r = 36 in. s_b = 5 in.	*PVC cap air distributor* d_a = 1.315 in.[a] s_s = 64 1/2 in.	h_s = 105 1/2 in.	Newtonian
SP-05	*Riser tube Type 2* d_r = 17.4 in. s_r = 2 1/8 in.[c]	h_r = 60 in. s_b = 5 in.	*PVC cap or open air distributor* d_a = 1.315 in.[a] s_s = 31 in.	h_s = ~96 in.[b]	Non-Newtonian
SP-05p	As SP-05, but with a second air tube installed next to the existing air tube. The second air tube was connected to the PHi mixer control box to provide a periodic burst of air in the riser tube.				

Test Series	Test Configuration				Simulant
GP-01	*Geyser Pump[d]* d_r = 3 15/16 in.[b] s_r = 2 7/8 in.	h_r = 32 5/8 in. s_b = 2 7/8 in.	*Dual air lines to Geyser pump* d_a = 1 3/8 in.[c] s_s = 70 in.	h_s = 105 1/2 in.	Newtonian
GP-02	*Geyser Pump[d]* d_r = 3 15/16 in.[e] s_r = 2 7/8 in.	h_r = 56 5/8 in. s_b = 2 7/8 in.	*Dual air lines to Geyser pump* d_a = 1 3/8 in.[f] s_s = 46 in.	h_s = 105 1/2 in.	Newtonian
GP-02	*Geyser Pump[d]* d_r = 3 15/16 in.[e] s_r = 2 7/8 in.	h_r = 56 5/8 in. s_b = 2 7/8 in.	*Dual air lines to Geyser pump* d_a = 1 3/8 in.[f] s_s = 36 1/2 in.	h_s = ~96 in.[b]	Non-Newtonian
PPM	PHi mixer with forming plate and control box: single 1-in. stainless steel tube connected to 8-in. diameter parallel plates resting on the tank bottom.				Non-Newtonian

(a) The air line in riser tube Type 2 is external to the riser tube. It was 1-in. Schedule 40 PVC pipe.

(b) The slurry level was measured from using a laser distance finder to the surface at three reference points and determined by subtraction. It is estimated the level is ±1/2 in., as the level would fluctuate due to operation (slurry loss via splatter) and evaporation of the slurry. Note the uncertainty extends to the value of s_s as well.

(c) During non-Newtonian testing the PVC cap was often removed from the air tube to eliminate the possibility that the air line would plug during test operations. With the cap removed, s_r is closer to 2 1/8 in.

(d) Many Geyser pump measurements were ± 1/4 in. due to the geometry of the pump and the difficulty of getting the tape measure in a stable position.

(e) Inside diameter of the outlet of the Geyser pump riser tube, i.e., 4-in. Schedule 40 clear PVC pipe. The inlet diameter is larger (> 6 in.).

(f) The air lines are external to the Geyser pump. Both air lines have the same diameter but the connection sizes (where they interface with the pump) are slightly different.

4.0   Liquid Velocity Measurements

In this section, estimates of liquid velocity and flow rate that were collected during testing are summarized. Measurements made to benchmark the PNNL test system against available data for a specific configuration are first discussed. Additionally, the data collected for almost all of the configurations tested in the Newtonian and/or non-Newtonian simulants is presented. The data was collected as each configuration was installed but is collated in this section for convenience of presentation. Following the presentation of the data, the section concludes with a short discussion comparing the results to correlations available in the literature.

4.1   Benchmark Testing

Initial testing was conducted to benchmark (BM) the ALC system constructed by PNNL against an ALC test conducted by Cook and Waters (1955)[1] using a 10-in. ID riser tube. Benchmarking the ALC system against available measurements provides confidence that the physics of the flow in the tank is similar to other ALC studies. This has a side benefit of confirming that the results of C&W are applicable to making design judgments regarding these (and any future) tests. Baseline testing also included shakedown activities to check functionality of support equipment and refine data collection procedures.

The initial set of benchmark tests (designated BM-01, see Table 3.4) was conducted using only water (no solids), with a newly constructed (by PNNL) air distributor that replicated the "sieve plate footpiece" (reproduced from Figure VIII in C&W, see Figure 4.1). The majority of the geometric parameters used in a C&W test were matched (with some small deviations) in the PNNL test stand.   The dimensions of the PNNL and the C&W test stands are compared in Table 4.1. The two major differences in the geometry of the test stands are that C&W used a much larger tank (the dimensions are unspecified in their report, but some dimensions can be inferred from other information) and had a weir box on top of their riser tube to measure liquid flow rate.
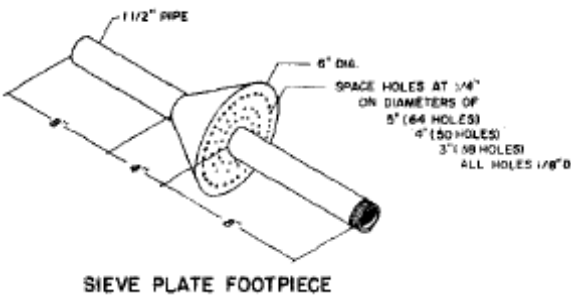
(a) Sieve-plate footpiece from C&W (1955).   (b) PNNL replica of sieve-plate footpiece.

Figure 4.1. Images of (a) the Original C&W Air Distributor and (b) the PNNL Replica Air Distributor Used in Benchmark Testing.

---

[1] Hereafter in this section, Cook and Waters (1955) is interchangeably referred to as C&W.

Table 4.1. Comparison of Dimensions in the C&W and PNNL Test Stands.

Dimension/Quantity	C&W Test	PNNL Test
Fluid	Water at 62 °F	Water at 69 °F
d_a	1.9 in. [a]	1 13/16 in.
d_r	10 in.	9 7/8 in.
d_t	Not specified	90 in.
h_r	108 in.	83 15/16 in.
h_s	258 in.	105 3/4 in.
h_t	Not specified	121.6 in.
s_b	Estimated at 102 in.	13 in.
s_r	24 in.	~0 in.
s_s	48 in.	8 1/4 in.
Length of riser tube above air distributor	84 in.	83 15/16 in.

(a) Assumes that the air line dimension, which is stated to be 1.5-in. pipe, is the nominal pipe size and that it is Schedule 40.

The key parameters that were matched in the PNNL test stand were the air tube diameter, the air distributor geometry, the riser tube diameter, and the length of the riser tube above the air distributor. The relationship between air flow rate and liquid flow rate in the riser tube was expected to be non-linear and approximately logarithmic based on the data available from C&W. Note that besides the geometric differences already mentioned, the C&W data was obtained using a weir box and differential pressure to determine the liquid flow as a function of air flow rate. In the PNNL test stand, liquid flow was determined using a propeller-style velocity instrument (see Section 3.2). The instantaneous velocity was measured and averaged over a period, typically 1 minute. Before it was recorded, the 1-minute average was monitored for a minimum of 1 additional minute to confirm the value was stable and not changing with time. The measured velocity was assumed to be the average velocity of the bulk fluid (water and air) at the riser tube outlet and was multiplied by the open cross-sectional area to obtain the flow rate of the bulk fluid, from which a liquid flow rate was determined, i.e.,

$$Q_{liquid} = \langle U \rangle \frac{\pi}{4}(d_r^2 - d_a^2) - aQ_{air,std} \tag{4.1}$$

where Q_{liquid} and $Q_{air,std}$ are the volumetric flow rates of liquid (gas-free simulant) and air at standard conditions, respectively, $\langle U \rangle$ is the velocity from the propeller instrument averaged over 1 minute, and a is an adjustment constant to correct to the actual air flow rate at the depth of the velocity measurement. The averaging was performed by the transmitter of the velocity instrument.[1] The air flow rate at the outlet of the riser tube was subtracted to obtain an estimate of the gas-free liquid flow rate. Subtracting the air flow rate is a simplification of the actual physics and should be considered an approximation. It is performed to account for the use of a propeller-based instrument to measure velocity in multiphase flow, and adds uncertainty as to the accuracy of the liquid flow estimates.

---

[1] Averaging the velocity data was appropriate because the flow was both multiphase and fully turbulent. Using the physical properties (ρ_L = density, μ_L = viscosity) of water, even a liquid velocity of 0.06 ft/s is sufficient enough to result in a Reynolds number (Re = $\rho_L U d_r / \mu_L$) of 5,000, implying that all of the measurements made in the PNNL test stand were collected at Re $\gg 10^4$, i.e., in the fully turbulent flow regime.

The volumetric air flow rate fed to the ALC devices ($Q_{air,rot}$) was measured using a rotameter (or series of rotameters) factory calibrated at standard conditions, i.e., standard cubic feet per minute or hour (scfm or scfh). For the rotameters used in these tests, standard conditions are 1 atm and 70 °F. Although the rotameter flow indication was given in standard units, the measured flow rate must be corrected for the air pressure (P_{rot}) and temperature (T_{rot}) on the downstream side of the rotameter to determine the true standard air flow rate, $Q_{air,std}$,[1]

$$Q_{air,std} = Q_{air,rot} \left(\frac{P_{rot}T_{std}}{P_{std}T_{rot}} \right)^{1/2} \tag{4.2}$$

where P_{std} and T_{std} are the pressure (1 atm) and temperature (70 °F) at standard conditions. In the absence of a pressure measurement at the flowmeter, P_{rot} can be estimated from the sum of the calculated pressure drop from the meter to the outlet of the air distributor and the hydrostatic pressure P_{ad} at the submergence of the air distributor h_{ad}. The hydrostatic pressure P_h at any height (depth) h below the simulant surface is

$$P_h = P_{atm} + \rho_{sim}gh \tag{4.3}$$

where P_{atm} is the atmospheric pressure, ρ_{sim} is the density of the simulant, and g is the gravitational acceleration. Neglecting the relatively small pipe flow pressure drop contribution,[2] as is done in this report, P_{rot} is approximately equal to P_{ad} (where $h = h_{ad}$ in Equation (4.3)). Using this approximation, $Q_{air,std}$ can be estimated from Equation (4.2).

To convert to actual volumetric air flow rate at depth h ($Q_{air,h}$), the standard flow rate given in Equation (4.2) is corrected for actual temperatures and pressures, i.e.,

$$Q_{air,h} = Q_{air,std} \frac{P_{std}T_h}{P_hT_{std}} = Q_{air,rot} \left[\frac{1}{\rho_{sim}gh+P_{atm}} \left(\frac{P_{std}P_{rot}T_{rot}}{T_{std}} \right)^{1/2} \right] \tag{4.4}$$

in which it is assumed that the temperature of air at depth h (T_h) is equal to T_{rot}. Poloski et al. (2005), for example, used this approach (right hand form of the equation) to define actual air flow rates at sparge tube nozzle depth from rotameter readings. Likewise, the actual air flow rate at the ALC air distributor is determined from Equation (4.4) by setting $h = h_{ad}$. Note that the submerged depth of the air distributor can be recast in terms of the geometric parameters shown in Figure 3.1, i.e., $h_{ad} = h_s - (s_b + s_r)$. Also note that the pressure ratio P_{std}/P_h is the factor a shown in Equation (4.1) if h is set to the depth of the velocity measurement (e.g., $h = s_s$).[1]

During the testing, P_{rot} and T_{rot} were not routinely measured, so P_{rot} was estimated by assuming that $P_{rot} = P_{ad}$ as already described. The temperature at the rotameter was measured once and found to be ~70 °F (essentially ambient). This value was used as T_{rot}, though it is unknown how much T_{rot} may have varied over the course of test operations. The $Q_{air,rot}$ values were corrected in some cases where data is being compared between configurations or to other data sets. In other cases, the air flow data shown in this report refers to flow rates measured by the rotameter manifold (written with units of cubic feet per

---

[1] This variable-area flowmeter (rotameter) correction method is shown, for example, in Dwyer technical Bulletin F-43 for Series RM flowmeters, which is available from www.dwyer-inst.com. Similarly, this method was applied in Poloski et al. (2005) to convert observed rotameter flow rates to actual air flow rates at sparger nozzle depth.

[2] The pressure drop was conservatively estimated to be 0.32 psi per 10 linear feet of 1-in. ID air line at an air flow rate of 30 cfm. The pressure drop would be lower for air flow rates < 30 cfm, and the IDs of the air line were always ≥ 1 in., thus 0.3 psi was an upper bound and small enough to be assumed negligible.

minute [cfm] or cubic feet per hour [cfh]). However, as the simulant densities and submerged depths were all known, the correction factors for the actual air flow rates at the riser outlet (units of actual cubic feet per minute) can be estimated using the assumed values of P_{rot} and T_{rot}. For the Newtonian (water) testing, ρ_{sim} = 0.998 kg/L and s_s ranges from 8.25 to 70 in. for the configurations tested, resulting in values a = 0.95 to 1.09 using Equation (4.4). For the non-Newtonian (clay slurry) testing, ρ_{sim} = 1.259 kg/L and s_s ranges between 30.875 and 36.5 in., resulting in values of a = 1.02 to 1.03 using Equation (4.4). The correction from $Q_{air,rot}$ to $Q_{air,std}$ via Equation (4.2) varies slightly with configuration but can be estimated by multiplying $Q_{air,rot}$ by a factor of 1.1.[1]

Limited measurements were also made using flow tracers (liquid-saturated sponge cubes that were ~1/4 in.) and a stop watch, where the flow rate was determined using an estimate of the riser tube volume and the transit time (t) of the tracers, i.e.,

$$Q_{liquid} = \frac{\frac{\pi}{4} h_r (d_r^2 - d_a^2)}{t} - Q_{air,avg} \qquad (4.5)$$

This equation incorporates a correction for the average volume of air in the riser tube during the transit time, which is the product of the average actual air flow rate, $Q_{air,avg}$, and t. The flow rate is averaged (integrated) over the height of the riser tube, which is necessary to account for gas expansion as it flows upward into an environment of progressively decreasing hydrostatic pressure. The average was computed by taking $Q_{air,rot}$ and correcting to $Q_{air,h}$ for $h = h_{ad}$ and $h = s_s$ using Equation (4.4), i.e., $Q_{air,avg} = (Q_{air,\,h}\,[h = h_{ad}] + Q_{air,h}[h = s_s])/2$.

The calculation shown in Equation (4.5) is an approximate method and is subject to the limitation that flow tracers could be held up in the riser tube interior as they traverse from the bottom to the top of the tube. For this reason, the measurement was repeated several times and the results were averaged. It was only possible to conduct this measurement at low air flow rates as the transit time became too small to measure accurately with a stopwatch.

The comparison of the PNNL benchmark test data with the data of C&W is shown in Figure 4.2. The liquid flow rates have similar relationships to the air flow rates, as evidenced by logarithmic fits that have very similar slopes. (A logarithmic fit is used for illustration only and is not indicative of the functional relationship between air flow and liquid flow.) The PNNL data is within 10% of the C&W data at air rates of 5 scfm and greater, with more significant differences (20% to 40%) at lower air flow rates. However, the majority of the difference is likely due to the data collection method, e.g., an average velocity determined using a propeller instrument at the riser tube outlet. The velocities that were measured by PNNL may have some inaccuracy (as discussed earlier) and the subtraction of the air flow rate per Equation (4.1) is a simple correction that does not account for the physics of two-phase flow. Even so, some difference between the data sets would be expected because the C&W geometry was not perfectly replicated in the PNNL test stand. Regardless, the PNNL data was consistent with the C&W data selected as a benchmark. This is also observed in the few PNNL tracer test results shown in Figure 4.2, which fall slightly below (within ~10% of) the C&W data. An important observation is that higher air flow rates diminish the liquid flow rate produced in the ALC. This is a consequence of the higher air flow filling the riser tube more completely and reducing the amount of liquid that can be entrained. The logarithmic fit is one mathematical way to represent that physical constraint, because it implies that air is

---

[1] Note that for all tested configurations, h_{ad} only varies between 88 and 100 in.

used more efficiently to generate liquid flow when the air flow rate is lower. Other non-linear empirical models for the liquid-air relationship that are closer to the form of Equation (2.1) are discussed later in this section.
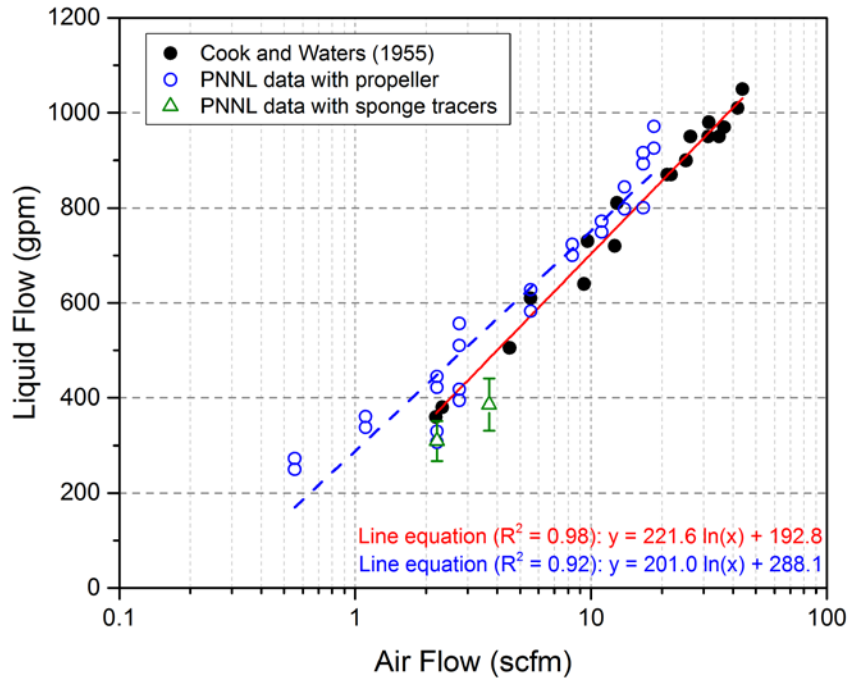
Figure 4.2. Data from Cook and Waters (1955) Compared to Data from PNNL Benchmark Tests. The C&W data (black closed circles) was collected at two submersion distances (s_s) in the original testing; it has been fit with a logarithmic function (red solid line). The PNNL data (blue open circles) was collected at a single submersion distance and fit with a logarithmic function (blue dotted line). The flow tracer measurements are shown as green open triangles (error bars indicate the standard error of the average measurement).

After performing the benchmark test, a second test was performed (BM-02) where the PNNL sieve plate air distributor was removed from the air line. This left only an open air tube pipe to disperse the air and generate the flow, leaving all the other geometric parameters the same. The purpose of the test was to determine the significance of the air distributor geometry on flow rates. The data from C&W collected with various air distributors is inconclusive on the effect of the air distributor geometry. Their data is consistent with the rest of the results in the literature, which are also inconclusive on the effect of the air distributor geometry. C&W asserted that differences were observed with changes in air distributor geometry, but the differences do not appear to be quantitatively significant (especially at lower air flow rates), as seen in the data reproduced in Figure 4.3. Note that the C&W data in Figure 4.3 was collected with a larger riser tube length ($h_r = 168$ in.) than in the benchmark data set shown in Figure 4.2. In general, the longer riser tube tends to produce higher liquid flow rates as a function of air flow (this is discussed later in conjunction with Figure 4.7).
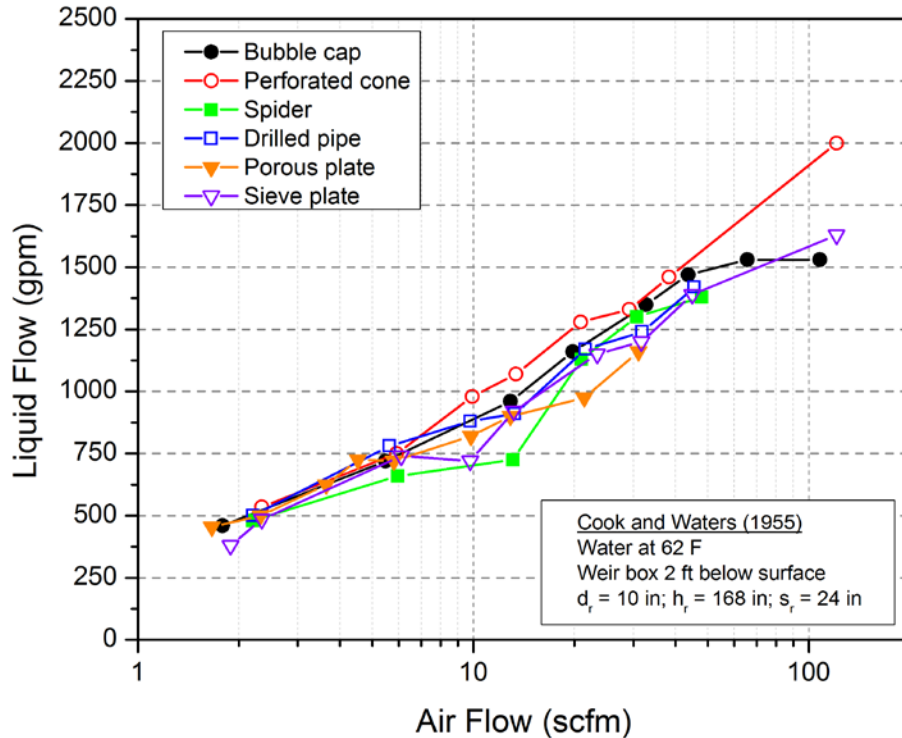
Figure 4.3. Comparison of Air Distributor (Footpiece) Types from Cook and Waters (1955). Refer to Figure VIII in C&W for the description of each air distributor listed in the legend.

The data collected during BM-02 testing in the PNNL test stand is shown in Figure 4.4. Data was only collected using the propeller instrument located at the riser tube outlet (no sponge tracers were used). By inspection of the data in Figure 4.4, it appears that air distributor geometry does not have an appreciable effect on liquid flow rates, and by extension, would not significantly affect mixing performance. If the average liquid flow rates (denoted by the solid lines) obtained at each air rate are compared directly, the BM-01 and BM-02 data are different by $\leq 20\%$. The differences are larger at lower air flow rates (≤ 3 scfm), where better air distribution would be expected to improve efficiency. The lack of significant difference between air distributor geometries is an important observation for future testing or design of an ALC system intended for use in WTP vessels, because open geometries that are less susceptible to plugging are preferable.
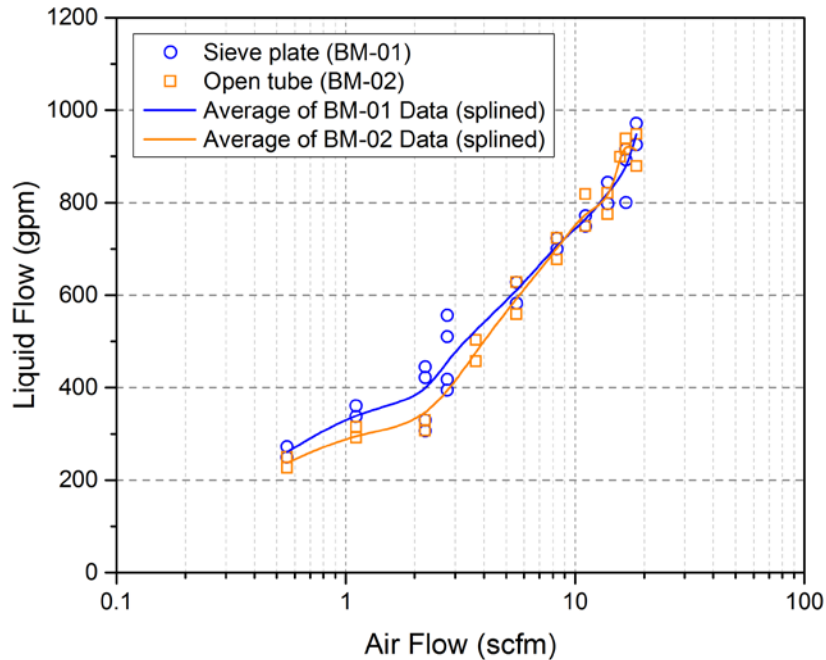
Figure 4.4. Comparison of Flow Rates Measured in Test Configuration BM-01 (sieve plate air distributor) and BM-02 (open tube air distributor). The average data is shown by the solid lines (the data has been B-splined for clear representation). All other geometric parameters were the same.

Another important observation from the BM-01 and BM-02 test data is that significant liquid flow rates can be generated using modest air flow rates.[1] For example, to achieve a liquid flow rate of ~500 gpm, only ~3 scfm of air was required in the PNNL test stand. For a working volume of a little less than 3000 gal, the entire liquid volume of the vessel was turned over in less than 6 minutes. Since tests BM-01 and BM-02 demonstrated that large liquid flow rates could be achieved, the focus on the testing shifted to the ability of an ALC system to lift and mobilize solid particles. This is discussed in Section 5.0.

4.2   Newtonian Liquid Flow Rates

The flow rate data collected from all the Newtonian test configurations is presented in Figure 4.5 and Figure 4.6. The difference between the data in the two figures is that Figure 4.5 is liquid flow rate data with an air correction (as in Equation (4.1)), whereas Figure 4.6 shows bulk fluid flow rate data with no air correction (i.e., directly measured using the propeller instrument). Note that, when corrected by the air flow rate, configurations SP-04 and GP-02 have liquid flow rates that are unchanged or even decrease with increasing air rate. Eventually, at a few higher air flow rates not shown in Figure 4.5, the calculated liquid flow rates in configuration GP-02, for example, were negative. Comparison with the uncorrected

---

[1] These air flow rates are only a small fraction of the total sparger air flows currently planned for use in the SHSV, which is projected to be ~200 scfm. Scaling the total sparger air flow rates for use in the 8-ft test vessel at MCE (a vessel that is similarly sized to the PNNL test vessel) results in estimated sparger air flow rates of between ~20 and ~50 scfm depending on the scaling approach. The liquid flow rates generated by a set of spargers have not historically been estimated, so it is difficult to compare the efficiency of air usage between an ALC and spargers.

data illustrates a limitation of the correction, that being it is unclear if the "true" liquid flow rate is increasing or decreasing at the highest air flow rates in these cases. The data sets also show that the liquid flow rates could be measured reproducibly. For instance, configurations BM-01, BM-02, SP-01, and SP-02 were all very similar geometrically, and the observed similarities in their data sets were expected. Likewise, the SP-03 configuration was measured twice (separated in time by measurements on other configurations) and the data sets are consistent with one another (see "PVC cap (SP-03)" [purple stars] and "10-in ALC (SP-03)" [grey asterisks] in Figure 4.5 and Figure 4.6).
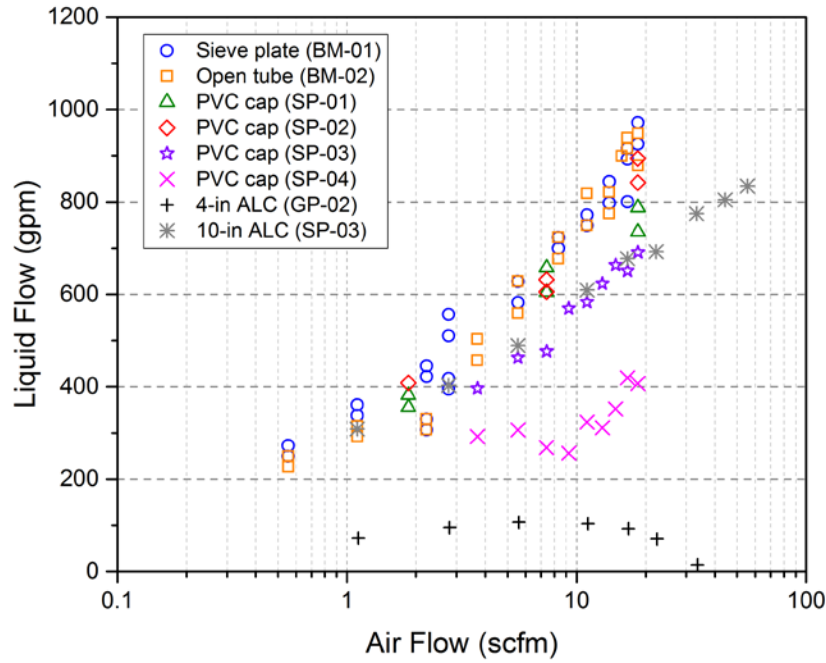
Figure 4.5. Measurement of Liquid Flow Rate versus Air Flow Rate in Various Test Configurations with an Air Flow Rate Correction (Equation (4.1)). Refer to Table 3.4 for parameters of each configuration.
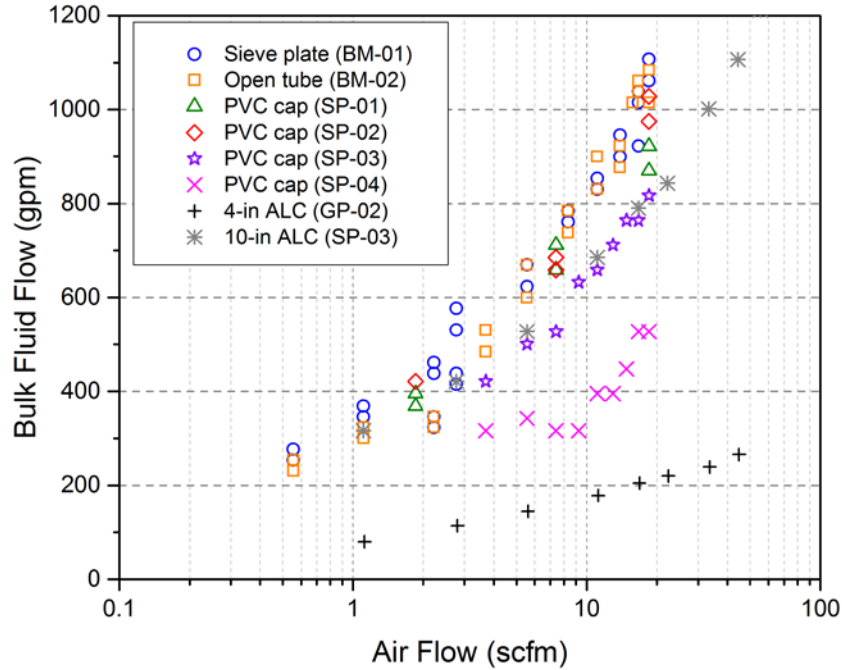
Figure 4.6. Measurement of Bulk Fluid Flow Rate versus Air Flow Rate in Various Test Configurations *Without* an Air Flow Rate Correction. Refer to Table 3.4 for parameters of each configuration.

The flow rate data also illustrates that increasing the diameter of the riser tube (with all other parameters held constant) increases the liquid flow rate, but it does not increase in proportion to the difference in the cross-sectional areas. In Figure 4.6, the nominally 10-in. ALC data (SP-03, grey asterisks and purple stars) is greater than the 4-in. ALC data (black crosses) that was collected using the Geyser pump by approximately a factor of 4 across the air rate range studied. This is only around two-thirds of the ratio of the cross-sectional areas, which are separated by a factor of approximately $10^2/4^2 \sim$ 6.25. Thus, there is a balance between efficiency (with respect to the air required) and the maximum achievable liquid flow rates when selecting a riser tube diameter.

The effect of the riser tube length was also apparent from the flow rate data collected. A shorter tube resulted in lower liquid flow rates (compare, for example, SP-02, SP-03, and SP-04 in Figure 4.5). Another way to present the data is shown in Figure 4.7, where the riser tube height is made dimensionless via the liquid surface height (which was fixed at ~105.5 in. for the Newtonian testing) and the corrected liquid flow rate is normalized by the average air flow rate in the riser, i.e., $Q_{air,avg}$. Increasing riser tube length ($h_r/h_s \to 1$) resulted in higher liquid flow rates for a fixed air rate. The effect is also much more pronounced at a lower air flow rate (black squares) than at an air flow rate an order of magnitude greater (green triangles). These data suggest that at increasingly high air flow rates, the effect of riser tube length may be negligible in determining the resultant liquid flow rate, whereas at low air flow rates the geometry makes a significant difference.
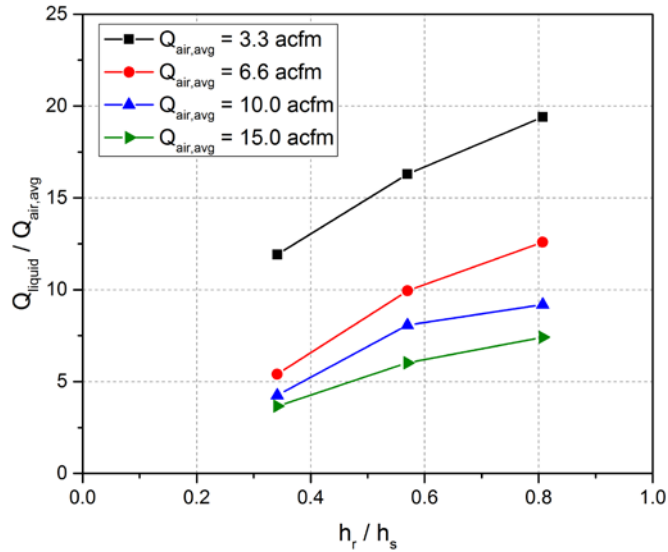
Figure 4.7. Flow Rate Ratio versus Dimensionless Riser Tube Height for Four Constant Air Flow Rates. Note that some of the data was interpolated to match the average air flow rates between each dimensionless riser tube height.

The propeller instrument was also used to measure the velocity at a location centered above the riser tube, but only 12 in. below the fluid surface. For example, Figure 4.8 shows the comparison of the uncorrected velocities measured with the propeller at the riser tube outlet and 12 in. below the surface for configurations SP-03 and SP-04. The approximate depth of the riser outlet below the fluid surface is also shown for reference. In both cases, the velocity was measured to be consistently higher 12 in. below the surface than at the riser tube. However, similar measurements taken with the 4-in. ALC riser tube (GP-02, data not shown)[1] showed the opposite trend: the velocities measured at 12 in. below the surface were consistently lower than at the riser outlet. The physical explanation for the difference is not clear. These observations imply that the measurement of the velocity, and profiling the liquid velocity in other locations in the vessel while an ALC is operating, is a complex undertaking. Attempts were made to better profile the velocities in the tank, but the propeller instrument was not suitable for the profiling measurements due to its sensitivity to orientation relative to the motion of interest and a minimum detection limit of 0.1 ft/s.

---

[1] In the GP-02 configuration, the riser outlet is located at approximately a depth of 49 in., so it is similar to the location where the SP-03 measurements were made for the data shown in Figure 4.8.
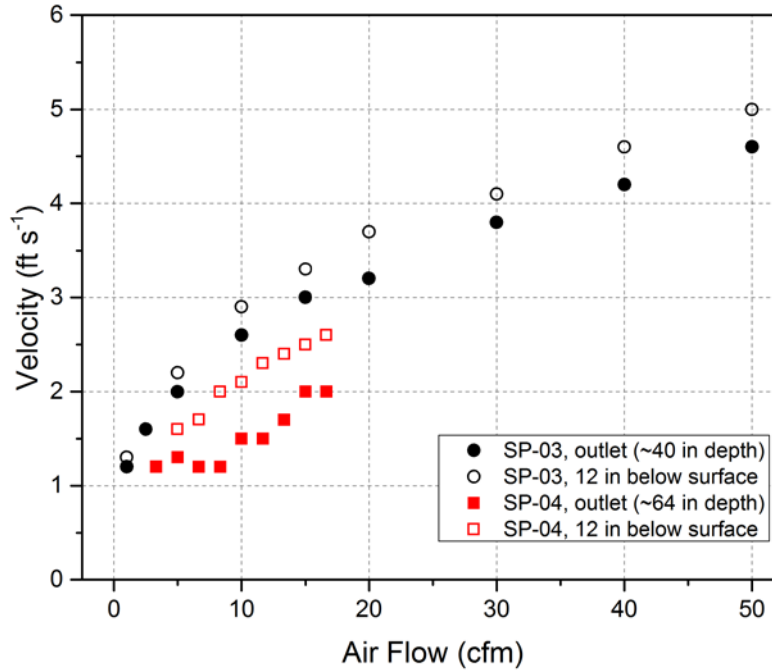
Figure 4.8. Comparison of Velocities Measured at the Riser Tube Outlet and 12 in. Below the Fluid Surface.

4.3   Non-Newtonian Liquid Flow Rates

The liquid flow rate measurements in the non-Newtonian simulant (corrected for air flow rate using Equation (4.1)) are presented in Figure 4.9, where they are compared with selected measurements from the Newtonian data set for reference. The ALC configurations studied in the non-Newtonian simulant were the nominally 10-in. diameter ALC (SP-03) and 18-in. diameter ALC (SP-05). The flow rate (or velocity) measured in the SP-03 geometry was greatly reduced in the non-Newtonian simulant compared to water. The larger diameter tube (SP-05) generated relatively higher flow rates in non-Newtonian slurry that approached, and in some cases exceeded, the flow rates achieved with a 10-in. ALC in water. Note that the SP-05 data shown in Figure 4.9 is an average of two data sets.
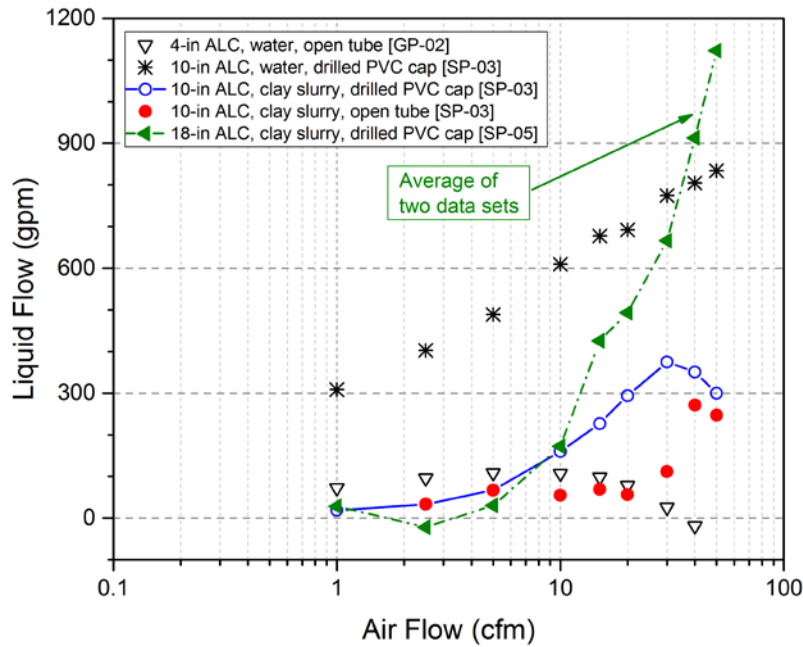
Figure 4.9. Measurement of Liquid Flow Rate versus Observed Air Flow Rate for Non-Newtonian and Newtonian Fluids in Various Test Configurations with an Air Flow Rate Correction (Equation (4.1)). Refer to Table 3.4 for parameters of each configuration.

The increased liquid flow rates achieved in SP-05 do not result from higher liquid velocities, but rather from the increased cross-sectional area of the tube. A comparison of measured velocities for different configurations and simulants is presented in Figure 4.10. The figure demonstrates that the ratio of velocities is approximately constant at air flow rates greater than ~10 cfm for the tests that are compared. This suggests that the differences in measured velocities are due to the geometry or simulant only and not a more complex interaction between the magnitude of the air flow and the ALC system. The observation that the three ratios shown all cluster around a factor of two is not necessarily meaningful and is likely coincidental. Based on air flow rates alone, for example, the velocity ratio should scale with the inverse ratio of cross-sectional areas, which is about 6.25 ($10^2/4^2$) for 4-in. (GP-02) vs. 10-in. (SP-03) ALCs and is ~3.2 ($18^2/10^2$) for 10-in. (SP-03) vs. 18-in. (SP-05) ALCs.
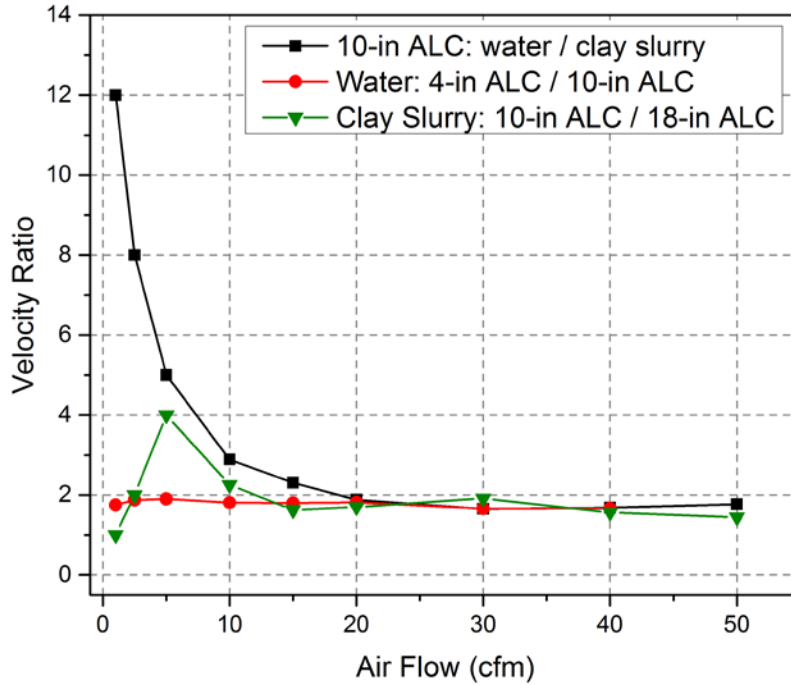
Figure 4.10. Ratio of Measured Velocities for Various Parameter Changes. The legend to the quantities present in each ratio shown.

Two important observations were made regarding the water data in Section 4.2: (1) the collection of flow rate data was repeatable, and (2) the air distribution geometry did not significantly affect the liquid flow rate. The velocity measurements were more challenging in the clay slurry and subject to larger errors, as the propeller was more erratic when used in the non-Newtonian simulant. In some cases, a propeller was observed to wear down (or out), and it was not possible to ascertain when the accuracy of the measurements collected beforehand was also adversely affected. The additional uncertainty in the non-Newtonian data does not allow the same observations to be made conclusively. The examples of repeated data sets shown in Figure 4.11, which were collected in configuration SP-05, illustrate this point.
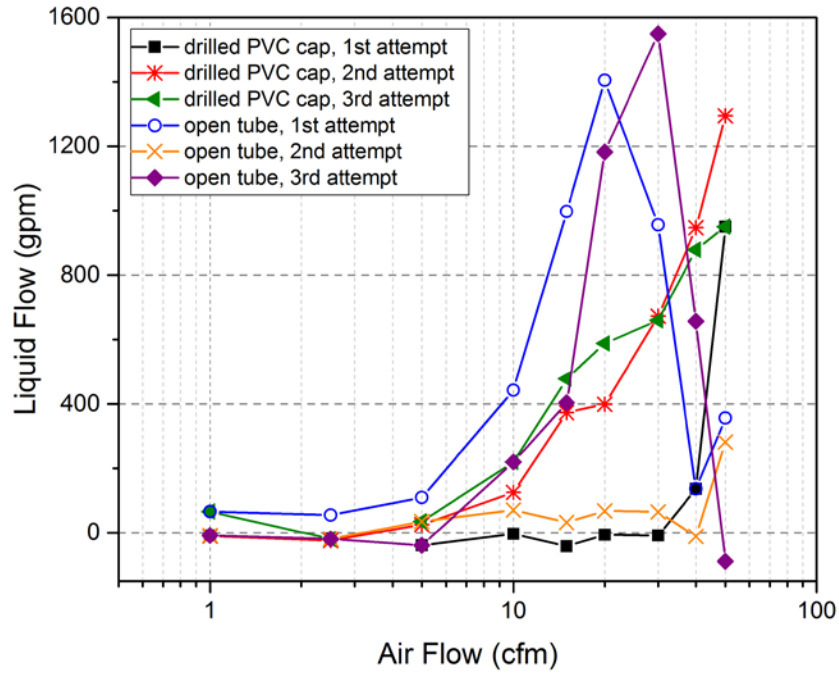
Figure 4.11. Various Measurements Collected in Configuration SP-05 Demonstrating the Erratic Nature of the Non-Newtonian Simulant Velocity (Flow Rate) Data.

4.4 Comparison with Literature Predictions

As described in Section 2.0, there are a variety of correlations available in the literature for liquid velocity in the riser tube, and most are of an empirical nature developed from the study of an ALC over a narrow range of geometries and fluids. The Newtonian velocity data that was directly measured[1] during testing was compared to some of these correlations. The expression of Chisti et al. (1988) given in Equation (2.2) was found to over predict the liquid velocity by a significant amount (see Figure 4.12 for an example), even when the riser tube length h_r is substituted for h_D as suggested by Wachi et al. (1991). Though they correlated data from 13 different airlift reactors, the expression was developed for ratios of A_r/A_d ranging from 0.5 to 9.1. The riser tubes used in this study all have $A_r/A_d \ll 0.1$, and since the square of this term appears in the denominator of Equation (2.2), the liquid velocity increases rapidly as that ratio becomes small. It is suspected that the applicability of the expression does not extend to the geometries tested in the PNNL study.

---

[1] "Directly measured" indicates that the velocity was *not* corrected for the presence of the air in the same manner that the liquid flow rate was using Equation (4.1)—the data measured by the propeller instrument at the riser tube outlet was used as is.
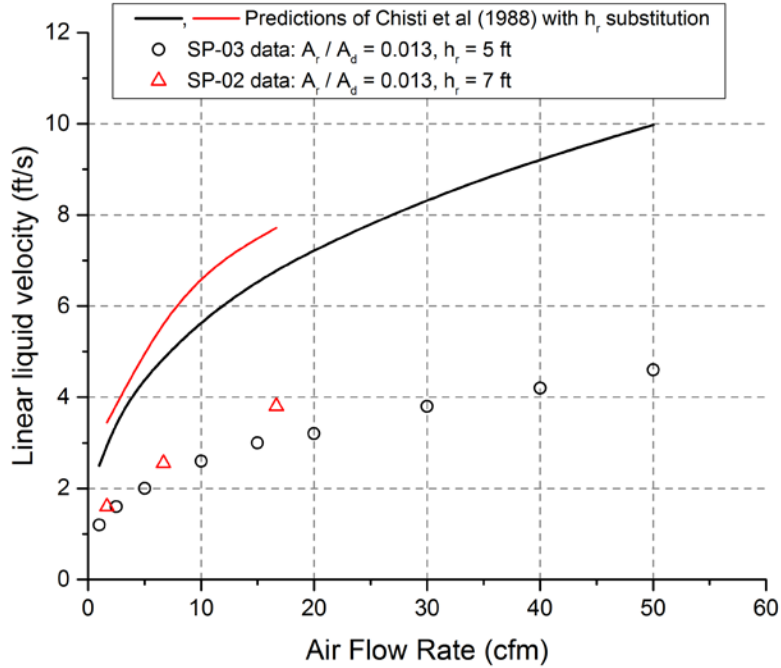
Figure 4.12. Comparison of Measured Liquid Velocities with Predictions Using the Methodology of Chisti et al. (1988). Note that the recommend substitution of Wachi et al. (1991) was used to replace h_D with h_r in Equation (2.2).

There was more success in correlating the data using the more general approach represented by Equation (2.1). The literature contains several variations on the geometric parameter(s) that are chosen for L_c (and in some cases L_c is absent entirely). Some examples include A_r/A_d or its reciprocal, fluid height or liquid dispersion height, and a ratio of diameters such as d_r/d_t, h_r, and s_b. All the correlations have in common a dependence on U^*_{gr}, which is the superficial gas velocity in the riser tube. In general, a height-averaged gas velocity is used to account for the changes in gas velocity with elevation in the tube/vessel. Chisti et al. (1989) present an expression to calculate the height-averaged U^*_{gr}, which is recast in terms of variables used in this report (see also Kuhn et al. 2013) and is limited to gas flow from the air distributor to the top of the riser tube (where velocity measurements were made):

$$U^*_{gr} = \frac{Q_{air,std}P_{atm}}{A_r(h_r - s_r)\rho_{sim}g} \ln\left(\frac{P_{atm} + \rho_{sim}gh_{ad}}{P_{atm} + \rho_{sim}gs_s}\right) \tag{4.6}$$

recall that $Q_{air,std}$ is in scfm and is equivalent to what Chisti et al. calls "the volume flow for the headspace pressure condition," i.e., atmospheric pressure, and ρ_{sim} is the density of the fluid (liquid) if it is assumed to be gas-free. One of the first correlations published for liquid velocity in the riser tube is described by Bello et al. (1984), which contains the empirical relationship

$$U_{lr} = \alpha \left(\frac{A_d}{A_r}\right)^{\beta} \left(U^*_{gr}\right)^{1/3} \tag{4.7}$$

where α and β are fitted parameters found to be 0.66 $(ft/s)^{2/3}$ and 0.78, respectively, for concentric tube ALCs and U_{lr} in ft/s. As in the case of the Chisti et al. prediction, the A_d/A_r ratio dominates Equation (4.7) and results in overestimates of liquid velocity for the data collected during PNNL testing if the

recommended values of α and β are used. However, the dependence of liquid velocity on superficial gas velocity to the 1/3 power was discovered to hold for all the water data collected in this study, using Equation (4.6) to translate air flow rate to the superficial gas velocity. Examples for two sets of water velocity data are shown in Figure 4.13, plotted against the Bello et al. correlation scaling given in Equation (4.7). The data sets are well-represented by linear fits, but the data does not collapse together owing to the assumed dependence on A_d/A_r that is likely not applicable for the PNNL configurations tested. Note also the values of the slope, which are much lower than the value Bello et al. gives of 0.66.
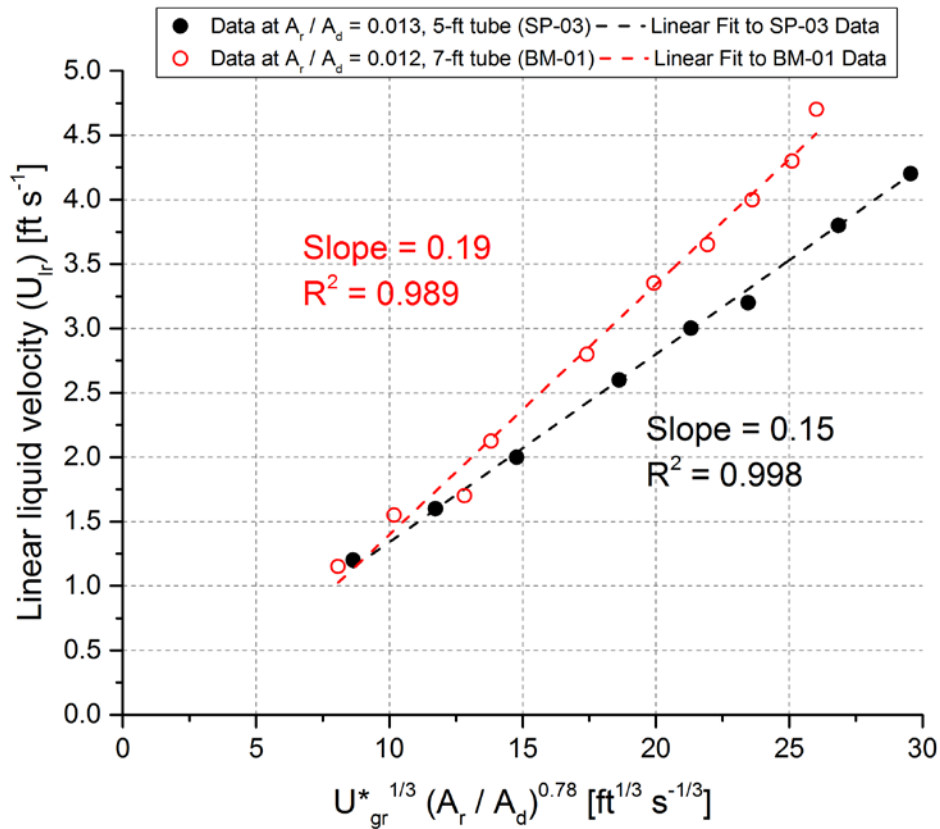
Figure 4.13. Newtonian Liquid Velocity Data Plotted Against the Correlation of Bello et al. (1984). The best fit lines are also shown on the plot with the slope and adjusted R^2.

By using combinations available in the literature and trial and error, a correlation was discovered that approximately collapsed all the water data collected in this study onto a single curve. The correlation that was identified has the form

$$U_{lr} = K \left(\frac{h_r}{h_s - s_b}\right)^{1/2} \left(U_{gr}^*\right)^{1/3} \tag{4.8}$$

where K is a fitting constant. The term in the square root is the ratio of the riser tube height to the height of the simulant from the bottom of the riser tube to the surface. The data shown in Figure 4.14 is plotted such that K represents the slope of a linear fit of the liquid velocity vs. the correlation factor (the right hand side of Equation (4.8)), with each data set identified separately. The linear fit shown in the figure incorporates all the data [$K = 1.58$ (ft/s)$^{2/3}$] with an adjusted $R^2 = 0.99$. Also shown are lines representing

4.16

$K \pm 20\%$ from the best fit; essentially all the data falls within these boundaries. Within the range of ALC geometric parameters and air flow rates tested with water, Equation (4.8) describes the expected liquid velocities in the riser tube quite well.
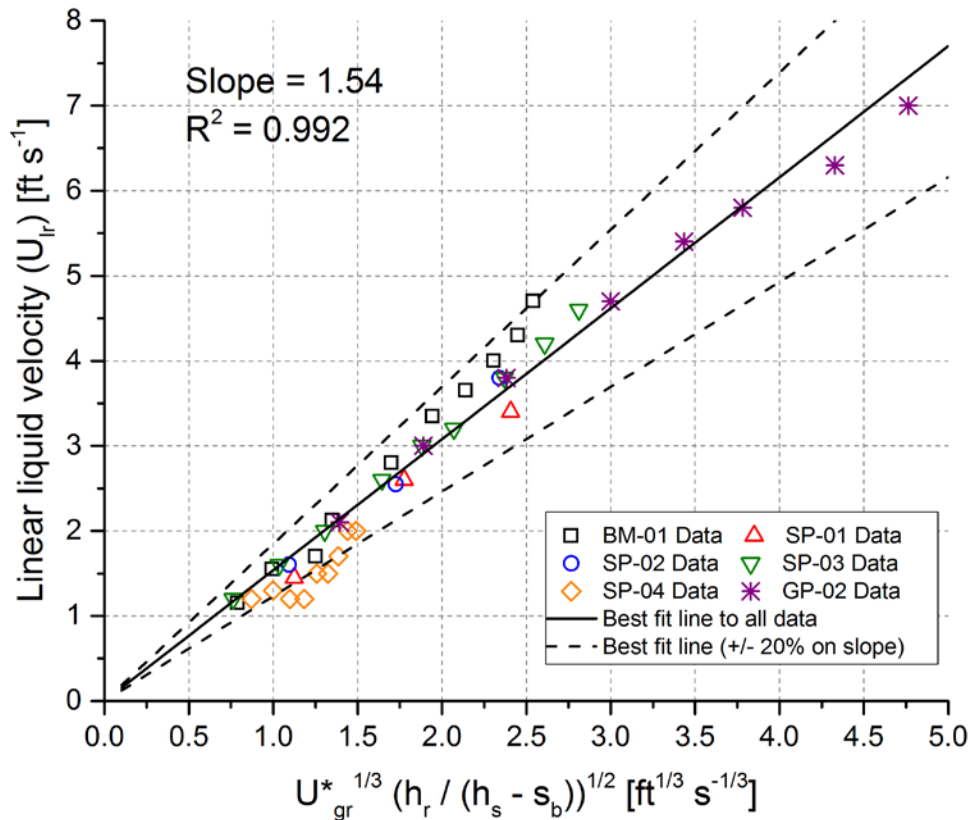
Figure 4.14. Newtonian Liquid Velocity Data Plotted Against Correlation Given by Equation (4.6). The solid line is the best fit line to all the data, and the dashed lines demonstrate how the best fit line is adjusted with changes to the K parameter of $\pm 20\%$.

   It was not expected that the non-Newtonian data would similarly collapse to a single expression (e.g., Equation (4.8)), given its additional uncertainty and the smaller number of sampled geometric parameters. Select data sets were plotted against the correlation of Equation (4.7) to assess whether the data scaled with superficial gas velocity. As shown in Figure 4.15, the relationship of U_{lr} versus $U^*_{gr}{}^{1/3}$ is not as well-represented by linear fits as the water data, though it is still reasonably approximated by the best fit line. The majority of the error in the fits is due to the data curvature at low U^*_{gr}, where the yield stress, and associated increases in effective viscosity at relatively low shear rate, may play a more important role in the physics. For a more rigorous investigation of the relationship between liquid and gas velocities in non-Newtonian fluids, a much larger data set is needed. This would include varying geometric parameters and formulating a more accurate method to measure liquid velocity. Some of the literature suggests that the apparent viscosity (Bingham consistency) and solid content (if solid particles are present – this would affect Newtonian systems as well) may also play a role. Increased viscosity has been observed to reduce U_{lr}, which was observed in PNNL testing by comparison of Newtonian and non-Newtonian simulants using the same geometric configuration and air flow rates. Quantifying the

influence of these parameters can only be accomplished by testing with multiple simulants, which was not within the scope of this study.
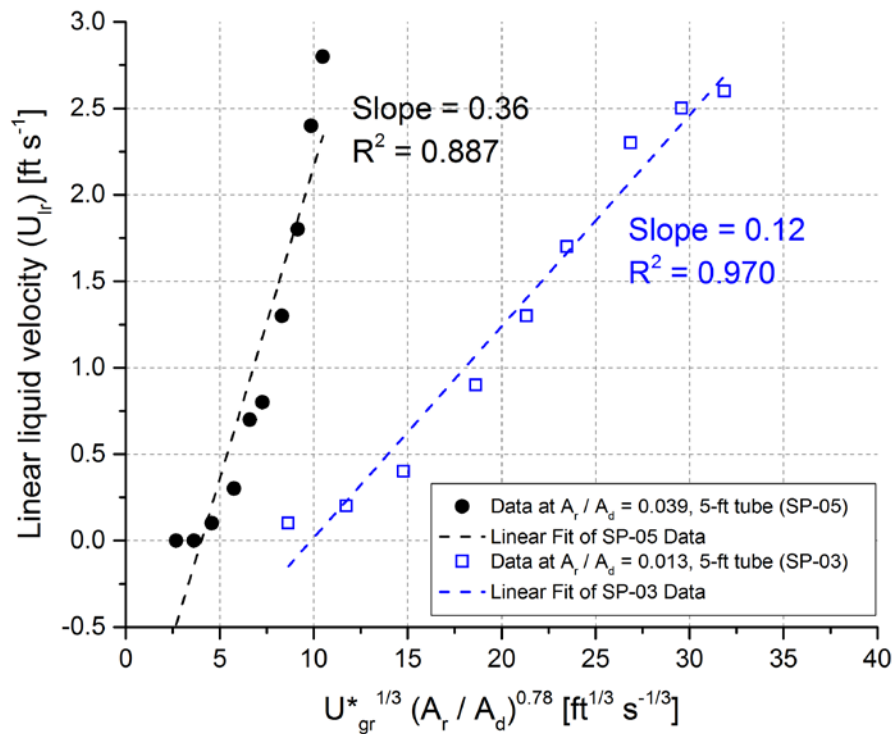
Figure 4.15. Non-Newtonian Liquid Velocity Data Plotted Against the Correlation of Bello et al. (1984). The best fit lines are also shown on the plot with the slope and adjusted R^2.

In general, the liquid velocity (and/or flow rate) data obtained by PNNL testing is consistent with data and correlations found in the bulk of the ALC literature. The Newtonian data was well-represented by a correlation that is a function of the cube root of the gas superficial velocity and the square root of a ratio of liquid heights in the tank. The non-Newtonian data was also approximately correlated with the cube root of the gas superficial velocity. In practice, the specification of an ALC system would be best classified as an optimization problem, where the ALC geometry and air flow rates would be manipulated to find a liquid velocity that achieves the required mixing performance and most efficiently uses (minimizes) the air to create the flow. The data presented in this section is not complete enough to solve that optimization problem, but provides a basis for discussing differences in mixing performance in other PNNL testing. Newtonian and non-Newtonian mixing performance testing, which is of more relevance to the WTP vessel mixing, is discussed in Sections 5.0 and 6.0.

5.0   Newtonian Testing

The Newtonian simulant performance testing of ALC (or similar) systems was conducted in two phases. The objective of the first phase was to demonstrate that particles could be transported (a) from the tank bottom to the surface, and (b) radially outward from the riser tube outlet (or towards the tank walls). Of particular interest were particles at or near the upper bound of particle sizes expected to be encountered in the WTP. In the second phase, the transport of particles was measured more quantitatively to compare the performance of the configurations shown in Table 3.4. These tests are referred to as particle capture experiments, as the method used to measure the particle distribution in the upper region of the tank was by capturing them with sieves. Both phases of the Newtonian testing are described in this section. The Newtonian testing preceded the non-Newtonian testing, so these results determined what configurations were tested in the clay slurry. The rationale for the configurations chosen for evaluation in non-Newtonian simulant is summarized at the end of this section.

5.1   Particle Transport

For completeness, the entire series of particle transport experiments that were conducted are described in chronological order. The first ALC installed was configuration SP-01. The initial attempts to definitively demonstrate particle transport were not successful. Before the implementation of the green beads, clear Potters Mil13 glass beads (diameters ranging from 45 to 90 µm) were loaded into the tank. These particles were mobilized quite readily by the ALC, but they clouded the water to such a degree that observation of their motion and/or distribution was not possible. Operation of the OBMS while these clear beads were present showed that there were significant dead zones on the tank floor (more than 50% of surface area) that were outside the influence of the four nozzles in the tank. An OBMS that consistently delivered particles to or near the ALC inlet was a critical test component, so the original nozzles were modified to improve the jet velocity and achieve more complete bottom-motion of the particles when the clear beads were removed.

In order to more clearly resolve the question of particle transport, measurements were attempted that did not require a functioning OBMS.[1] For these demonstration tests, the green beads were loaded in small batches and exposed to the ALC inlet directly. A simple diagram of the test is given in Figure 5.1. A long, 1-in. stainless steel tube was located with one end near the riser tube inlet and the other accessible outside the tank. A GoPro camera was attached to the tube to view the particle injection and behavior at the inlet; a second GoPro camera was also installed at a fixed location in the tank (not shown in the figure) to provide another angle of the loading events. The particles were loaded in small batches of 100 to 500 g through a funnel at the top of the tube and allowed to settle down to the ALC inlet. Because the particles have some inertia as they settle down the tube, this particle loading procedure is more challenging (with respect to transporting the particles vertically upward) than the situation that would occur in typical operation. Before batches of particles were loaded, the air flow rate to the ALC was set to a fixed value to observe its effect on particle transport.

---

[1] In WTP vessels, off-bottom suspension of particles is expected to occur, driven by the mixing energy provided by PJMs. Thus, the method used to bring the particles in proximity to the air lift suction was not considered important to the evaluation of the ALC technology.
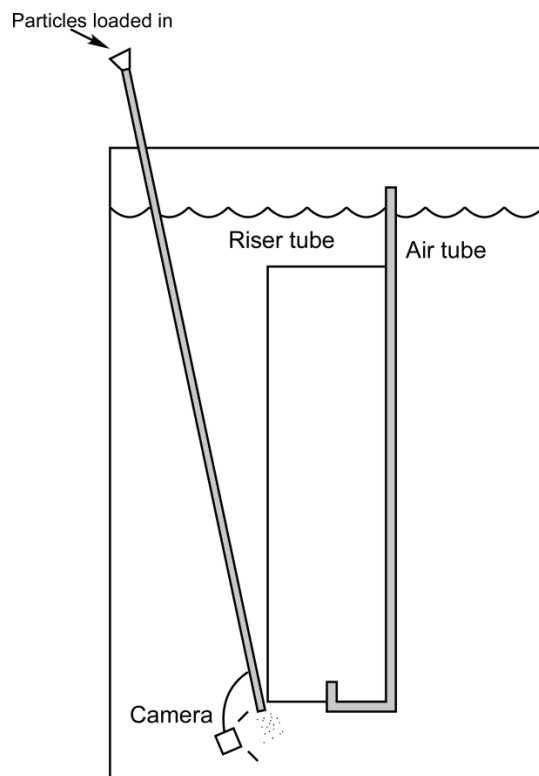
Figure 5.1. Diagram Illustrating Localized Particle Introduction Approach.

The ALC was found to successfully lift all the green beads at air flow rates as low as 300 cfh (5 cfm). At air flow rates < 300 cfh (5 cfm), green beads were lifted, but not 100% of them. The lowest air flow rate tested was 150 cfh (2.5 cfm). In addition to the video evidence, green beads were collected using simple containers or nets near the surface,[1] including near the walls of the tank (not measured quantitatively). Thus, the particles were being transported from the bottom of the tank to the surface, even out to the tank walls. Following these tests, there was approximately 1 kg of green beads in the tank from all the batches loaded into the system.

The second iteration of the OBMS with modified nozzles was tested using the green beads that were present. Though performance was improved, the nozzles still left significant dead zones on the tank floor (~1/3 of the floor surface area) where particles were not mobilized. Since particles would eventually find their way into these dead zones, assessment of the mixing performance would be dependent on time and sensitive to the initial condition in the tank. Thus, the OBMS was modified for a third time in order to have a system that repeatedly swept particles near the ALC inlet with minimum dead zones.

In the interim, the green beads were moved to the side and the loading procedure shown in Figure 5.1 was used to introduce batches of pea gravel. The pea gravel was loaded in small batches, again changing the air flow rate before each batch was added. All the gravel was lifted when the air flow rate was ≥ 400 cfh (6.7 cfm), with ~80% of the gravel lifted at 300 cfh (5 cfm) and approximately 50% at 200 cfh (3.3 cfm, the lowest flow rate tested). The gravel was also captured at the surface, though only occasionally was a gravel particle collected near the tank wall. The majority of the pea gravel was observed to be within 2 to 3 ft (radially in all directions) from the ALC centerline in the 3.75-ft radius tank. The ability

---

[1] "Near the surface" was loosely defined as the top ~12 in. of the fluid present in the tank.

of the ALC to lift both the green beads and the pea gravel confirmed that the technology can convey the expected range of particle sizes in WTP vessels.

Despite the relative ineffectiveness of the first two OBMSs, it was consistently observed that the collision of the jets from the nozzles 180° apart from one another had enough energy to drive the flow up the riser tube. This was observed in three ways: (1) when the OBMS was in use but the ALC was not in operation (no air flow), water motion manifested as small ripples on the surface; (2) the flow was sufficient to cause the propeller velocity instrument to rotate; and (3) both the clear glass beads and the green beads were visually observed to exit out of the top of the riser tube. These observations are relevant to the implementation of an ALC system with PJMs, as it suggests that PJM jets colliding near the ALC inlet may drive significant upwelling flow even without the ALC in operation. Testing an integrated system containing both an ALC and PJM would help refine the placement of an ALC to take maximum advantage of this effect. Other design choices could enhance this effect, such as a properly configured diverter, for example.

The third and final version of the OBMS was implemented and tested just prior to conducting the particle capture tests described in the next section. Instead of a single nozzle at each of the four locations along the tank periphery, a set of two inverted sprinkler heads was used at each location (refer to Figure 5.2 for an image of their installation and an image of the sprinkler head). The advantage of the sprinkler heads was that they rotated 360° and thus could move particles anywhere in the tank, even particles located between the head and the tank wall. The sprinkler-head OBMS was found to reliably move (or more accurately, sweep) particles to the center of the tank, with the AOD typically operated at 40 to 45 psi. Note that the particles were not truly suspended in the fluid but were moved into the vicinity of the airlift suction constantly during ALC operation, instead of settling into dead zones. Figure 5.2(a) provides an example of what the particle distribution looked like when the OBMS was used without the ALC in operation.
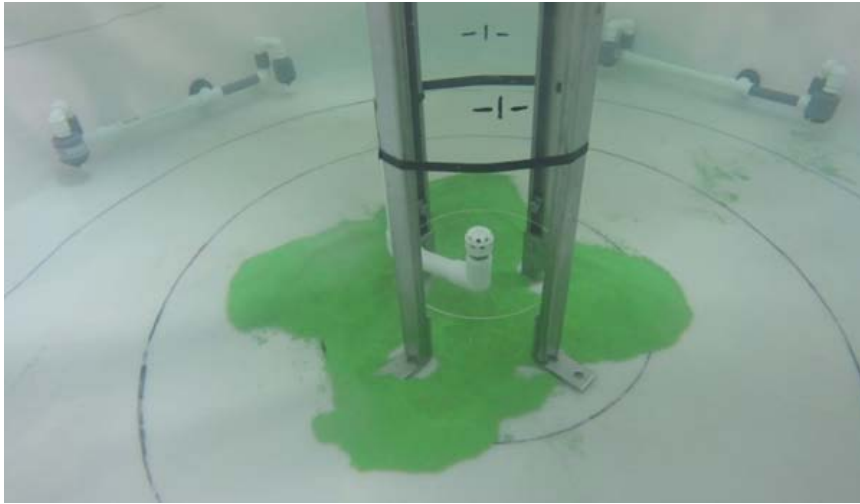
(a) In-tank image showing sprinkler installations near the wall to the left and right of the riser tube, with two sprinkler heads on each side. The majority of the green beads have been swept to the center of the tank under the riser.

(b) Close-up of 1/2-in. gear driven sprinkler head. They can be observed in the image at left pointing upside-down.

Figure 5.2. Images of Final OBMS Used in Newtonian Testing and Resulting Typical Particle Distribution.

Prior work can also be used to estimate how other particles of different densities and sizes might be lifted in an ALC system. The estimate can be built following the approach outlined in Meacham et al. (2012). Using a typical value of the measured liquid velocity (say at 10-cfm air, where $U_{lr} = 2.6$ ft/s in the 10-in. SP-03 configuration), the methodology in Section 7.2.1.2 of Meacham et al. (2012) can be used to solve for combinations of particle diameter and density that would have a net upward velocity of 0.1 ft/s, for example, and be lifted vertically in the tube.[1] The methodology is based on calculating the relative velocity of the fluid surrounding a solid particle from a particle frame of reference, U_r, defined as

$$U_r = \sqrt{\frac{4dg}{3C_D}\left(\frac{\rho_S}{\rho_L} - 1\right)} \tag{5.1}$$

where d is the spherical particle diameter, ρ_s is the density of the solid particle, $\rho_L = \rho_{sim,}$ and C_D is the dimensionless drag coefficient. C_D is a function of Re_r, which in turn is a function of U_r. The particle Reynolds number based on the surrounding fluid is

$$Re_r = \frac{\rho_L d U_r}{\mu} \tag{5.2}$$

where μ is the fluid viscosity. As noted above, the net particle velocity, $V = U_{lr} - U_r$, was designated to be 0.1 ft/s. The value of U_r that results in the chosen value of V is a function of particle diameter and density. For each chosen particle size, the value of C_D is iterated upon by changing the particle density

---

[1] This is an arbitrary and relatively conservative choice compared to the flow rate of the liquid in the tube, e.g., 2.6 ft/s. A particle with a net velocity of 0.0 ft/s would still be carried along with the upward flow and would be most conservative.

until the value of Re_r gives the same value of C_D (a guessed parameter) that is being used as an input to the U_r calculation (refer to Meacham et al. 2012 for additional information on this process). The combinations of diameters (abscissa) and densities (ordinate) that solve this system of equations generates a stability curve, where particles having density below the curve would be lifted in the riser tube and more-dense particles would not.

A similar curve can be built using a different criterion: the terminal settling velocity of a single particle. The terminal settling velocity of a particle v_T can be calculated using an expression given in Camenen (2007) with the Dallavalle (1948) coefficients for spherical particles (also shown in Camenen), which becomes

$$v_T = \frac{\mu}{\rho_L d}\left(\sqrt{15 + \sqrt{\frac{10Ar}{3}}} - \sqrt{15}\right)^2 \tag{5.3}$$

where Ar is the Archimedes number, defined as

$$Ar = \frac{\left(\frac{\rho_S}{\rho_L}-1\right)gd^3}{\left(\frac{\mu}{\rho_L}\right)^2}. \tag{5.4}$$

Equations (5.3) and (5.4) were used to solve for a set of particle diameters and densities by setting the settling velocity to 1/5 of the riser tube velocity (~0.52 ft/s).[1] With a fixed value of v_T, Equation (5.3) can be solved for one particle property by fixing the other. The variable U_r in the Meacham et al. (2012) analysis approach, e.g., 2.5 ft/s for $V = 0.1$ ft/s, can be considered an effective settling velocity and is most directly comparable to v_T.

The stability curves for both of these approaches are shown in Figure 5.3, along with the two particle types tested in the PNNL study for reference. The curve generated using the method in Meacham et al. (denoted "V of 0.1 ft/s") demonstrates that the ALC would be expected to lift very large and heavy particles, ranging up to particle sizes and densities not expected to be processed in the WTP. The terminal velocity curve (denoted "$v_T = 0.52$ ft/s") is more conservative; the pea gravel that was transported in the testing falls above the line, which suggests that a factor of five times the terminal velocity is probably overly conservative. Both curves indicate that, at minimum, the ALC should readily lift particles with diameters ≤ 2000 μm (2 mm) and densities ≤ 3 kg/L.

---

[1] Requiring that the fluid velocity be five times the settling velocity of solid particles was suggested to the authors by DOE-ORP staf. It is a conservative heuristic used to assess vertical pipe runs in the WTP.
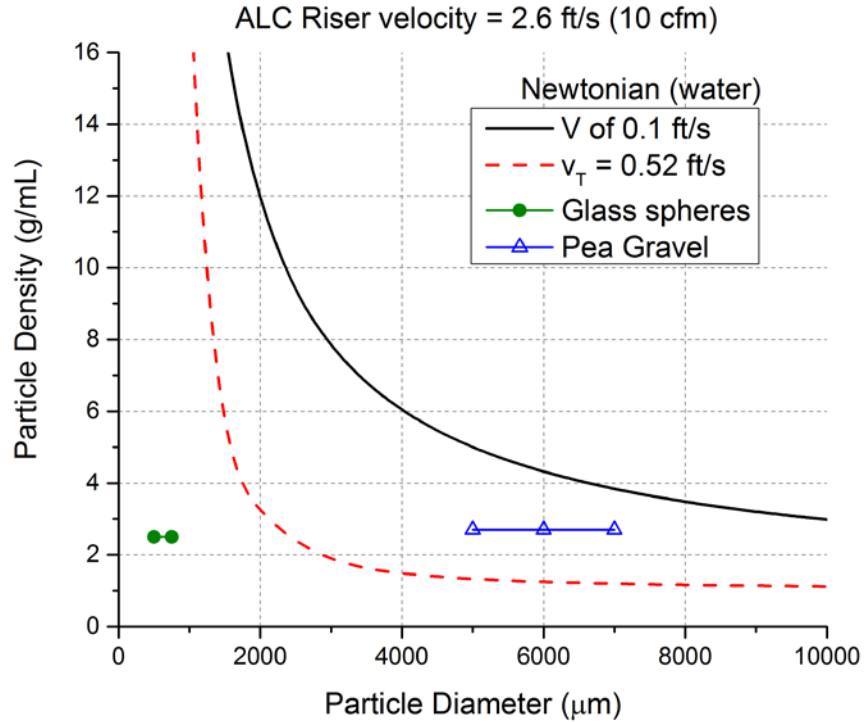
Figure 5.3. Stability Curves Developed for ALC Riser Tube Velocity of 2.6 ft/s (10 cfm). The solid black line was estimated using the approach in Meacham et al. (2012), and the dotted red line is calculated using the settling velocity as given by Camenen (2007). The green beads (glass spheres) and pea gravel are shown on the figure for reference.

5.2   Particle Capture Tests

After both the green beads and pea gravel were confirmed to be lifted in the ALC, the Newtonian testing moved into a second phase where the focus was on system performance as a function of changing geometric parameters and air flow rate. The testing was not intended to be an optimization of the system, but to collect enough data to facilitate downselection of ALC features and operating conditions for further study in a non-Newtonian simulant. At various points in the installation of other ALC and GHP configurations, it was confirmed that changes in the configuration did not restrict the device's ability to lift the particles prior to conducting the particle capture test. Particles were observed to be lifted by every configuration listed in Table 3.4 that was used in Newtonian fluid.

The tests described in the previous section demonstrated that the particles were transported up the riser tube but did not quantify how they were distributed in the tank once they exited the riser. The most desirable outcome for a supplemental mixing technology in a WTP vessel is for the upwelling flow created by the mixing apparatus to distribute solids into the upper region (near-surface) of the fluid, preferentially dispersing them homogeneously in the radial direction. In order to study the particle distribution as a function of various parameters, a set of particle capture tests was devised. Initial qualitative to semi-quantitative studies were followed by more quantitative experiments, which are discussed toward the end of this section.

The particles were captured using a set of 100-mesh, 8-in. OD sieves placed in a fixed location using a holder constructed by PNNL for that purpose. The sieve holder design drawing and an as-built picture are shown in Figure 5.4.
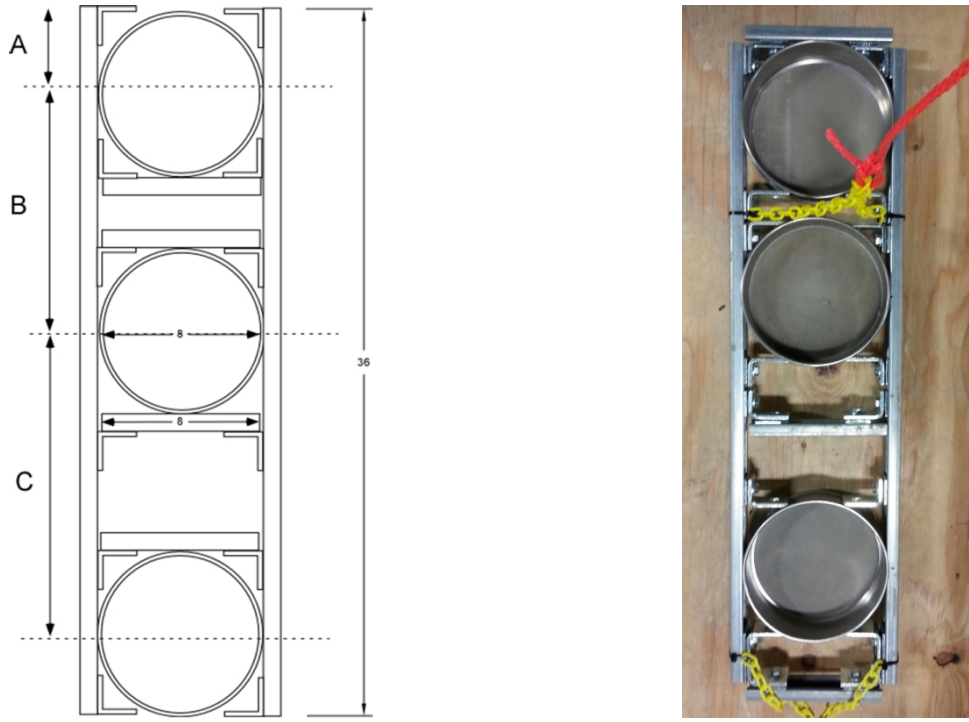
(a) Design drawing of sieve holder. Dimensions A, B, and C are for reference only – see Table 5.1 for as-built dimensions.

(b) Image of as-built sieve holder in Unistrut frame. The chains shown in the image were used to affix the holder during testing.

Figure 5.4. Representations of the Sieve Holder: (a) design drawing and (b) an as-built image.

The three sieves installed in the holder were used to represent three equal cross-sectional areas of the tank (see Figure 5.5) and typically installed approximately 12 in. below the liquid surface.[1] The relationship to satisfy for each sieve to be representative of the same area fraction in the tank is

$$\frac{A_{s1}}{A_{z1}} = \frac{A_{s2}}{A_{z2}} = \frac{A_{s3}}{A_{z3}} \tag{5.5}$$

where A is a cross-sectional area, with subscripts s and z referring to a sieve and a zone (annular region) in the tank, respectively (refer to Figure 5.5). Using the area ratio equality above and the constraint that

$$A_{z1} + A_{z2} + A_{z3} = A_t - A_r, \tag{5.6}$$

where the subscript t refers to the tank, the sieve holder dimensions were specified using their known sizes (fixed at 8-in. diameter). Equations (5.5) and (5.6) were used to determine sieve placements for a

---

[1] Measurements using sieves at various depths confirmed the expectation that transporting the particles to a near-surface region was the limiting case with respect to the number of particles collected. Note that the sieves were located above the top of the riser tube in all the configurations that were tested (SP-02, SP-03, SP-04, GP-01 and GP-02), as shown by the s_s values in Table 3.4.

nominally 10-in. riser tube and remained unchanged when later testing was performed with a smaller riser tube (GP-01 and GP-02). Relocating the sieves would have shifted the target sieve locations by < 1 in.
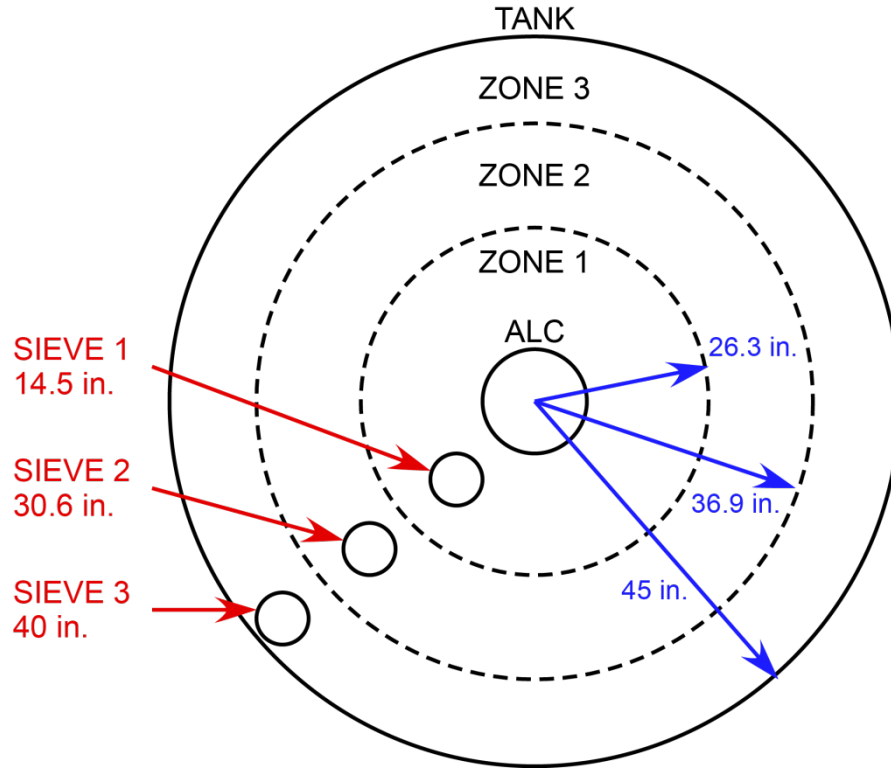
Figure 5.5. Conceptual Schematic of Zones and Sieve Placement for Particle Capture Testing. The placement of the sieves in the diagram is approximately where they were located during testing but the drawing is not to scale. Sieve locations are to the sieve center.

    The radial locations of the sieves, both target (near the radial centers of the zones) and actual, are compared in Table 5.1. Note that the actual positions were shifted towards the center of the tank by ~1 in.; this was solely due to the need for a crossbar on the end of the sieve apparatus (refer to the top of the image in Figure 5.4b). The small deviation from the target dimensions was not expected to introduce any significant error. The use of a fixed-location sieve holder in combination with collecting particles over a fixed time period, i.e., an integrated measurement, also reduced the uncertainty that would be introduced from sampling the tank contents at discrete points in time.

Table 5.1. Target vs. Actual Dimensions for the Sieve Holder. Dimensions are referenced to the center of each sieve, which is 8 in. in diameter.

Sieve	Target dimensions (in.)		Actual dimensions (in.)		Difference from target (in.)
	From tank center	*From tank wall*	*From tank center*	*From tank wall*	
Zone 1 Sieve	15.8	29.2	14.5	30.5	1.3
Zone 2 Sieve	31.6	13.4	30.6	14.4	1.0
Zone 3 Sieve	40.9	4.1	40.0	5.0	0.9

In the experiments using the sieve holder shown in Figure 5.4, it was installed 12 in. below the liquid surface at the approximate angular location shown in Figure 5.5 (roughly southwest if the text "Tank" is taken as north).[1] The green beads, which were present at ~0.05 wt% in the water (a total mass of 12 lb) were moved to the middle of the vessel floor using the OBMS to achieve the initial condition (or a very similar distribution to that) shown in Figure 5.2a. Once this initial condition was visually confirmed, ALC operation commenced at the selected air flow rate for the experiment. The ALC, with the OBMS also in operation, was run for 10 minutes. At the completion of this period, the ALC was turned off and the sieve holder was carefully removed from the tank to avoid disturbing the captured particles. Particle data was collected from the sieves and then the particle inventory was returned to the tank, after which the process could be repeated for a different air flow rate.

The initial evaluations were performed by taking photographs of the sieves and making qualitative comparisons. The uncertainty in this approach was that the depth of the particle layer (if any) in each sieve was not discernable from the photographs, but some simple judgments were made by comparison of the images with one another. Two examples of the comparisons are given in Table 5.2 and Table 5.3.

Comparison of the images from different riser tube lengths in Table 5.2 reveals two important conclusions. The first is that the length of the riser tube does not significantly affect the amount of particles captured. By zone, sieves captured similar amounts of particles as the riser length was shortened from 7 ft to 3 ft. This result seemed reasonable, since the driving force for the circulation flow generated by the ALC is localized near the bottom of the riser tube where the air inlet is located. Thus, the length of the tube does not drastically change the ability of the ALC to lift particles and send them vertically upward provided a certain minimum air flow rate is used. The length of the tube will primarily dictate how the flow field will manifest above the riser tube: a shorter tube permits the bubbly flow to expand further radially as it moves upward in comparison to a longer tube, which channels the flow in a narrower region upward. The expansion of the bubbly flowing region was observed visually on the surface as well as *in situ* using GoPro cameras. The second conclusion is that the near-wall sieve (Zone 3) is the most challenging location to mobilize the particles to, although some particles were able to reach that location in each of the three configurations.

Given the error inherent in visual assessments, it is difficult to assess whether any of the configurations shown in Table 5.2 performed better than the others. However, it appeared that the shorter tubes (SP-03, SP-04) captured slightly more particles than the 7-ft riser tube (SP-02), particularly in Zones 1 and 2. This suggests that a shorter ALC tube could be used in a WTP vessel, making it easier to operate at lower fill levels and reducing the risk of the ALC causing surface splatter due to more localized air flow that leads to undesirable aerosol generation or other complications. The PNNL test stand was not capable of collecting data to predict if the use of a short ALC tube[2] would also be appropriate for a larger scale vessel, i.e., the SHSV, where the fluid level (and thus the submergence distance s_s) would be much larger.

_____
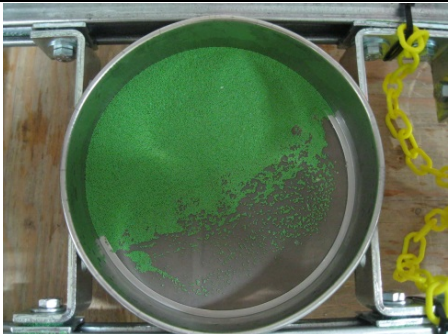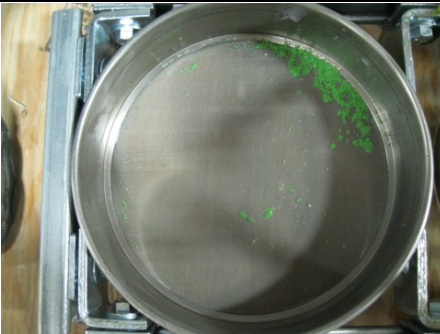
[1] An experiment was conducted to test the sieve holder in a different angular location that was ~90° in the counter-clockwise direction from the standard location (or roughly southeast if the text "Tank" is north in Figure 5.5). No significant difference in the amount of particles captured was observed.
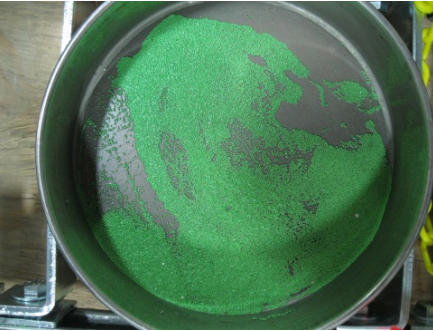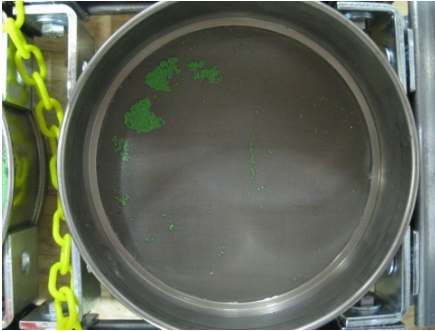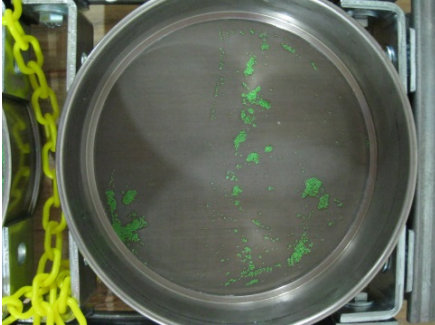
[2] In this case, short refers to a riser tube where the top of the tube is more than 16 in. below the working fluid level of the PNNL vessel (which was not the case for the 7-ft riser tube used in some of the testing reported here). For example, both SP-03 and SP-04 would be considered short tubes by this criterion. In the SHSV, if the SP-03 or SP-04 configuration was used the value of s_s would become ~127 in. or ~151 in., respectively, if the fluid was at the nominal operating level.

The images in Table 5.3 demonstrate how performance is not greatly affected by air flow rate, as the amount of particles captured in configuration SP-03 (5-ft riser tube) at 200, 500 and 800 cfh (3.3, 8.3, 13.3 cfm) are visually similar in all three zones. There is expected to be a lower air flow rate (likely ≤ 150 cfh [2.5 cfm], based on earlier experiments) where particle transport would be reduced appreciably. All three air flow rates in Table 5.3 are above this threshold. The similarity with different air flow rates is consistent with the observation that there is a minimum air flow rate required to lift and transport the particles. Above this minimum, higher air flow rates were observed to only slightly increase the amount of particles captured.

Table 5.2. Comparison of Particle Capture in Sieves as a Function of Riser Tube Length. The riser tube diameter was 10 in. and the air flow rate was 500 cfh (8.3 cfm).

Test [h_r]	Sieve 1 (Zone 1)	Sieve 2 (Zone 2)	Sieve 3 (Zone 3)
SP-02 [7 ft]			
SP-03 [5 ft]			
SP-04 [3 ft]			

Table 5.3. Comparison of Particle Capture in Sieves as a Function of Air Flow Rate. The test configuration was SP-03: 10-in. diameter riser tube, 5-ft tube length, 5-in. off-bottom distance.

Air Flow Rate	Sieve 1 (Zone 1)	Sieve 2 (Zone 2)	Sieve 3 (Zone 3)
200 cfh (3.3 cfm)			
500 cfh (8.3 cfm)			
800 cfh (13.3 cfm)			

5.12

The results shown in Table 5.2 and Table 5.3 are subject to the important caveat that the performance was not assessed across the entire range of liquid levels expected in WTP vessels. With the operating level typically fixed at 105.5 in. (8.8 ft), the testing was conducted at approximately half-scale, compared to a nominal operating level in the WTP SHSV of 16 ft. Were the sieves to be stationed 12 in. below a 16-ft liquid level with riser tubes of the same lengths and off-bottom separation distances, the differences in particle capture may be more significant. However, the results presented illustrate that over the length scales tested in the current study, the effect of riser geometry and air flow rate is relatively minor once a minimum air flow rate threshold is exceeded.

Other assessments that were conducted during the initial particle capture experiments but are not discussed in great detail in this report include:

- Confirming the green beads reach the near-wall region at greater depths in the fluid when the ALC was in operation. This was performed by moving the sieve holder to lower depths (as low as ~70 in. below the surface in the same angular location) and observing that an appreciable number of particles was still collected over the same 10 minute period. In fact, the number of green beads collected in the Zone 3 sieve was noticeably higher at lower depths. This suggests that the particles are more evenly distributed in the radial direction by the ALC at lower depths.

- Mapping out the radial distribution of pea gravel when it was lifted in the ALC. The pea gravel was lifted out to as far as ~3 ft from the tank center, but very few particles were transported out to the 12- to 18-in. region nearest the wall of the tank.

- Installing the GHP and observing GHP performance when only the pulse air flow rate was operating. The pulse-only mode was found to be inferior for particle lifting and capture, and for data reported here, the GHP was run either as an airlift only or hybrid.

- Identifying an operational range suitable for the hybrid mode of the GHP, i.e., a ratio of pulse air flow rate to continuous air flow rate of 2:1. This was based on recommendations from the manufacturer and confirmed by a couple of trials with the GHP. Once the 2:1 ratio was established, it was used in all other GHP testing.

- Comparing the suction radius of an ALC to the GHP (assessed by running only the ALC or GHP with particles covering the tank floor). One of the features quoted by the manufacturer of the GHP was a 2 to 3 ft suction radius, i.e., a region around the riser tube inlet in which the GHP could motivate and lift particles without the assistance of another mixing device. ALCs tested in this study had a small suction radius that was only observed to extend 2 to 4 in. radially from the riser tube outer wall. The GHP was found to have an approximately 2-ft radial region of influence, and over time, even particles > 2 ft away slowly moved toward the tank center.

In later performance testing, more quantitative particle capture methods were developed. The particles in the sieves were transferred into buckets by rinsing the sieves with water. The wetted particles were then carefully loaded into graduated cylinders and shaken to get the particles to pack together, and a volume measurement was taken. Once this measurement was recorded and photographed (refer back to Figure 3.6 for an example), the particles were returned to the tank. This method was used to compare the particle transport performance of two ALC configurations (SP-03, GP-02) and the GHP (GP-01). Note that GP-02 testing was conducted using the GHP with no pulsed air flow, in which case it becomes a "traditional" ALC with a nominal riser diameter of 4 in.

The results of the evaluation are shown separately for the three sieve zones in Figure 5.6 (Zone 1), Figure 5.7 (Zone 2), and Figure 5.8 (Zone 3), each as a function of air flow rate. From inspection of these data, the GHP was the best performer, followed by the 10-in. ALC (SP-03). Since the sieve technique was an integrated measurement, the larger suction radius of the Geyser pump allowed it to lift a larger amount of particles over time. In other words, the GHP was less dependent on the presentation of particles to the inlet of the riser tube by the OBMS. The measurements that were made cannot differentiate between increased suction and improved particle transport once it leaves the riser tube, so it is not clear if the larger suction radius of the GHP was the sole explanation for its superior performance. The data also demonstrates that a larger diameter ALC is a better choice for lifting and transporting particles radially (e.g., comparing SP-03 and GP-02).
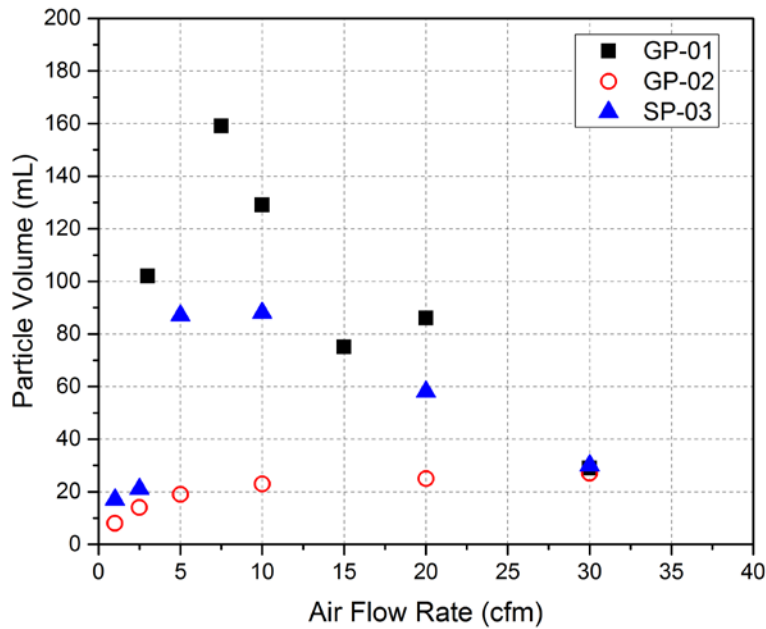
Figure 5.6. Comparison of Particles Captured by Various ALC Configurations in the Zone 1 Sieve (location closest to the tank center). Note the air flow rate for GP-01 (run in pulsed mode) is the sum of the two air flow rates used in the test. GP-02 (4-in. diameter) and SP-03 (10-in. diameter) were both traditional ALC tests and only had a single air flow rate.
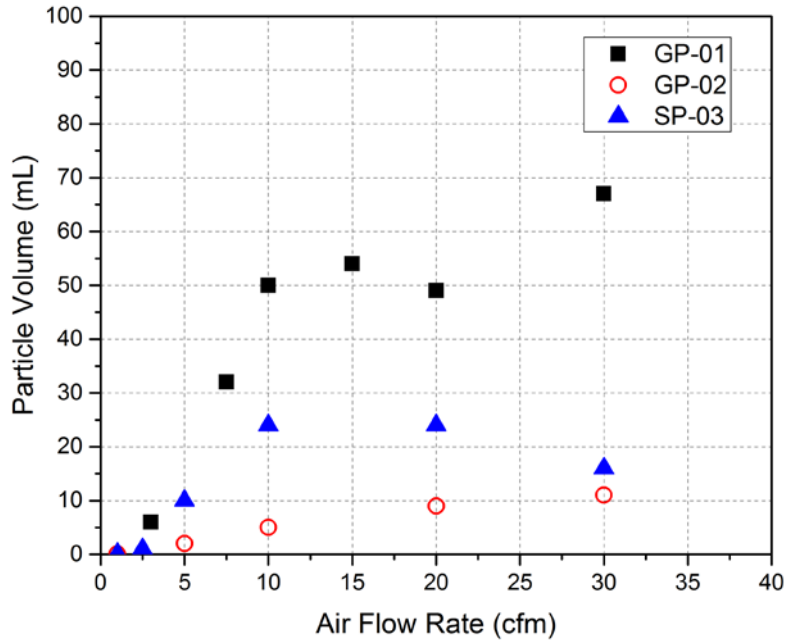
Figure 5.7. Comparison of Particles Captured by Various ALC Configurations in the Zone 2 Sieve (middle location). Note the air flow rate for GP-01 (run in pulsed mode) is the sum of the two air flow rates used in the test. GP-02 (4-in. diameter) and SP-03 (10-in. diameter) were both traditional ALC tests and only had a single air flow rate.
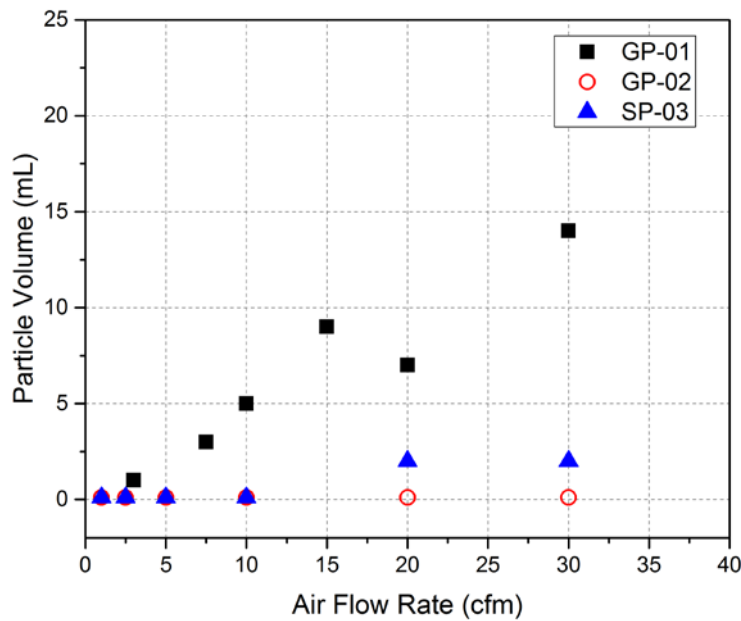
Figure 5.8. Comparison of Particles Captured by Various ALC Configurations in the Zone 3 Sieve (location closest to the tank wall). Note the air flow rate for GP-01 (run in pulsed mode) is the sum of the two air flow rates used in the test. GP-02 (4-in. diameter) and SP-03 (10-in. diameter) were both traditional ALC tests and only had a single air flow rate.

Examination of the particle capture data as a function of sieve radial position, given in Figure 5.9, also illustrates that the highest air flow rates tested were, in general, not as effective at transporting particles to the sieve capture zone as intermediate air flow rates (~10 cfm). This is likely explained by the nature of the flow field above the riser tube: as the air flow rate increases, the liquid velocity increases and the flow has more inertia; consequently, more of the flow is directed upward instead of spreading out radially. A larger fraction of energy (that could be used for mixing or particle transport) is lost when the plume/jet breaks the surface of the fluid. At the highest air flow rate tested (30 cfm), the GHP mixing became vigorous enough that it either displaced green beads out of the Zone 1 sieve, forcing them out of the sieve from below, or transported the particles right past the sieve at a high velocity, which tended to favor the middle sieve. The result is that the GHP performance (as measured by Zone 1 particle capture) appears similar to the other ALC configurations at 30 cfm.
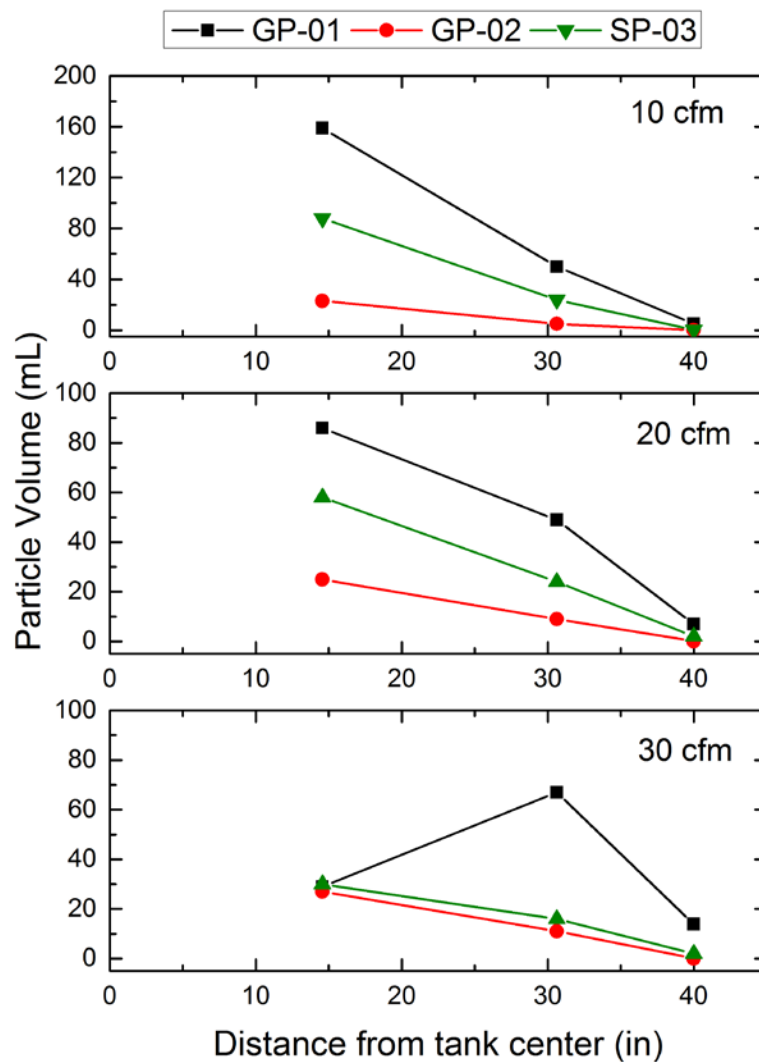
Figure 5.9. Comparison of Particle Volumes Collected as a Function of Sieve Radial Position at the Highest Air Flow Rates Tested. Note: The energetic upward flow from GP-01 was observed to push beads out or past the innermost sieve location at 30 cfm.

It is worthwhile to discuss the particle volumes collected and shown in Figure 5.6 through Figure 5.9 in context of the total particle inventory. There were 12 lb of green beads in the tank initially, which has an approximate intrinsic particle volume of 2200 cm^3. Hypothetically, if the particles were evenly distributed across the surface of the tank and then allowed to settle, ~17 cm^3 would drop into each of the three sieves. Alternatively, assuming that an entire particle volume equivalent to 2200 cm^3 passes exclusively through one of the zones over the course of 10 minutes, a sieve would collect ~52 cm^3 of particles based on its area fraction. Since the particles have interstitial space when the volume is measured in the graduated cylinder, the actual bulk volumes measured would be greater by a factor of 1/0.64 (assuming the spheres randomly close pack with a void fraction of 0.36). Many of the particle volumes measured in PNNL testing are of a similar magnitude to, and in a number of cases exceed, these hypothetical values, suggesting that appreciable particle transport is occurring over the course of the 10-minute particle capture test.

5.3 Recommended Configurations for Non-Newtonian Testing

Due to the success of the ALC and the GHP in both lifting and transporting particles throughout the test tank, other systems that were considered for testing in the Newtonian fluid were not pursued. The testing indicated that large particles (up to nominally 6 mm in size) could be lifted by the ALC and GHP, and that particles of 500 to 750 μm diameters could be distributed radially throughout the test vessel. The particles were lifted at air flow rates as low as 5 cfm. The amount of particles collected near the surface using sieves in fixed positions over 10-minute test runs was appreciable considering the available particle inventory in the vessel and the small area fraction covered by the sieves (~0.8% each). However, successfully transporting solid particles in Newtonian fluid does not suggest how the ALC systems might perform in a non-Newtonian fluid.

In order to conduct non-Newtonian simulant testing, a configuration was downselected from those tested in the Newtonian fluid. The downselection was based on performance in the PNNL test stand and the expected compatibility with operating conditions in the 8-ft diameter test stand at Mid-Columbia Engineering (MCE). The MCE test vessel has a similar vessel diameter and maximum operating level, but is expected to be tested at varying fluid levels to simulate processes that occur in the WTP. The recommended ALC technology needs to provide sufficient fluid energy and influence at an ~8-ft fill level, but must also be able to operate effectively when the fluid level is much lower.[1] A 10-in. riser tube was preferred to a 4-in. riser tube because it performed better in Newtonian fluid. In the Newtonian testing, the difference in performance between different tube lengths (3, 5, and 7 ft) with a 10-in. riser tube diameter was not determined to be significant (quantified visually). Thus, the riser tube length should be selected to influence the near-surface fluid when the vessel is at a maximum operating level (could be a 16-ft fluid level in the SHSV) while keeping the length similar to the lowest expected fluid level (so the tube could nearly always be submerged in the fluid). It is unknown precisely how an ALC would impact operation of the PJMs at lower fluid levels, though the ALC could be turned off or ramped down as the level is decreased, if needed. To strike a balance between these competing effects, a 5-ft riser tube length was selected for the non-Newtonian simulant testing, i.e., configuration SP-03.

---

[1] "Operate effectively," in this case, means performing the same mixing functions the ALC is designed to perform while avoiding undesirable aerosol production when the fluid level is lowered. The simplest way to minimize the aerosol may be to maximize (if possible) the distance of the outlet of the riser tube from the fluid surface.

As discussed, the 10-in. ALC (SP-03) did not perform as well as the GHP (GP-01) in particle capture testing, though it still lifted and transported significant amounts of particles to the fluid surface. The ALC geometry would likely be preferred for use in WTP vessels due to its simpler geometry and design. However, to avoid arbitrarily discarding a potentially suitable technology, the GHP (in the ~5-ft riser configuration GP-02) was also selected for non-Newtonian simulant testing. The GHP is considered a feasible alternative to an ALC system and provided a system for comparison of performance.

6.0 Non-Newtonian Testing

The non-Newtonian testing was performed in two discrete parts. The initial testing focused on examining the performance of the recommended devices mentioned in Section 5.3 (SP-03, GP-02 in GHP mode). A later phase of testing concentrated on improving the initial performance of the tested devices with new configurations (SP-05, SP-05p, and PPM). Both the SP-05p and PPM configurations were only briefly tested to confirm the plausibility of each device to mobilize clay slurry (proof-of-principle style experiments). In all cases, the objectives were to determine if the clay slurry was sheared and in motion when the ALC was operated and, if not, to identify regions that were not in motion. Regions that are influenced in the tank during the PNNL testing described in this report bear some resemblance to the historical quantity "zone of influence" (e.g., of spargers in Poloski et al. 2005) but should not be interpreted as such.

This section describes all the non-Newtonian slurry testing conducted in the PNNL test stand through December 2014. First, the method that was used to perform the evaluations is described. Then the results of the initial testing and the follow-on testing are presented. At the end of the section, the results are discussed and summarized.

6.1 Non-Newtonian Test Method

The purpose of the non-Newtonian simulant testing was to assess the capacity of an ALC to motivate the fluid throughout the tank, and most critically, the top region of the tank. The clay slurry chosen as the non-Newtonian fluid was opaque and did not allow *in situ* flow visualization, so another measurement method was required to detect fluid motion. Several methods were considered, based on either observing motion directly (a more accurate velocity instrument, for example) or indirectly (e.g., radio frequency tags, chemical tracers or dyes, observing bubbles with a submerged camera). All of these methods may have been effective, but a particle seeding method was chosen. The other methods were deemed slower (more time elapsed before obtaining results) and more complex to implement than the seeding method. Acquiring results quickly was important so that the test apparatus could be adjusted in response to data. The clay slurry also has a finite usable lifetime before biological growth (controlled for an initial period with the addition of biocide) and aging effects on rheology compromise the material.

The seeding method depended on the assertion that particles (the Airsoft pellets described in Section 3.3.2) could be placed in the clay slurry and would not move on their own (due to buoyancy), but instead would effectively act as tracers. If the fluid was sheared sufficiently to begin moving, the particles would follow along with the motion until there was no longer sufficient shear to continue the motion. To verify that the particles would be stable, i.e., not move of their own accord, previous work was consulted. Stability calculations of this type are based on a dimensionless number known as the yield-gravity number Y, written in Jossic and Magnin (2001), for example, as

$$Y = \frac{\tau_0}{gl|\Delta\rho|} \tag{6.1}$$

where l is the characteristic dimension of the particle (typically the diameter for a sphere), $\Delta\rho$ is the density difference between the fluid and the particle, and τ_0 is the yield stress of the fluid. Equation (6.1) is the ratio of the restraining force of the material to the gravitational force on the particle (i.e., yield

stress/buoyancy). Jossic and Magnin (2001) found that spherical particles (where $l = d$) were stable at $Y \geq \sim 0.06$. A similar calculation by Beris et al. (1985) was based on a derivative of the yield-gravity number, which they call the yield-stress parameter Y_g:

$$Y_g = \frac{3\tau_y}{2g|\Delta\rho|R_0} \tag{6.2}$$

where $\tau_y = \tau_0$ and R_0 is the radius of a sphere ($d/2$). Equation (6.2) differs from Equation (6.1) by a factor of 3 when $l = d$, e.g., $Y_g = 3Y$. Beris et al. (1985) found that the stability criterion for Y_g was 0.143. Consistent with these other studies, Stewart et al. (1996) identified in the literature and through analysis yield-gravity numbers (Y) ranging from < 0.1 to ~ 0.2, where the lower values were applicable to use of the Bingham yield stress and higher values for static strength determination methods such as shear vane measurements. They applied the yield criterion to gas (bubble) retention and release in Hanford tank waste and non-Newtonian simulants. Using values of $Y = 0.06$ and $Y_g = 0.143$ for reference, the calculated value of the dimensionless number (Equation (6.1) and Equation (6.2), respectively) with the starting yield stress of the clay slurry (~22 Pa) and typical Airsoft pellet properties ($d = 0.006$ m, $\Delta\rho = 200$ kg/m^3) was more than 30 times the critical value (see Table 6.1). Even if the Bingham yield stress were to drop significantly over the course of testing, the Airsoft pellets would still not be expected to move in the fluid when the fluid is at rest. This was also confirmed in a simple experiment where the particles were placed in a small volume of slurry overnight and found at the same location where they were placed the next day.

Table 6.1. Stability Criterion Values Y and Y_g for 6-mm Diameter Airsoft Pellets in Clay Slurry.

τ_0 or τ_y (Pa)	Y	$Y/0.06$	Y_g	$Y_g/0.143$
2	0.17	2.8	0.51	3.6
6	0.51	8.5	1.53	11
10	0.85	14	2.55	18
16	1.36	23	4.08	29
22	1.87	31	5.61	39

Based on the analysis just discussed, the Airsoft pellets were not expected to move when the clay slurry was stagnant or quiescent. However, if the clay slurry was yielded during ALC operation and could be approximated locally as a fluid with an apparent viscosity similar to the Bingham consistency, all of the pellets except the red ones would have small positive (upward) velocities due to buoyancy. The velocities would vary due to the differences in density of the particles of various colors (see Table 3.3). Even so, the likelihood of local fluid disturbances causing the pellets to slowly rise through the clay independent of the flow fields created by the ALC was considered small. This is supported by two observations: (1) except for above the ALC riser outlet, the majority of fluid is traveling vertically down toward the ALC suction, a flow that would counter the possible small rise velocity of the pellets, and (2) when the slurry was pumped out after conducting an experiment, particles of all colors were found at locations below their initial starting locations (and often at or near the bottom of the vessel), indicating that the rise velocity of the pellets is not large enough to overcome the flow created by the ALC. Thus, the Airsoft pellets were treated as tracers and assumed to be located where found because they had been moved there by an external force and not buoyancy.

The seeding method was used to determine if selected locations in the tank were sheared and in motion when an ALC system was operated. Lifting and transporting of settling solid particles, such as the green beads or pea gravel described in Section 5.0, was not a significant concern. Calculations repeated using the approach outlined in Meacham et al. (2012) for solid particles in clay slurry demonstrated that the stability curve for a net particle velocity of 0.1 ft/s shifts up and to the right on Figure 5.3 for a non-Newtonian fluid, despite a lower fluid velocity of 0.4 ft/s in the riser tube at 10-cfm air. In this case, the yield stress and consistency of the non-Newtonian fluid (and their contributions to a reduction in the relative particle velocity) is the dominant term affecting solid particle transport.

Consequently, the experimental approach using the Airsoft pellets did not depend on motivating solid particles at the tank bottom. This led to several changes in the test stand configuration. The OBMS was removed from the vessel, and the 3/4-in. bulkhead fittings were replaced with 2-in. bulkheads to facilitate pumping clay slurry in and out of the vessel. The recirculation inlets at the 3- and 6-ft levels were valved out and not used. Two 2-in. AOD pumps were staged to assist with pump in or pump out as needed. A pair of floor scales were brought in proximity to the tank so that totes of clay slurry simulant could be weighed during operations.

Generally, each ALC configuration tested in the non-Newtonian simulant had a similar test evolution (exceptions are discussed in the corresponding sections that follow). The empty test tank was loaded with clay slurry to achieve a level of ~96 in. (8 ft). As mentioned, level measurements were conducted using a laser distance finder and were taken from three reference points around the tank perimeter. These distances were subtracted from similar measurements made when the tank was empty to estimate slurry level. The ALC device being tested was then installed in the test vessel. Initially, the device was operated over a range of air flow rates to collect video of the surface motion and confirm the target air flow rates to use during particle seeding tests.

Airsoft pellets (referred to from here on as particles for simplicity) were placed in various locations and distinguished by color. Particles were seeded according to the diagrams shown in Figure 6.1 and the quantities given in Table 6.2. The yellow particles were placed randomly (by hand) on the slurry surface in an approximately 18-in. by 45-in. rectangle. The other colored particles were loaded on the surface in an approximately 8-in. diameter circle and then slowly driven to the target depth using an inverted sieve attached to a pole. In the cross-section schematic shown in Figure 6.1, *R* refers to the tank radius. The "discs" of particles at various depths in Column A were centered on the half radius of the vessel, and the particle discs in Column B were centered 4 in. away from the wall (the southern edge of each disc was at the wall).
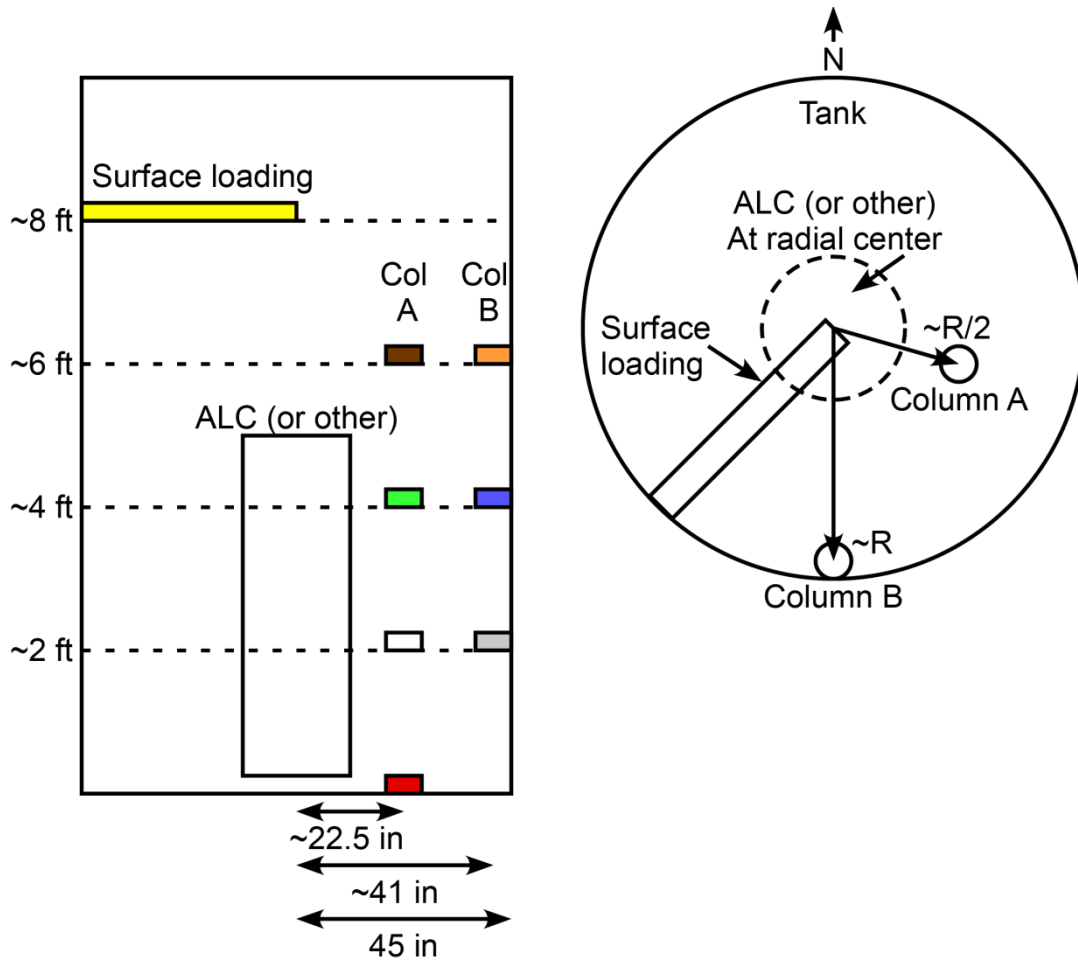
Figure 6.1. Loading Diagrams for Particle Seeding Tests in Clay Slurry. The quantity *R* in the cross-section diagram on the right refers to the radius of the tank; the side view is shown schematically on the left.

Table 6.2. Particle Quantities Added to the Tank During a Particle Seeding Test. The load sequence refers to the order in which the particles were loaded into the vessel.

Load Sequence	Particle Color	Column	Distance Below Surface [Elevation (ft)]	Target Mass (g)[a]	Approximate Number (ct)
1	Red[b]	A	~96 in. [0 ft]	100.0	670
2	White	A	~72 in. [2 ft]	100.0	890
3	Green	A	~48 in. [4 ft]	100.0	760
4	Brown	A	~24 in. [6 ft]	100.0	845
5	Grey	B	~72 in. [2 ft]	100.0	845
6	Blue	B	~48 in. [4 ft]	100.0	880
7	Orange	B	~24 in. [6 ft]	100.0	860
8	Yellow	Surface	~0 in. [8 ft]	319.5	2710

(a) Target masses shown were actual masses (within 0.1 g) in all the tests.
(b) The red particles were ~0.15 g each (and denser than the simulant).

After loading the particles, the ALC system was operated continuously for 1 hour. An hour was chosen to give any slow-moving regions of the tank ample time to migrate to a faster-moving region in the vessel. After an hour, the ALC system was stopped. A sampling device (a net) was used to sweep the top ~12-in. region of the slurry, and any particles captured in the net were collected. The sample region was swept a second time to collect any particles that were missed during the first pass (in most cases, >75% of the particles recovered were collected in the first pass). Finding particles in the top layer of the slurry indicated that the particles had been moved from their starting location, motivated to the suction of the ALC, and transported to the surface along with the fluid carrying them. Note that if the particles were able to move around the entire tank during operation and were distributed homogeneously, ~1/8 of the particles would be recovered from the 1-ft surface layer (of 8-ft total depth) when it was sampled. After the two-step sampling process, the top 12-in. of slurry was considered clear of particles, the ALC system was operated again, and the process was repeated until either enough data was collected or the particle population in the tank became depleted.

The final step was to pump down the clay slurry in a controlled manner to characterize the distribution of the remaining particles in the fluid. This was done using a single 2-in. AOD pump and a hose suspended using the Gantry crane and hoists. The inlet hose was submerged only a couple of inches and moved around the surface of tank so that the suction point was not stationary. The slurry was pumped out in eight 1-ft increments from the top to the bottom. Slurry leaving the vessel was passed through a Y-strainer to collect the particles. Each batch of particles collected in the strainer during a 1-ft incremental pump out were removed, cleaned, separated, and measured (by mass and/or number). Slurry was returned to the totes until the next device was ready to be tested.

6.2   Initial Tests: SP-03 and GP-02

In the initial non-Newtonian testing, the two configurations recommended after Newtonian testing were evaluated. The GP-02 test was conducted first; however, the SP-03 test is discussed first in the report as it is the baseline against which data from other tests are compared. The objective was to assess which regions of the tank were motivated or moved by the ALC as determined by relocation of the seeded particles. A configuration would be considered successful if, at minimum, the ALC mobilized the entire top half of the tank contents. This was considered to be a good target based on the assumption that this is the region most likely to require supplemental mixing in a WTP vessel.

The SP-03 non-Newtonian test was conducted in six segments. In the first three segments, the air flow rate was set at 15 cfm and the ALC was run for 1 hour. In the fourth segment, the air flow rate was raised to 20 cfm for an hour. The fifth and sixth segments were shorter and run at 25 and 30 cfm, respectively. The shorter duration was due to air flow restrictions, which were later attributed to plugging in the air tube distributor. The plugging occurred because the drilled PVC cap was used for the SP-03 testing. Once the plugging was discovered in the cap, the balance of the non-Newtonian tests were conducted using an open tube air distributor, which mitigated the plugging problem. This was not expected to affect comparisons of the data because the velocity measurements described in Section 4.0 demonstrated that the air distributor geometry did not impact the ALC riser velocity at the outlet. Data collected is shown in Figure 6.2 as the mass of particles of each color recovered from the top 1-ft of slurry versus operating time (refer to Figure 6.1 for the original location of each particle color). The legend entries in Figure 6.2 and similar ones to follow show the initial location of particles in terms of distance below the surface and radius. The data at each operating time is the discrete mass of particles recovered

using the sampling process, and does not include particles recovered in previous segments. The air flow rate used in each segment is shown across the top of the figure.
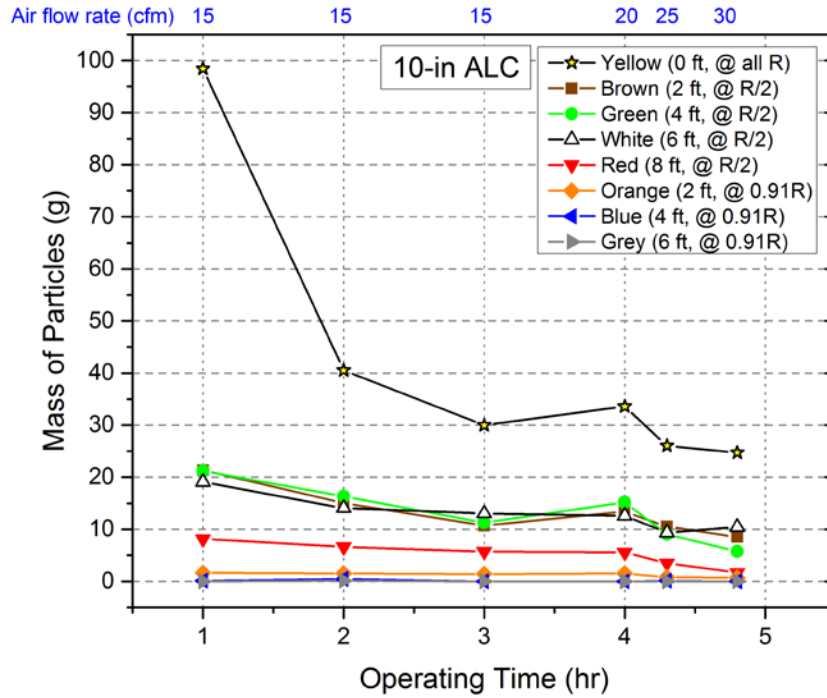
Figure 6.2. Mass of Particles Recovered from 1-ft Surface Layer During SP-03 (10-in. ALC) Non-Newtonian Testing. Air flow rates used prior to each particle collection event shown along the top of the figure.

For all tests, the mass data was normalized in order to compare more easily between tests where the amount of particles in the tank at a given time might not be the same. The normalization was calculated as a mass fraction of particle color j recovered in sampling after segment i (where segment is just a sequential test counter variable, i.e., run 1, run 2, etc.) from the 12-in. surface region, f_{ij}, defined as

$$f_{ij} = \frac{m_{ij}}{m_{0j} - \sum_{n=1}^{i-1} m_{nj}[i \geq 2]} \tag{6.3}$$

where m_{ij} is the mass of particle color j recovered after segment i and m_{0j} is the original mass of particle color j loaded into the tank. Thus, as defined by Equation (6.3), f_{ij} is the mass recovered from the vessel as a fraction of the mass left in the tank prior to system operation in run segment i. All data sets presented subsequently in this report show the normalized mass fractions, such as the SP-03 data in Figure 6.3 converted from the masses shown in Figure 6.2. For the actual particle masses recovered during each test, refer to Appendix B.

6.6
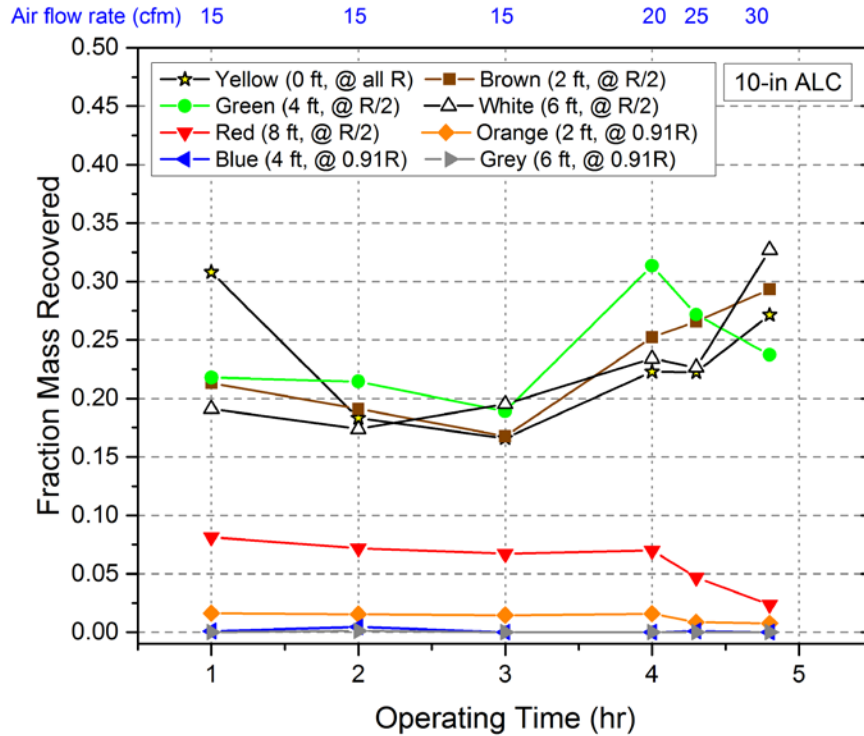
Figure 6.3. Fraction of Particle Mass Recovered During SP-03 (10-in. ALC) Non-Newtonian Testing. Air flow rates used prior to each particle collection event are shown along the top of the figure.

The data from SP-03 indicates that there was little or no motion out to the wall region of the tank, as the orange, blue and grey particles were not recovered at the surface in large amounts (or at all), and a large fraction of yellow particles were recovered after the first hour of operation (suggesting they never moved from their original location).[1] When a lack of recovery of near-wall particles (except yellow) was observed after operating the ALC at 15 cfm for three segments, the air rate was increased in an attempt to improve performance. With respect to the near-wall particles, there was no change. It appeared from this test evaluation that the influence of the 10-in. ALC did not extend out radially to the tank wall even at the top of the tank, with an interface between well mobilized and poorly mobilized slurry somewhere between ~0.5R and ~0.8R.[2]

The pump-down data, shown in Figure 6.4, confirmed that the near-wall particles (Airsoft pellets) had not been mobilized. The data is given as the fraction F_{kj} of the mass recovered of particle color j in each layer k of slurry that was pumped down, i.e.,

---

[1] That a large fraction of yellow particles was recovered is not, on its face, indicative of little motion out to the tank wall. However, since a net was used to sweep the surface, it provides additional information about where the recovered particles were located, and almost all of the yellow particles recovered after the first hour of operation were within 12 in. of the tank wall. Combined with the lack of recovery of the orange, blue, and grey particles, it is reasonable to conclude that the influence of the SP-03 configuration did not extend to the tank wall at the fluid surface.

[2] The edge of the particles loaded in column B extended ~8 in. into the interior of the tank since they were loaded as discs. With $R = 45$ in., 8 in. is located at $1 – 8/45 = 0.82R$. The column A particles were centered at 0.5R, which sets the lower bound.

$$F_{kj} = \frac{M_{kj}}{m_{0j} - \sum_{i=1}^{N} m_{ij}} \tag{6.4}$$

where M_{kj} is the mass of particle color j collected during pump-down of layer k and N is the total number of segments run in a particular configuration. Equation (6.4) describes the mass of particle color j found in a particular layer as a fraction of the total mass that was in the tank prior to pump-down. The pump-down data in Figure 6.4 shows that almost all of the particles near the wall (orange, blue, grey) were found in the layer where they were originally loaded (or just below that elevation). Almost all of the red particles were also found on the bottom, where they were originally. Particles that were detected in appreciable amounts in the top foot of slurry during testing (yellow, brown, green, and white) were spread reasonably uniformly throughout the tank height, but with a general trend of increasing concentration at higher elevations.
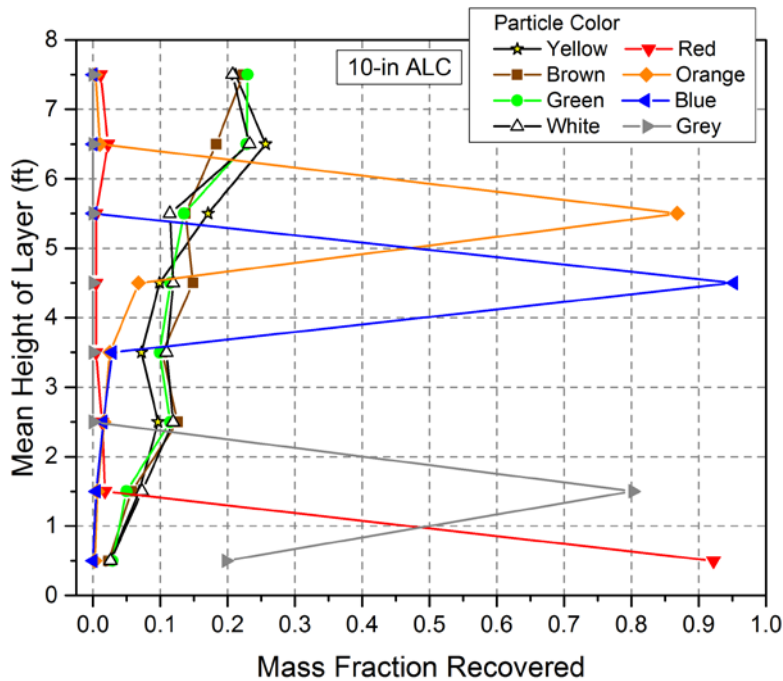
Figure 6.4. The Distribution of Particle Fractions Recovered During Slurry Pump-Down Following SP-03 Testing. The mean height is the mid-point of the layer that was pumped out, i.e., the first layer was pumped from 8 ft to 7 ft so the layer height is represented as 7.5 ft.

The Geyser pump non-Newtonian test, since it occurred first, was performed a little differently to support the development of the test protocols that were used for all the other tests. For the first 4 hours of operation, only the yellow surface particles were present. The yellow particles were used to develop the sampling and analysis methodology and confirm particles did not move around in the tank when the slurry was quiescent. After the fourth segment of operation, all the other colored particles were loaded into the tank and the operation time was reset to zero. The implication for interpreting the data given in Figure 6.5 is that the yellow particle inventory was already reduced from what had been initially loaded, and they were distributed in the tank and not on the slurry surface. All the GP-02 tests were conducted in hybrid pulsed-mode with air flow rates of 5 cfm (airlift) and 10 cfm (pulse), for a total of 15 cfm.
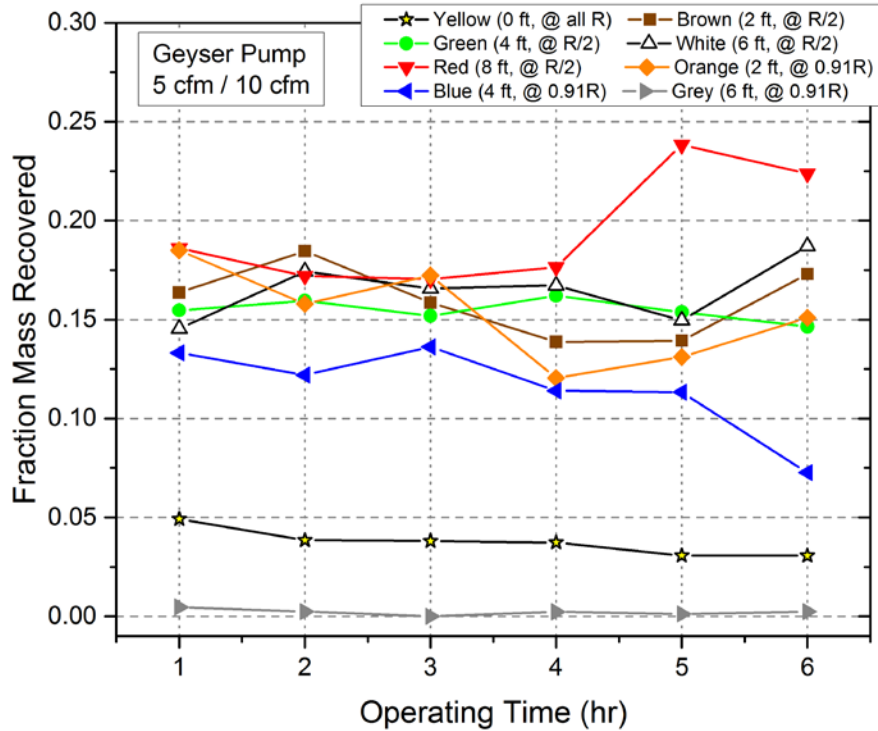
Figure 6.5. Fraction of Particle Mass Recovered During GP-02 (GHP operated in pulsed-mode) Non-Newtonian Testing. The GHP was operated in four segments prior to this data with the yellow particles only; this data is not included in the plot.

In comparison to the SP-03 data in Figure 6.3, the GP-02 data has a few key differences. First, the orange particles initially located near the wall and 2 ft below the surface were mobilized by the GHP and were recovered at the surface in approximately the same amounts as the particles originally located at $R/2$ (green, white, and brown). The red particles (at $R/2$, bottom of tank) were also recovered in similar amounts, which was not surprising based on the size of the suction radius around the GHP observed in the Newtonian testing. The blue particles were found in appreciable amounts, though slightly less than many of the other particles. This suggests that at least a portion of the region where the blue particles were loaded was influenced or in motion, but there was not enough energy imparted to the fluid to motivate all the blue particles at or near the wall at an elevation 4 ft below the surface. Similar to the SP-03 test, the grey particles did not appear to be mobilized and negligible amounts of them were found at the surface during the test. The explanation for the reduced fraction of yellow particles is that testing had already been performed with them and the inventory was significantly reduced. Preliminary testing using only the yellow particles demonstrated that particles at the surface migrated down, even at the wall. This was observed by initially sweeping the net near the wall in the process of quantifying the amount of yellow particles present in the top foot of slurry after running the GHP. The majority of yellow particles that were originally on the surface near the wall were not found in the top foot and thus had been displaced to a lower elevation in the tank by GHP operation.
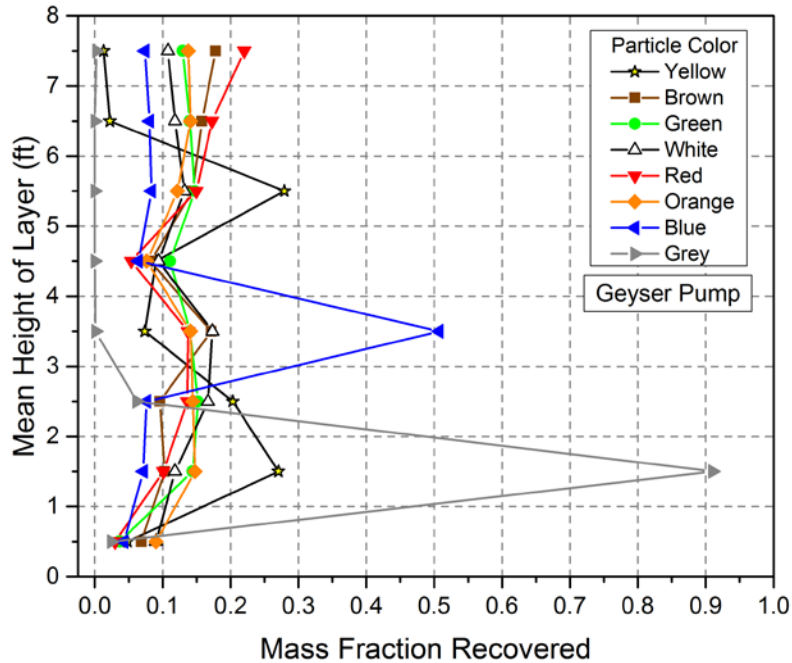
Figure 6.6. The Distribution of Particle Fractions Recovered During Slurry Pump-Down Following GP-02 Testing. The mean height is the mid-point of the layer that was pumped out, i.e., the first layer was pumped from 8 ft to 7 ft so the layer height is represented as 7.5 ft.

The pump-down data presented in Figure 6.6 confirms the observations made from the data collected during testing. The grey particles were found at the elevation where they were loaded; this implies that fluid in that region near the wall was not mobilized substantially (or at all). Approximately half of the blue particles were distributed throughout the tank height, with half found at the elevation where they were originally loaded. As mentioned in the previous paragraph, it appears that some of the blue particles were located in a region of fluid that was moving and the rest were not, e.g., most likely those at or close to the tank wall at that elevation. Particles of all other colors were found well-distributed in all the slurry layers, with the greatest variability present in the yellow particles. At the close of GP-02 testing, the yellow particle inventory was fairly low and they had been moving around the tank for 10 hours of operation; the increased variability in the yellow particles' vertical distribution is not considered representative of any unusual phenomena.

The GHP (GP-02) had better performance than the ALC (SP-03) based on the data from the particle seeding tests. The GHP influenced slurry out to the wall in the upper region of the tank, and mobilized material down to an elevation of approximately 4 ft (as indicated by the distribution of blue particles). However, the GHP was considered a less-favorable alternative system due to its complexity, so additional testing was conducted to evaluate whether other ALC configurations could offer improved performance over SP-03. This is described in the next section.

6.3 Follow-On Tests: SP-05, SP-05p, and PPM

A variation of the SP-03 configuration was to maintain the riser tube length and off-bottom distance but increase the tube diameter. A nominally 18-in. ID tube was selected, and this configuration was

designated SP-05. Based on estimates of liquid velocity/flow rate discussed in Section 4.3, the 18-in. diameter tube was observed to produce much greater liquid flow rates for a given air flow than smaller tubes (despite the reduction in velocity due to increased cross-sectional area). Thus, SP-05 was tested in the same way as SP-03 and GP-02 to determine if the increase in recirculation rate produced a corresponding improvement in fluid mobilization in the test vessel.

The data collected from SP-05 testing in five segments is shown in Figure 6.7. The segments had increasing air rates starting at 15 cfm (first two segments) up to 30 cfm (last segment) as shown on the top of the figure. Similar to SP-03 testing, the air rate was increased over the starting value of 15 cfm to ascertain if the near-wall particles could be mobilized at higher air flow rates. The primary difference in performance between the SP-03 (Figure 6.3) and SP-05 configurations is that SP-05 mobilized the orange particles (near-wall at 6-ft elevation) whereas SP-03 did not. The lower initial fraction of yellow particles recovered in SP-05 and their radial distribution observed during particle collection also indicated that the slurry was motivated out to the wall at the surface, which was not achieved with SP-03. However, there was little difference between the two ALCs in terms of the amount of blue and grey particles recovered. The reduction in the presence of red particles at 15 cfm in SP-05 is likely attributed to the reduced velocity on the tank floor with the larger riser tube diameter. The fluid "suction" velocity at 15 cfm with SP-05 appeared to be insufficient to move fluid near the tank floor at $R/2$, whereas ≥ 20 cfm was enough.
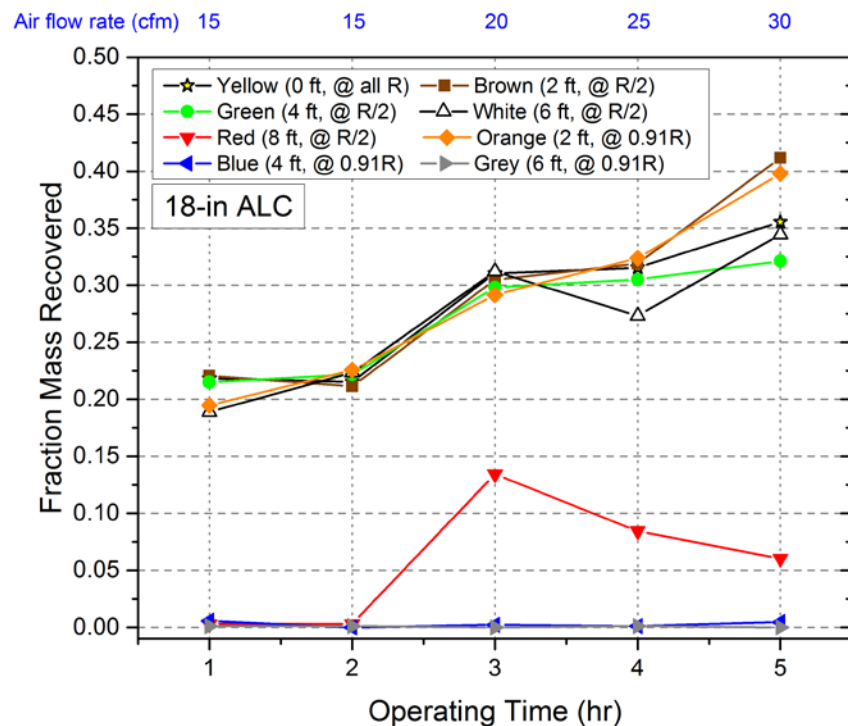
Figure 6.7. Fraction of Particle Mass Recovered During SP-05 (18-in. ALC) Non-Newtonian Testing. Air flow rates used prior to each particle collection even shown along the top of the figure.

The pump-down data collected following the SP-05 non-Newtonian test is shown in Figure 6.8. The near-wall particles that were not collected in appreciable amounts (blue and grey) are not as "focused" at a single elevation as they were in the SP-03 testing. Only the red particles were found concentrated at the elevation where they were originally loaded. The distribution of the blue particles and grey particles

6.11

(grey to a much lesser extent) were spread across the bottom four or five layers. This may suggest that the 18-in. ALC provided enough energy to generate small or slow downward motion where those particles were initially placed, but the motion was not sufficient to move those fluid elements radially toward the ALC suction. Absent additional information, a more precise explanation for the SP-05 pump-down particle distributions cannot be offered. Based on comparing the results of the SP-03 and SP-05 testing, the 18-in. ALC offers improved performance over the 10-in. ALC. At minimum, the top 2 ft of the slurry exhibited downward motion across the entire tank diameter as indicated in Figure 6.8 by the low concentrations of particles in the upper two layers. The GHP still outperformed the 18-in. ALC, as greater overall vertical redistribution of the particles at the 4-ft level near the wall was observed during the GP-02 test (comparing blue particles in Figure 6.5 to Figure 6.7 and Figure 6.6 to Figure 6.8).
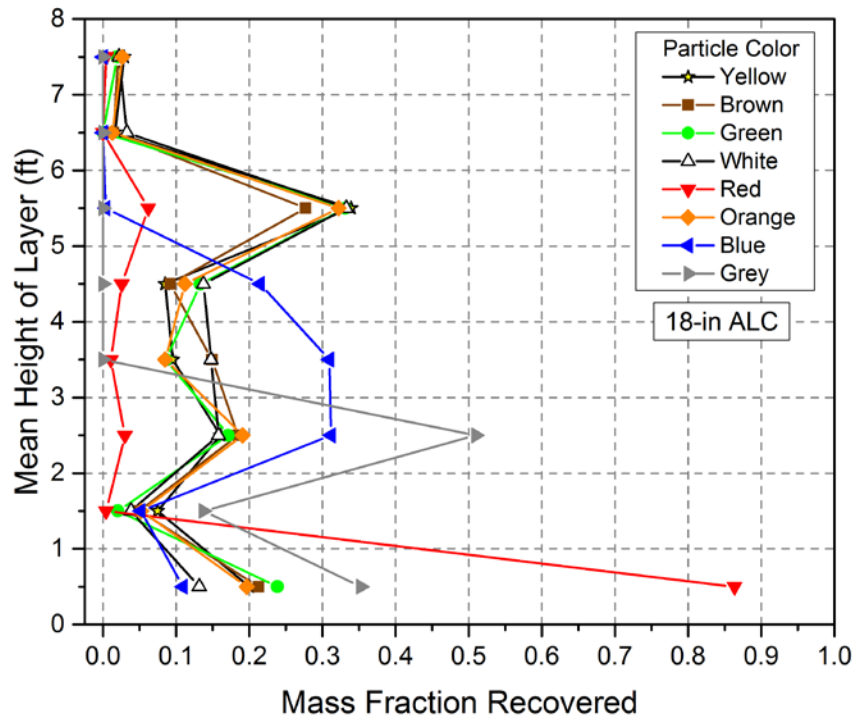
Figure 6.8. Distribution of Particle Fractions Recovered During Slurry Pump-Down Following SP-05 Testing. The mean height is the mid-point of the layer that was pumped out, i.e., the first layer was pumped from 8 ft to 7 ft so the layer height is represented as 7.5 ft.

Other devices were investigated to establish if a larger region of slurry could be mobilized using a mixing technology other than a "true" ALC or the GHP. Two other tests were conducted (configurations SP-05p and PPM) with a more limited set of particles, where particles of various colors were only loaded in the blue and grey positions. These two locations had already been established as the most difficult to mobilize in the previous tests. This was followed by a repeat of the 10-in. ALC test (SP-03) with the full suite of particles loaded as shown in Figure 6.1. Pump-downs were not conducted between these three tests, as substitute colored particles were used for the SP-05p (green for blue and white for grey) and PPM tests (orange for blue and brown for grey). Four "new" replacement colors were then used in the SP-03 repeat test. Thus, when a pump-down was completed after the 10-in. ALC repeat test, there were 12 particle types in the tank (see Table 3.3). The effect of small density differences between the 12 particle types on their transport is undetermined, but it is expected to be small.

The average of the mass percentages of "blue" and "grey" equivalent particles (based on initial location) collected for all non-Newtonian tests are summarized in Table 6.3. The mass fractions determined using Equation (6.3) for all segments were averaged and multiplied by 100 to convert to the percentages shown in the table. Using this metric, both the SP-05p and PPM configurations were significant improvements over GP-02, as they both mobilized significant fractions of even the grey particles (or more precisely, particles loaded in the grey location 6 ft below the surface). Since they were not tested using a full distribution of particles, it cannot be concluded that either the SP-05p or PPM configuration mobilized the clay slurry to a greater extent than GP-02, SP-03, or SP-05. However, the data in Table 6.3 (except for the SP-03 repeat test discussed below) implies that more comprehensive mobilization would be probable using either of those mixing devices.

Table 6.3. Average Percentage of Particles Recovered During Testing from Hardest-To-Mobilize Regions of the Vessel. The results are presented in chronological order.

Device	Segments of Operation[a]	Rheology Measurements from Samples (yield stress in Pa / consistency in cP)[b]	Average Percentage of Particles Collected from the Top Foot During Testing that Were Originally Placed at **4 ft** Below the Surface, Near the Wall (Blue Particles)	Average Percentage of Particles Collected from the Top Foot During Testing that Were Originally Placed at **6 ft** Below the Surface, Near the Wall (Grey Particles)
GHP (GP-02)	6	After Segment 3: 16.3 Pa / 32.6 cP	11.5%	0.2%
10-in. ALC (SP-03)	6	Prior to Operation: 14.3 Pa / 32.5 cP After all Segments: 11.5 Pa / 32.5 cP	0.1%	0.0%
18-in. ALC (SP-05)	5	Prior to Operation: 11.3 Pa / 31.4 cP After all Segments: 10.2 Pa / 31.9 cP	0.3%	0.1%
18-in. modified ALC (SP-05p)	4	n/a	16.8%	14.0%
PHi-300 mixer (PPM)	4	n/a	18.6%	17.6%
10-in. ALC (SP-03), repeat test	3	After Segment 2: 10.1 Pa / 30.8 cP	14.8%	9.6%

(a) This corresponds approximately to the number of hours the device was operated, as the majority of the segments had duration of 1 hr.
(b) The point in operation referred to with each rheology sample measurement is when the sample was collected from the tank. The analysis was performed on the samples 7 to 10 days after the sample was collected.

The 10-in. ALC test was repeated to assess the potential effect of a downward drift in the yield stress of the clay slurry on the non-Newtonian simulant test results. Archive slurry samples were collected from the tank (at a fixed location: ~18 in. from wall and ~2 ft below the surface) at intervals over the course of testing, but not necessarily coinciding with the individual tests. The rheology (Bingham parameters) and solids content were later (typically 7 to 10 days after sample collection) measured on these samples. Despite the solids content remaining unchanged, the yield stress decreased to just over 10 Pa (from 22 Pa at the start of testing) by the time the PPM was tested. The consistency dropped slightly over the same period but was still > 30 cP. Thus, the 10-in. ALC was retested to see if performance was different with a non-Newtonian simulant that had a greater than 50% reduction in the yield stress from the starting material (note that the difference between the two 10-in. ALC tests was closer to 4 Pa). According to the data shown in Table 6.3, collection of particles from the hardest to mobilize regions of the vessel improved significantly in the repeat 10-in. ALC test. The results are similar to the percentages of particles collected when testing with the SP-05p and PPM configurations and are also indicative of better performance than the earlier test configurations (GP-02, SP-03, and SP-05). The significant improvement in the repeated SP-03 results with decreasing simulant yield stress and the timing of the tests make it difficult to establish conclusively that the SP-05p and PPM configurations performed better than earlier tested configurations.

The reduction in yield stress appeared to be related to a shift in pH, which increased by around 0.5 units over the course of testing. The cause of the pH shift is not clear. Regardless of the cause, the shift introduces uncertainty in the interpretation of the results collected in the non-Newtonian testing. It also suggests that as the yield stress decreases, the effectiveness of the ALC in mobilizing the clay slurry improves. The 10-in. ALC, which did not motivate the particles at the wall 2 ft below the surface (orange particles) when it was initially tested, mobilized particles 6 ft below the surface (grey particles) in the repeat test.

6.4   Discussion of Non-Newtonian Results

The recommendation of the Newtonian testing was for a nominally 10-in. diameter ALC (SP-03) to be used in non-Newtonian testing. The initial testing with clay slurry demonstrated that SP-03 was not as effective at mobilizing a non-Newtonian fluid as the GHP, which had superior performance. The GHP mobilized the slurry to approximately the 4-ft level near the wall, or nearly the entire top half of the tank contents. However, an ALC system is preferred for implementation in the WTP vessels due to its simplicity relative to the GHP. This consideration led to additional testing to determine if an ALC other than the SP-03 configuration performed better in non-Newtonian fluid (e.g., SP-05).

Based on the fractions of colored particles collected during the testing and initial seeding locations, a qualitative picture of the shape of the region that is moving/being sheared was built. A conceptual representation of the regions for each configuration tested (except the SP-03 repeat) is displayed in Figure 6.9. The outlines for GP-02, SP-03, and SP-05 can be thought of as an approximation of the shear boundary in the slurry; all the fluid inside (toward the center of the vessel) each outline is considered to be moving and all fluid outside the outline is apparently not sheared sufficiently to move. The dimensions labeled "< 37 in." are approximately where the fluid is mobilized out to 37 in. radially (or less). This corresponds to the centermost location of near-wall discs of particles (recall they had a diameter of 8 in.). The regions mobilized by the testing performed with configurations SP-05p and PPM

are also shown, but without the entire complement of seeded particles a region of influence could not be constructed for those devices. The SP-03 repeat test is also not shown in Figure 6.9; the test data indicated that its profile would be similar to that of SP-05p and PPM and extend further to the wall than GP-02. The improved performance in the SP-03 repeat, as well as in the SP-05p and PPM configurations, may be attributed to a reduction in the yield stress of the simulant, as noted in the previous section.

One criterion for a successful test was mobilization of the top half (4-ft elevation and above) of the slurry in the tank. By this measure, none of the devices that were tested (in full) were successful as determined by the particle seeding test results. SP-03 (initial test) did not achieve mobilization out to the wall at any elevation in the test vessel. GP-02 and SP-05 had similar performances to each other, with the GHP being marginally better. Both of these configurations influenced the slurry across the entire radius in the top few feet. The GHP afforded a slight improvement in collection of particles from the 4-ft near-wall location compared to SP-05. This small improvement is not significant enough to recommend the GHP over a "traditional" ALC device due to its more complex design and concerns regarding its implementation. For this reason, SP-05 is the recommended configuration for the 8-ft MCE test vessel. However, the successful use of both SP-05p and PPM to motivate fluid and seeded particles in the hardest to mobilize locations (as shown in Figure 6.9 by the orange circles) warrants additional study. Assessment of these devices for implementation in the 8-ft MCE vessel is also recommended based on the preliminary results, in particular to confirm if the improved performance that was observed translates to materials with a Bingham yield stress closer to 30 Pa.
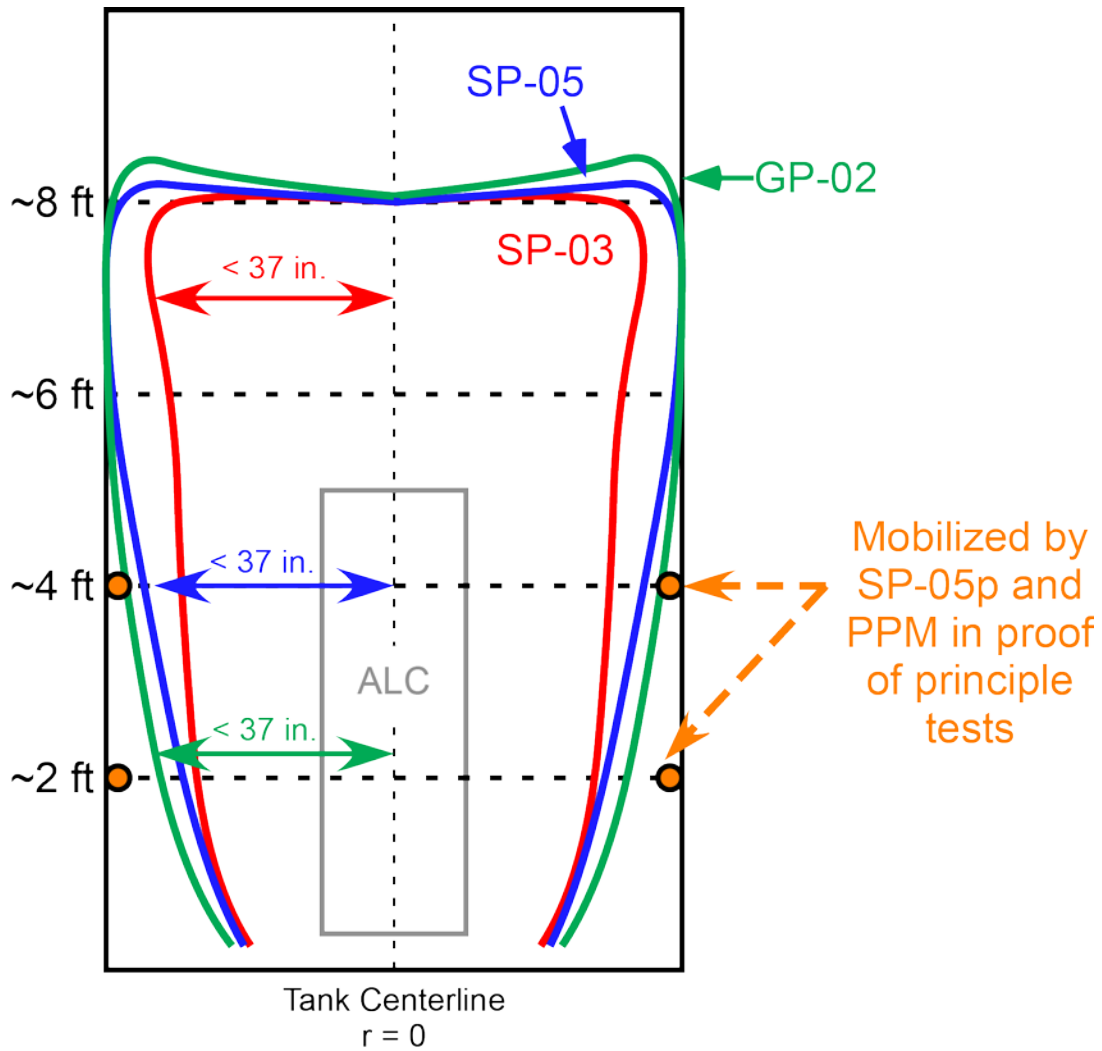
Figure 6.9. Conceptual Representation of the Shear Boundary for Devices Tested in Clay Slurry. Slurry inside of the boundary was mobilized during operation and slurry outside the boundary was quiescent or not moving with the bulk fluid. The "< 37 in." dimension indicates approximately where the device was influencing fluid out to 37 in. or less, which corresponds with the edge of a near-wall disc of particles. Note: The SP-03 repeat test shear boundary is not shown in this conceptual representation.

7.0   Summary of Results

The testing conducted at PNNL described in this report covers three different aspects of performance in ALC systems (or similar systems): liquid velocity (flow rate), transport of solid particles in a Newtonian fluid, and mobilization of a non-Newtonian fluid with a yield stress. This section summarizes the major conclusions of the testing with respect to performance in these three areas.

The liquid flow rate increased non-linearly with the air flow rate injected into the ALC riser, and flow rates of > 500 gpm were achieved using air flow rates of ≤ 20 cfm in several ALC geometries and in both Newtonian and non-Newtonian fluids. The liquid velocity at the riser outlet increased with the superficial gas velocity to the 1/3 power in both the Newtonian and non-Newtonian fluids. All of the Newtonian data was collapsed with and fit reasonably well by a single empirical constant. The data was collapsed by incorporating a second term in a correlation: the square root of a ratio of liquid heights in the vessel (see Equation (4.6)). The non-Newtonian simulant flow rate data was too sparse and uncertain to perform any additional analysis. Developing a similar correlation for non-Newtonian data would require a more dependable measurement technique and testing with multiple simulants (or over a range of Bingham parameters).

The ALC system testing with Newtonian fluid (water with small amounts of solid particles) demonstrated successfully that particles as large as ~6 mm can be lifted by the vertical riser flow. Testing also demonstrated that particles with diameters between 500 and 750 μm were transported radially throughout the test vessel using several different configurations of the ALC and the GHP. The minimum air flow rate at which all particles can be lifted in water was determined to be ~5 cfm, and it is expected that at higher air flow rates an ALC could lift particles expected to be encountered in a WTP vessel provided a second mixing device (PJMs) suspends the particles off the tank bottom and exposes them to the ALC suction. Above the minimum air flow rate, the capture of lifted solid particles just beneath the fluid surface was not appreciably improved. The ALC riser tube height (3-, 5-, and 7-ft diameters were tested) also did not greatly affect particle capture performance. Based on these evaluations, a 10-in. diameter and 5-ft long riser tube located ≥ 5 in. off the tank bottom was recommended for further testing in non-Newtonian fluid (SP-03). The GHP was also a promising candidate in Newtonian liquid testing, as it had superior performance to SP-03 with respect to solid particle transport, and it was recommended for testing as an alternative to the ALC.

The non-Newtonian testing established that the recommended ALC configuration (SP-03) did not impart enough energy into the clay slurry (initial Bingham parameters: ~22 Pa yield stress, ~34 cP consistency) to mobilize the slurry out to the tank wall in the upper half of the vessel. The GHP had better performance. A larger ALC (nominally 18-in. diameter, SP-05) was tested and exhibited improved performance, as it very nearly mobilized the upper half. In all these configurations, the air flow rate required to mobilize significant regions of the simulant was typically ≥ 20 cfm. Other mixing devices were operated in proof-of-principle tests (but not formally tested) and showed much better performance, as both a pulsed ALC (SP-05p) and a pulsed plate mixer (PPM configuration) mobilized the clay slurry in the most challenging tank locations. There is some uncertainty in the relative performance of these devices as the yield stress of the clay slurry decreased gradually during the testing evolution, reaching a value of ~10 Pa by the end of the testing. This was evidenced by improved performance in the SP-03 configuration from near the beginning of the test period to the end. Since the GHP is likely more complicated to operate and implement, SP-05 was the recommended ALC configuration for non-

Newtonian fluids in vessels similar in dimension to the one used in PNNL testing. The selected ALC configuration for use in the 8-ft vessel at MCE should provide sufficient supplemental mixing to the vessel; additional improvements may be achieved by undertaking additional study.

8.0   Recommendations and Future Work

The objective of the PNNL study was to provide a recommendation for testing in the 8-ft vessel located at MCE. The study included a Newtonian liquid testing phase, where several ALC configurations were demonstrated to be effective in lifting (solid particles up to ~6 mm) and distributing (solid particles with diameters between 500 and 750 μm) throughout the upper region of the fluid in the test vessel. However, the non-Newtonian simulant testing showed that effective mobilization of a yield stress fluid, where "effective" was defined as shearing/moving the slurry in the upper half of the tank, was more challenging for the ALC. Based on the work conducted in this study, investigating the mobilization of a non-Newtonian fluid at or near the rheological boundary of 30 Pa/30 cP is proposed as the most critical test scenario for selecting an ALC configuration. Note that a Newtonian simulant with high solids content (solid loadings did not exceed 1 wt% in PNNL testing) or a different non-Newtonian simulant with fast-settling solids may be more limiting in terms of ALC performance, but they have not yet been examined experimentally.

Assuming performance in a non-Newtonian fluid is the limiting case for this study, an ALC that is centrally located in the tank with the following features is recommended for use in the 8-ft MCE vessel:

- Nominally 18-in. ID riser tube, 5 ft in length

- Riser tube installed at least 5 in. off the bottom

- Air tube running along the outside of the riser tube, with at least 1-in. ID, capable of supplying at least 30 scfm of air

- Air injection point at or near the bottom, open geometry air distributor, and centrally located in the riser tube cross-section.

The last two recommended features are not considered to be as critical as the first two recommended features, and variations on the air tube configuration may yield similar performance. The PNNL configuration possessing the same recommended features was designated SP-05. SP-05 mobilized nearly the entire upper half of the clay slurry in the PNNL test vessel and should provide adequate supplemental mixing in a vessel of similar dimensions. Note that preliminary successful testing with SP-05p (the same configuration as SP-05 with a second air tube that supplied pulses of air) suggests that, with regard to non-Newtonian fluid mobilization, it may be possible to motivate nearly all the non-Newtonian fluid in the tank. It is also recommended that this modification to the "traditional" ALC be investigated further, or alternatively, a similar pulsed air technology using a parallel plate device, e.g. PPM.

The testing described in this report indicates the ALC is a mixing system that generates significant recirculating flow that can transport solid particles and mobilize yield stress fluids in the upper parts of a vessel. The upwelling circulating flow supplied by a centrally located ALC system has some overlap with the expected performance of a PJM system, which may form a cavern in a non-Newtonian fluid that the ALC could disrupt or enhance by its influence on flow fields. Any disruption might be mitigated by increasing the elevation of the bottom of the riser tube, for example. Both the configuration and operation of an ALC device are relatively simple and it appears to be suitable as a potential supplemental mixing system for WTP vessels (SHSVs).

The scope of the testing did not allow an evaluation of the ALC against all anticipated conditions in the WTP, and thus there remains some uncertainty regarding the robustness of its performance, though this could likely be mitigated by "tuning" operation of the ALC in response to changing conditions in the SHSV. It is strongly recommended that uncertainties be evaluated with other testing (for instance, in the 8-ft MCE vessel) in order to provide confidence that the ALC will perform its intended functions across a range of processing conditions. There is not a sufficient amount of applicable prior work (specifically for non-Newtonian fluids) to predict ALC performance for this application. For example, one of the reasons mobilizing/shearing fluid in the vessel is important is the requirement that flammable gas be released continuously in normal operations and periodically in off-normal events to prevent a hazardous build-up of retained gas. Thus, performing a gas release test with the ALC in a non-Newtonian fluid is important. A successful gas release test would confirm that the mobilization observed in the APEL test vessel was sufficient to release most of the retained gas.

There are additional design, performance, and operability considerations that may affect the suitability of an ALC as a supplemental mixing system that have not been investigated experimentally in this report. Some of these considerations are related to refining elements of the system and others concern installation or implementation of the ALC in a WTP vessel. These considerations include the following items (the list is not intended to be exhaustive):

- The use of a diverter to channel PJM jets and reduce the tendency of solids to pile up underneath ALC suction

- The generation of aerosol during ALC operation (particularly if the outlet of the riser tube is exposed at lower slurry fill levels) and mitigation of same, if needed

- Probability of plugging of ALC air line(s), particularly if a continual flow of air is not used during operation and prevention of same, if needed

- Operation of the recommended ALC system (5-ft riser length) when the liquid is at full working level (~16 ft) or the minimum batch level, which may approach the riser tube length or be below the riser tube outlet

- Changes in ALC performance with a prototypic semi-elliptical tank floor geometry, though this is expected to be a beneficial change, e.g., in terms of "funneling" particles and slurry toward the ALC inlet, compared to the use of flat-bottom tank in PNNL testing

- Interface of ALC circulation pattern with PJM jets when they are in the drive phase, and/or the interaction of PJM upwell with ALC upwell

- Effect of any internal structures, such as PJM bodies, other instruments, etc., present in the tank on the flow patterns generated by operation of the ALC (by contrast, the PNNL test tank was open and had essentially no obstructions)

- Method to install and secure the ALC in a WTP vessel

- Scale-up of recommended device to the expected full-scale vessel (16-ft diameter), which could require, for example, a larger riser tube (either in diameter, height, or both) than was tested by PNNL or multiple riser tubes

The considerations listed are provided for reference and likely will require additional experimental studies or design work to address. These topics are, by and large, refinements to the design and

implementation of an ALC and do not represent serious obstacles to the technology performing its intended function. Some of these issues could be investigated in the interim prior to implementation of an ALC system in the 8-ft MCE test vessel.

9.0 References

Arbib Z, J Ruiz, P Alvarez-Diaz, C Garrido-Perez, J Barragan, and JA Perales. 2013. "Long term outdoor operation of a tubular airlift pilot photobioreactor and a high rate algal pond as tertiary treatment of urban wastewater." *Ecological Engineering*, 52: 143-153.

Ballou RA. 1994. *Identification of Single-Shell Tank In-Tank Hardware Obstructions to Retrieval at Hanford Site Tank Farms*. WHC-SA-2447-FP, Westinghouse Hanford Company, Richland, Washington.

Bamberger JA, PA Meyer, JR Bontha, CW Enderlin, DA Wilson, AP Poloski, JA Fort, ST Yokuda, HD Smith, F Nigl, MA Friedrich, DE Kurath, GL Smith, JM Bates, and MA Gerber. 2005. *Technical Basis for Testing Scaled Pulse Jet Mixing Systems for Non-Newtonian Slurries*. PNWD-3551 (WTP-RPT-113, Rev. 0), Battelle – Pacific Northwest Division, Richland, Washington.

Bello, RA, CW Robinson, and M Moo-Young. 1984. "Liquid Circulation and Mixing Characteristics of Airlift Contactors." *Canadian Journal of Chemical Engineering*, 62: 573-577.

Beris AN, JA Tsamopoulos, RC Armstrong, and RA Brown. 1985. "Creeping motion of a sphere through a Bingham plastic." *Journal of Fluid Mechanics*, 158: 219-244.

Blazej M, M Kisa, and J Markos. 2004. "Scale influence on the hydrodynamics of an internal loop airlift reactor." *Chemical Engineering and Processing*, 43: 1519-1527.

Calvo EG. 1989. "Comments on liquid circulation in airlift reactors." *Chemical Engineering Science*, 44(5): 1269.

Camenen B. 2007. "Simple and General Formula for the Settling Velocity of Particles." *Journal of Hydraulic Engineering*, 133: 229-233.

Cerri MO, L Futiwaki, CDF Jesus, AJG Cruz, and AC Badino. 2008. "Average shear rate for non-Newtonian fluids in a concentric-tube airlift bioreactor." *Biochemical Engineering Journal*, 39: 51-57.

Chisit MY and M Moo-Young. 1987. "Airlift Reactors: Characteristics, Applications and Design Considerations." *Chemical Engineering Communications*, 60: 195-242.

Chisti MY and M Moo-Young. 1988. "Gas Holdup Behaviour in Fermentation Broths and Other Non-Newtonian Fluids in Pneumatically Agitated Reactors." *The Chemical Engineering Journal*, 39: B31-B36.

Chisti MY, B Halard, and M Moo-Young. 1988. "Liquid Circulation in Airlift Reactors." *Chemical Engineering Science*, 43(3): 451-457.

Chisti MY and M Moo-Young. 1989. "Authors' reply to comments by E. Garcia Calvo." *Chemical Engineering Science*, 43(5): 1270-1271.

Cook MW and ED Waters. 1955. *Operational Characteristics of Submerged Gas-Lift Circulators*. HW-39432, Hanford Atomic Products Operation, Richland, Washington.

Cozma P and M Gavrilescu. 2012. "Airlift Reactors: Applications in Wastewater Treatment." *Environmental Engineering and Management Journal*, 11(8): 1505-1515.

Daymo EA. 1997. *Industrial Mixing Techniques for Hanford Double-Shell Tanks.* PNNL-11725, UC-721, Pacific Northwest National Laboratory, Richland, Washington.

Dunn J and WJ Van Slyke. 1964. *Evaluation of Prototype Air-Lift Circulator for 241-AX Tank.* HW-81666, Hanford Atomic Products Operation, Richland, Washington.

Gavrilescu M and RZ Tudose. 1998. "Hydrodynamics of non-Newtonian liquid in external-loop airlift bioreactors. Part 2: Study of the liquid circulation velocity." *Bioprocess Engineering*, 18: 83-89.

Gumery F, F Ein-Mozaffari, and Y Dahman. 2009. "Characterisitics of Local Flow Dynamics and Macro-Mixing in Airlift Column Reactors for Reliable Design and Scale-Up." *International Journal of Chemical Reactor Engineering,* 7(1): Review R4.[1]

Heijnen JJ, J Hols, RGJM van der Lans, HLJM van Leeuwen, A Mulder, and R Weltevrede. 1997. "A simple hydrodynamic model for the liquid circulation velocity in a full-scale two- and three-phase internal airlift reactor operating in the gas recirculation regime." *Chemical Engineering Science*, 52(15): 2527-2540.

Jin B, P Yin, and P Lant. 2006. "Hydrodynamics and mass transfer coefficient in three-phase air-lift reactors containing activated sludge." *Chemical Engineering and Processing*, 45: 608-617.

Jossic L and A Magnin. 2001. "Drag and Stability of Objects in a Yield Stress Fluid." *AIChE Journal*, 47(12): 2666-2672.

Kassab SZ, HA Kandil, HA Warda, and WH Ahmed. 2007. "Experimental and analytical investigations of airlift pumps operating in three-phase flow." *Chemical Engineering Journal*, 131: 273-281.

Kassab SZ, HA Kandil, HA Warda, and WH Ahmed. 2009. "Air-lift pumps characteristics under two-phase flow conditions." *International Journal of Heat and Fluid Flow*, 30: 88-98.

Kawase Y and M Moo-Young. 1986a. "Influence of Non-Newtonian Flow Behavior on Mass Transfer in Bubble Columns With and Without Draft Tubes." *Chemical Engineering Communications*, 40: 67-83.

Kawase Y and M Moo-Young. 1986b. "Mixing and Mass Transfer in Concentric-Tube Airlift Fermenters: Newtonian and non-Newtonian Media." *Journal of Chemical Technology and Biotechnology*, 36: 527-538.

Kennard M and M Janekeh. 1991. "Two- and Three-Phase Mixing in a Concentric Draft Tube Gas-Lift Fermentor." *Biotechnology and Bioengineering*, 38: 1261-1270.

Kojima H, J Sawai, H Uchino, and T Ichige. 1999. "Liquid circulation and critical gas velocity in slurry bubble column with short size draft tube." *Chemical Engineering Science*, 54: 5181-5185.

---

[1] ISBN 1542-6580 – no page numbers associated with this publication.

Khalil MF, KA Elshorbagy, SZ Kassab, and RI Fahmy. 1999. "Effect of air injection method on the performance of an air lift pump." *International Journal of Heat and Fluid Flow*, 20: 598-604.

Kondo M, R Slaby, R Rubin, and BK Barringer Jr. 2008. "Enhanced Grit Removal in Small and Large Wastewater Operations with Geyser Hybrid Pump." Presented 20 October 2008 at Water Environment Federation Technical Exhibition and Conference (WEFTEC), Chicago, Illinois.

Krieg SA, WW Jenkins, KJ Leist, KG Squires, and JF Thompson. 1990. *Single-Shell Tank Waste Retrieval Study*. WHC-EP-0352 (UC-721), Westinghouse Hanford Company, Richland, Washington.

Kuhn WL, DR Rector, SD Rassat, CW Enderlin, MJ Minette, JA Bamberger, GB Josephson, BE Wells, and EJ Berglin. 2013. *Scaling Theory for Pulse Jet Mixed Vessels, Sparging, and Cyclic Feed Transport Systems for Slurries*. PNNL-22816, Pacific Northwest National Laboratory, Richland, Washington.

Kurath DE, BD Hanson, MJ Minette, DL Baldwin, BM Rapko, LA Mahoney, PP Schonewill, RC Daniel, PW Eslinger, JL Huckaby, JM Billing, PS Sundar, GB Josephson, JJ Toth, ST Yokuda, EBK Baer, SM Barnes, EC Golovich, SD Rassat, CF Brown, JGH Geeting, GJ Sevigny, AJ Casella, JR Bontha, RL Aaberg, PM Aker, CE Guzman-Leong, ML Kimura, SK Sundaram, RP Pires, BE Wells, and OP Bredt. 2009. *Pretreatment Engineering Platform Phase 1 Final Test Report*. PNNL-18894; WTP-RPT-197 Rev 0, Pacific Northwest National Laboratory, Richland, WA.

Lamont AGW. 1958. "Air agitation and pachuca tanks." *Canadian Journal of Chemical Engineering*, 36: 153-160.

Lewis BE. 1986. *Solids Suspension and Transfer Studies in a Model Digester Tank*. ORNL/TM-9886, Oak Ridge National Laboratory, Oak Ridge, Tennessee.

Li S, T Qi, Y Zhang, and C Liu. 2009. "Hydrodynamics of a Multi-Stage Internal Loop Airlift Reactor." *Chemical Engineering Technology*, 32(1): 80-85.

Liang N-K and H-K Peng. 2005. "A study of air-lift artificial upwelling." *Ocean Engineering*, 32: 731-745.

Lu W-J, S-J Jwamg and C-M Chang. 1994. "Liquid Mixing in Internal Loop Airlift Reactors." *Industrial Engineering and Chemistry Research*, 33: 2180-2186.

Luo H-P and MH Al-Dahhan. 2008. "Macro-mixing in a draft-tube airlift bioreactor." *Chemical Engineering Science*, 63: 1572-1585.

Margaritis A and JD Sheppard. 1981. "Mixing Time and Oxygen Transfer Characteristics of a Double Draft Tube Airlift Fermentor." *Biotechnology and Bioengineering*, 23: 2117-2135.

Martinez AMM and EME Silva. 2013. "Airlift Bioreactors: Hydrodynamics and Rheology Application to Secondary Metabolites Production." Chapter 15 in Mass Transfer - Advances in Sustainable Energy

and Environment Oriented Numerical Modeling, H Nakajima (Ed.), ISBN: 978-953-51-1170-2, InTech, DOI: 10.5772/53711.[1]

McQuillan KW and PB Whalley. 1985. "Flow Patterns in Vertical Two-Phase Flow." *International Journal of Multiphase Flow,* 11(2): 161-175.

Meachem JE, SJ Harrington, JS Rodriguez, VC Nguyen, JG Reynolds, BE Wells, GF Piepel, SK Cooley, CW Enderlin, DR Rector, J Chun, A Heredia-Lagner, and RF Gimpel. 2012. *One System Evaluation of Waste Transferred to the Waste Treatment Plant*. RPP-RPT-51652, Rev. 0, Washington River Protection Solutions LLC, Richland Washington.

Mehrotra SP and R Shekhar. 2000. "Studies on particle suspension in air-agitated Pachuca tanks." *Proceedings of Processing of Fines*, PROF-2000 (NML, Jamshedpur, November 2000): 345-361.

Mehrotra SP and Shekhar. 2001. "Particle suspension in air agitated tanks: Investigation of hysteresis and novel split air injection technique." *Metallurgical Transactions B,* 32B: 223-231.

Merchuk JC. 1986. "Gas Hold-Up and Liquid Velocity in a Two-Dimensional Air Lift Reactor." *Chemical Engineering Science*, 41(1): 11-16.

Merchuk JC. 1990. "Why use air-lift bioreactors?" *Trends in Biotechnology*, 8: 66-71.

Merchuck JC, A Contreras, F Garcia, and E Molina. 1998. "Studies of mixing in a concentric tube airlift bioreactor with different spargers." *Chemical Engineering Science*, 53(4): 709-719.

Miller RL and MB Cain. 1986. "Prediction of Flow Regime Transitions in Vertical Upward Three Phase Gas-Liquid-Solid Flow." *Chemical Engineering Communications*, 43: 147-163.

Miron AS, M-CC Garcia, FG Camacho, EM Grima, and Y Chisti. 2004. "Mixing in Bubble Column and Airlift Reactors." *Chemical Engineering Research and Design*, 82(A10): 1367-1374.

Morrison GL, TI Zeineddine, M Henriksen, and GB Tatterson. 1987. "Experimental Analysis of the Mechanics of Reverse Circulation Air Lift Pump." *Industrial Engineering and Chemistry Research*, 26: 387-391.

Poloski AP, ST Arm, JA Bamberger, B Barnett, R Brown, BJ Cook, CW Enderlin, MS Fountain, M Friedrich, BG Fritz, RP Mueller, F Nigl, Y Onishi, LA Schienbein, LA Snow, S Tzemos, M White, and JA Vucelick. 2005. *Technical Basis for Scaling of Air Sparging Systems for Mixing in Non-Newtonian Slurries.* PNWD-3541 (WTP-RPT-129, Rev. 0), Battelle – Pacific Northwest Division, Richland, Washington.

Powell MR. 1997. *Retrieval Process Development and Enhancements Pulsed-Air Mixing DOE Site Assessment.* PNNL-11584, Pacific Northwest National Laboratory, Richland, WA.

---

[1] Available from: http://www.intechopen.com/books/mass-transfer-advances-in-sustainable-energy-and-environment-oriented-numerical-modeling/airlift-bioreactors-hydrodynamics-and-rheology-application-to-secondary-metabolites-production

Powell MR and CR Hymas. 1996. *Retrieval Process Development and Enhancements FY96 Pulsed-Air Mixer Testing and Deployment Study*. PNNL-11200, Pacific Northwest National Laboratory, Richland, Washington.

Russell AB, CR Thomas, and MD Lilly. 1994. "The Influence of Vessel Height and Top-Section Size on the Hydrodynamics Characteristics of Airlift Fermentors." *Biotechnology and Bioengineering*, 43: 69-76.

Russell RL, SD Rassat, ST Arm, MS Fountain, BK Hatchell, CW Stewart, CD Johnson, PA Meyer, and CE Guzman-Leong. 2005. *Final Report: Gas Retention and Release in Hybrid Pulse Jet Mixed Tanks Containing Non-Newtonian Waste Simulants*. PNWD-3552 (WTP-RPT-114, Rev. 1), Battelle—Pacific Northwest Division, Richland, WA.

Salser BR and CR Mock. 1973. "An Air-Lift Circulator for Algal Culture Tanks." *Proceedings of the Annual Workshop – World Mariculture Society,* 4 (1-4): 295-298.

Samaras VC and DP Margaris. 2005. "Two-phase flow regime maps for air-lift pump vertical upward gas-liquid flow." *International Journal of Multiphase Flow*, 31: 757-766.

Schlotelburg C, M Gluz, M Popovic, and JC Merchuk. 1999. "Characterization of an Airlift Reactor with Helical Flow Promoters." *Canadian Journal of Chemical Engineering*, 77: 804-810.

Schonewill PP, MK Edwards, C Smith, R Tranbarger, RW Shimskey, and RA Peterson. 2011. *Integrated Near-Tank Treatment System Pilot Demonstration*. PNWD-4298, Battelle—Pacific Northwest Division, Richland, Washington.

Serne RJ, GA Whyatt, SV Mattigod, Y Onishi, PG Doctor, BN Bjomstad, MR Powell, LM Liljegren, JH Westsik, Jr., N. Aimo, KP Recknagle, GR Golcar, TB Miley, GR Holdren, DW Jeppson, RK Biyano, and GS Barney. 1996. *Fluid Dynamics, Particulate Segregation, Chemical Processes and Tank Inventory Discussions that Relate to the Potential for Criticality in Hanford Tanks.* WHC-SD-WM-TI-757, Rev. 0, Westinghouse Hanford Company, Richland, Washington.

Siegel MH, JC Merchuk, and K Schugerl. 1986. "Air-Lift Reactors Analysis: Interrelationships Between Riser, Downcomer, and Gas-Liquid Separator Behavior, Including Gas Recirculation Effects." *AIChE Journal*, 32(10): 1585-1596.

Sorenson PF. 1985. "A simple mathematical model for the calculation of pumping rate in an air-agitated pachuca tank." *Journal of the South African Institute of Mining and Metallurgy*, 85(1): 23-27.

Stewart CW, MS Fountain, JL Huckaby, LA Mahoney, PA Meyer, and BE Wells. 2005. *Effects of Globally Waste-Disturbing Activities on Gas Generation, Retention, and Release in Hanford Waste Tanks*. PNNL-13781, Rev. 3, Pacific Northwest National Laboratory, Richland, Washington.

Stewart CW, ME Brewster, PA Gauglitz, LA Mahoney, PA Meyer, KP Recknagle, and HC Reed. 1996. *Gas Retention and Release Behavior in Hanford Single-Shell Tanks*. PNNL-11391, Pacific Northwest National Laboratory, Richland, Washington.

Sun S, C Liu, W Wei, and X Bao. 2006. "Hydrodynamics of an annulus airlift reactor." *Powder Technology*, 162: 201-207.

Taitel Y, D Bornea, and AE Dukler. 1980. "Modelling Flow Pattern Transitions for Steady Upward Gas-Liquid Flow in Vertical Tubes." *AIChE Journal*, 26(3): 345-354.

Tobajas M, E Garcia-Calvo, MH Siegel, and SE Aptiz. 1999. "Hydrodynamics and mass transfer prediction in a three-phase airlift reactor for marine biotreatment." *Chemical Engineering Science,* 54(21): 5347-5354.

Velan M and TK Ramanujam. 1992. "Hydrodynamics and mixing in down flow jet loop bioreactor with a non-Newtonian fluid." *Bioprocess Engineering*, 7: 193-197.

Wachi S, AG Jones, and TP Elson. 1991. "Flow Dynamics in a Draft-Tube Bubble Column Using Various Liquids." *Chemical Engineering Science*, 46(2): 657-663.

Washenfelder DJ, DA Barnes, JW Ficklin, JG Field, MA Fish, DG Harlow, and EC Shallman *Tank 241-SX-110 Leak Assessment Report.* RPP-ASMT-47140, Rev 0, Washington River Protection Solutions, Richland, Washington.

Waters ED. 1994. *Background and Status of Hanford's DST Retrieval Technology.* WHC-SD-WM-TI-593, Rev. 0, Westinghouse Hanford Company, Richland, Washington.

Whyatt GA and CR Hymas. 1997. *Bench-Scale Feasibility Testing of Pulsed-Air Technology for In-Tank Mixing of Dry Cementitious Solids with Tank Liquids and Settled Solids*. PNNL-11690, Pacific Northwest National Laboratory, Richland, Washington.

Wyatt GA, RJ Serne, SV Mattigod, Y Onishi, MR Powell, JH Westsik, Jr., LM Liljegren, GR Golcar, KP Recknagle, PM Doctor, VG Zhimov, and J Dixon. 1996. *Potential for Criticality in Hanford Tanks Resulting from Retrieval of Tank Waste.* PNNL-11304, Pacific Northwest National Laboratory, Richland, Washington.

Yu W, T Wang, F Song, and Z Wang. 2009. "Investigation of the Gas Layer Height in a Multistage Internal-Loop Airlift Reactor." *Industrial and Engineering Chemistry Research*, 48: 9278-9285.

Yu W, T Wang, M Liu, and F Song. 2010. "Investigation of Operation Regimes in a Multistage Internal-Loop Airlift Reactor." *Industrial and Engineering Chemistry Research*, 49: 11752-11759.

Zabaras G, AE Dukler, and D Moalem-Maron. 1986. "Vertical Upward Concurrent Gas-Liquid Annular Flow." *AIChE Journal*, 32(5): 829-843.

Zenz FA. 1993. "Explore the Potential of Air-Lift Pumps and Multiphase." *Chemical Engineering Progress*, August 1993: 51-56.

Appendix A

Description of Experimental Equipment and Methods

Appendix A

Description of Experimental Equipment and Methods

This appendix includes details of the experimental equipment and methods used to perform the testing of ALC and related mixing systems described in the report. It includes methods that may not have been used to collect data that is reported. The appendix has three main sections. Section A.1 presents a full description of the test stand and associated equipment. Section A.2 describes the general test set-up, instruments used to collect information, and methods to perform test operations. Section A.3 contains a description of all the various ALC mixing systems that were investigated during the testing.

A.1 Description of Test Stand

A.1.1 General Layout

All airlift circulator (ALC) testing was done in the Pacific Northwest Nation Laboratory (PNNL) Applied Process Engineering Laboratory (APEL) high bay facility designated as Room 184. The test area is fenced and access is limited to authorized personnel only. The main test support components were a 3000-gal test tank sitting inside a secondary 24 mil polyvinyl chloride (PVC) 4488-gal portable containment berm (UltraTech / Economical Design part no. 8627), 1-ft high and 12 ft × 50 ft, with a 7-ft-high and 2-ft-wide scaffolding with wood deck around three sides of the tank and a moveable A-frame gantry crane that could bridge both the tank and scaffolding (see Figure A.1).
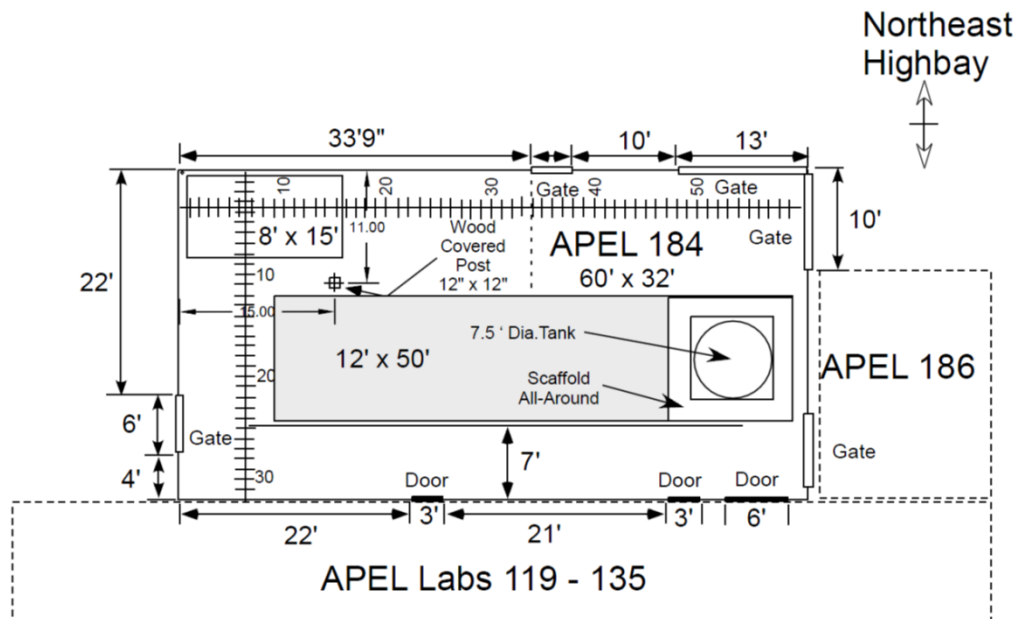
Figure A.1. General Space Layout – APEL 184.

A.1

A.1.2   Tank and Plumbing for Fluid Transfers

All ALC testing was done in a 3000-gal vertical plastic tank from Snyder Industries (part no. 5130000N) with a flat bottom and domed top. The tank had a diameter of 90 in., was 125.6 in. high, and had a maximum fluid fill height of 109.5 in. (see Figure A.2a). The tank dome area was modified to allow general access through a large center cutout and instrumentation and visual access through eight holes along the outer edge (see Figure A.2b). The tank was also modified on the sides to insert bulkhead pipe fittings for the pumping used to fill, recirculate, decant, and drain the tank fluid.
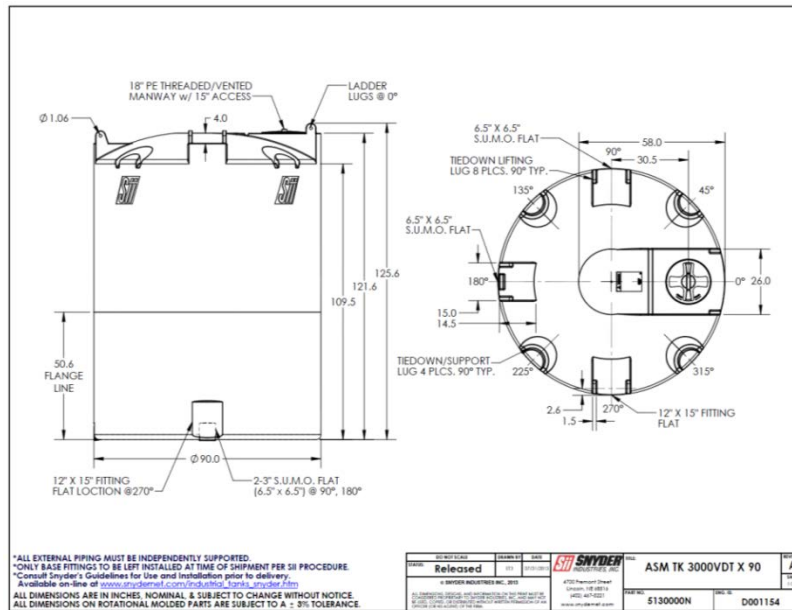
(a)
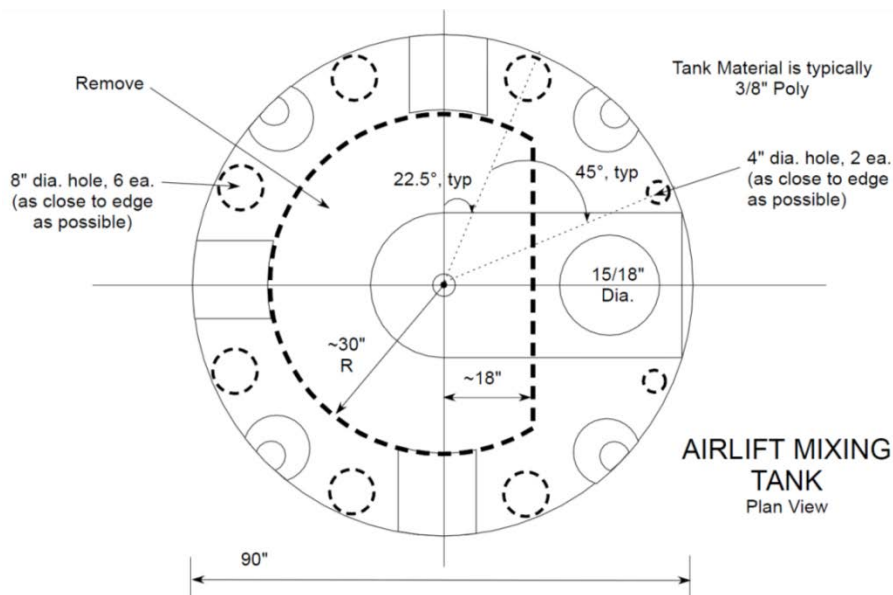
(b)

Figure A.2. Original Tank Detail (a) and Tank Dome Modification Detail (b).

A.1.3   Scaffolding and Gantry

For personnel access to the tank, metal scaffolding with a wood floor, a ladder, and a top safety gate was built around three sides of the tank approximately 8 ft above ground level (see Figure A.3). To move ALC equipment in and out of the tank, a moveable 5-ton-capacity A-frame gantry crane (Wallace Model 5T19-20AC) with an overall height of 19 ft 1 in. (229 in.) and a clear span of 14 ft 1 in. (160 in.) was used. During ALC testing, the A-frame gantry crane was fitted with three hoists/chain falls on roller trollies riding on the overhead beam, providing 191 to 196 in. lift range above the floor. They were as follows:

- One 2-ton electric chain trolley suspension (plain trolley); Coffing JLC Model JLCET-4008, serial number JMA1650YC. Total lift distance of 194 in. above floor.

- One 2-ton manual chain fall, Harrington CF4. Total lift distance of 191 in. above floor.

- One 1-ton manual chain fall, CM Series 622. Total lift distance of 196 in. above floor.

Because of the limited building height and crane height, two chain hoists were sometimes used to lift ALC devices over the tank end for insertion into the tank.

Figure A.3. Scaffolding and Gantry (before two additional cranes/hoist installed).

A.1.4   Test Fluid Use, Transfer, and Disposal

ALC testing used test simulants of either a Newtonian fluid (water) or a non-Newtonian clay slurry (80/20 wt% kaolin/bentonite clay mix). Prior to ALC testing, the tank was filled with the test fluid (water or clay slurry). Water and clay slurry were moved in and out of the tank using building water supply, gravity drain, or diaphragm pumping between totes/tanks. When water was no longer needed for testing, it was typically sent to the city drain after appropriate separation of solid particles by decant. When applicable, water samples were taken and analyzed prior to draining. Water material that could not be drained was held in totes/tanks for reuse or alternate disposal.

The clay slurry material was made at PNNL using dry powder from bags and various mixing devices. Completed clay slurry material was analyzed for constituents and rheology prior to use and was stored in totes. During testing, clay slurry samples were taken periodically and either analyzed or held for archive. Totes were used exclusively for all clay slurry transfers between the ALC test tank, and offsite disposal is planned after clay slurry is no longer required. During ALC testing, the clay slurry changed from its initial conditions even though no intentional adjustments were made. Details of the clay slurry can be found in Section 3.3.2.

Diaphragm pumps and associated hoses were used to move water and clay slurry to and from the PNNL ALC test tank during fill and empty operations. Totes and smaller tanks were used as buffer tanks for fluid that was not approved to be discharged to building drain. Two diaphragm pumps were used during ALC testing to pump fluids:

- Wilden M8 2-in. Double Diaphragm Pump Model M8 (see Figure A.4) – Air driven, self-priming, flow rate 0 to 75 gpm, maximum pressure 125 psi, maximum solids handled 0.25 in., dimensions 16 in. long × 14 in. wide × 26 in. high, weight 90+ lb.

- Sandpiper HDF2 DP6SI Type 6, Serial #1633195 (see Figure A.5) – Air driven, self-priming, flow rate 0 to 140 gpm, maximum pressure 125 psi, maximum solids handled 2 in., dimensions 22 in. long × 14 in. wide × 21 in. high, weight 86+ lb.

The diaphragm pumps used building air, and an air valve on each pump was adjusted to change pumping speed as required by testing activity.

A.1.4.1 Bottom Sweeping – Newtonian Water Testing Only

For ALC Newtonian testing with water and particles, two methods were developed to clear particles that settled on the flat tank bottom edge and move these particles toward the center of the tank where the ALC inlet was located. In both methods, water was drawn from an upper elevation of the tank through one of two bulkhead fittings on the side of the tank with valving and fed to a diaphragm pump that pressurized the water and distributed it to four evenly spaced radial locations at the bottom of the tank using a manifold, four 1-in. hose lines, and four 1-in. bulkhead fittings near the tank bottom (see Figure A.6 and Figure A.7).

Figure A.4. Diaphragm Pumps: Wilden.

Figure A.5. Diaphragm Pumps: Sandpiper.
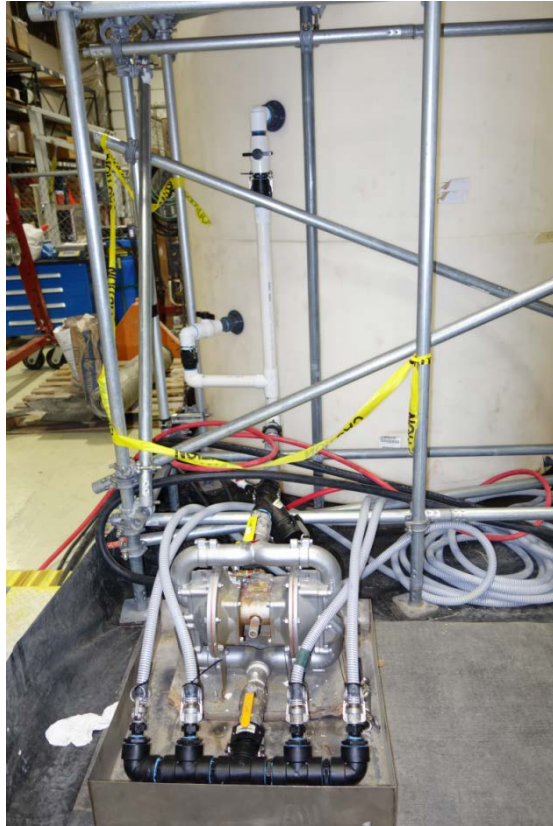
Figure A.6. Bottom Sweeping Pumping Arrangement.

Figure A.7. Tank Bottom with Bulkhead Fittings and Tank Markings (bottom and sides).

Nozzles

Initially four nozzles, each with a different configuration (see Figure A.8), were constructed, installed, and tested. These fixed nozzles provided some particle motivation but left "dead zones" between the nozzles where particles were not moved (see Figure A.9) and were not efficient for the amount of flow they required to move solid particles.
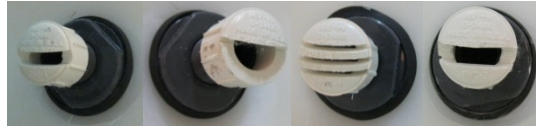
Figure A.8. Nozzle Configurations.
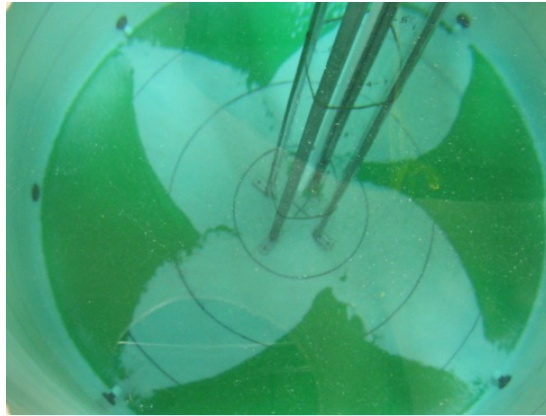
Figure A.9. Bottom Clearing Results Using Nozzles.

Sprinklers

The four nozzles were replaced with eight sprinklers (two at each nozzle location) that rotated 360 degrees and constantly swept the floor with a jet stream (see Figure A.10). The rotating nozzles were not synchronized, so particles were not always immediately moved to the ALC suction (as they moved between adjacent sprinkler zones), but eventually they were moved to the center. The sprinkler arrangement could adequately move the particles used in water testing to within a ~1.5-ft radius of center but did not have a large enough motivating force to push particles to or through the tank center. Not moving the particles under the ALC was the desired PNNL testing parameter to limit the influence of ALC operation by any outside forces. It is likely that the sprinkler system could have been modified by adding sprinklers and/or moving it further from the wall to allow the particles to be pushed directly under the ALC inlet on the floor.

The specific sprinklers used were Nana 525 sprinklers installed with red 4-mm nozzles (see Figure A.11). Per the vendor literature, flow output from each nozzle is approximately 4.53 to 5.20 gpm at 43 to 58 psi discharging in air. In this testing application, discharge pressure was estimated to be around 45 psi but instead of air it discharged into water at a depth of approximately 8 ft. Zone of influence of these sprinklers for bottom clearing was estimated at around 3- to 4-ft radius.
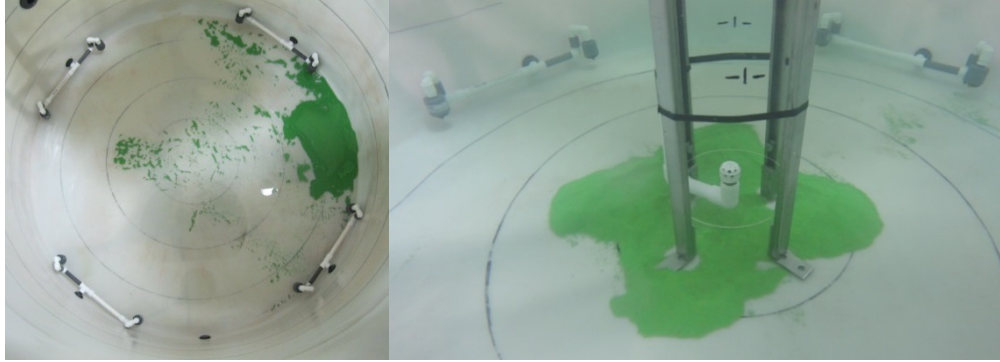
Figure A.10. Sprinkler Installation in Tank: all eight sprinklers (left), bottom clearing results using sprinklers (right)

Figure A.11. Sprinkler Details.

A.1.4.2 Tank Fill – Water

The building water supply or water stored in tanks/totes was used to fill the ALC tank. Water was added to the tank using a secured hose that discharged into the open tank top.

A.1.4.3 Tank Draining – Water

Emptying the tank was more involved than filling as there are restrictions on what can be discharged to the APEL building drain. Effectively clean process water in the tank could be pumped directly to the drain, but the more typical case was to pump into totes. Water in totes was discharged to the APEL drain after sample approval and often included storage tank decanting and a filter system to trap residual particles.

A.1.4.4   Tank Fill – Clay Slurry

Clay slurry tank filling was done from the bottom of the tank through one or more of the four 2-in. bulkhead connections (see Figure A.12). The four 1-in. connections used for water nozzles/sprinklers were removed for clay slurry testing. Pipe/hose extensions were added to the 2-in. bulkhead in the tank to route the clay slurry discharge at the tank floor and toward the center of the tank. These extensions, along with an inline static mixer outside the tank and simulated gas release injection port were added in anticipation of gas release testing to determine operating parameters and characteristics (e.g., fill rate) if gas release testing was done (ultimately, gas release testing was not performed[1]). After initial testing of clay slurry tank filling, it was found that for non-gas release testing, one fill point in the tank was adequate and extensions were not necessary, so some of the extensions were removed. The inline static mixer was left in, even though it was not needed for non-gas release testing, because it did not impede tank filling with clay slurry. The start of a tank filling with clay slurry using only one extension is shown in Figure A.13 and was the normal mode of operation for most of the tank clay slurry fills.
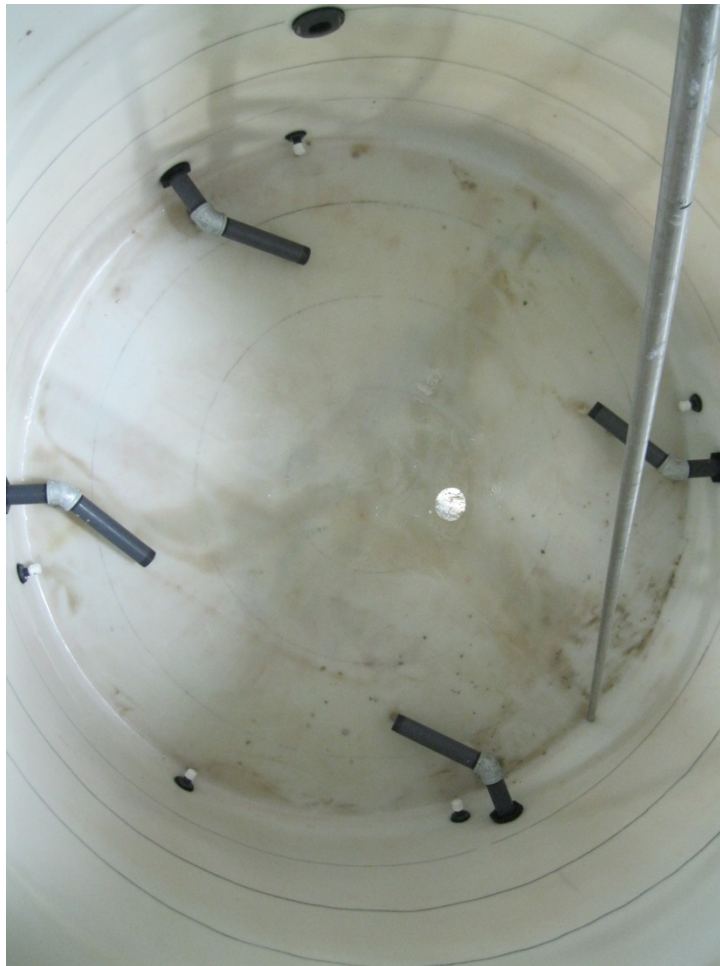
Figure A.12. Tank Clay Slurry Fill Configuration with Extensions at All Fill Locations.

---

[1] A small-scale gas release test was conducted using the clay slurry in preparation for a larger scale experiment. Details of this experiment can be found in LRB BNW-61799, pgs. 119-123 but they are not reported here.
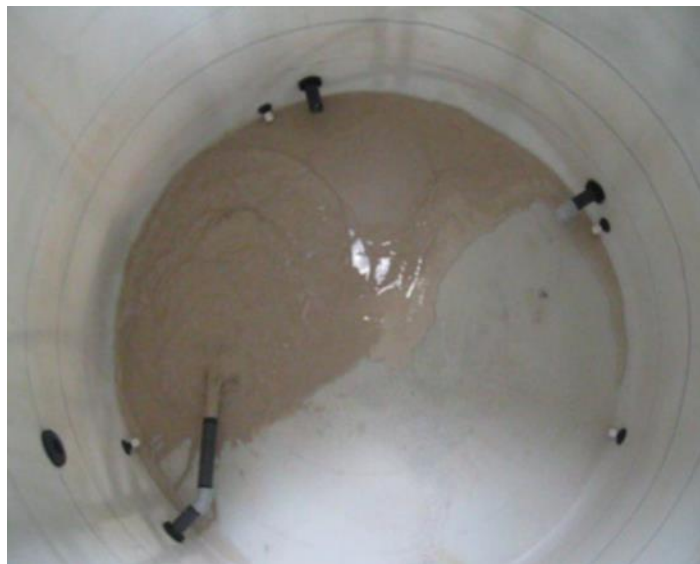
Figure A.13. Tank Clay Slurry Fill Configuration, Typical for Testing.

All clay slurry tank fills were done from totes. The clay slurry material was stored in totes of sizes ranging from nominally 250 and 300 gal capacity. Each clay slurry tote was moved into location for pumping and connected to the suction side of a diaphragm pump using a 2-in. hose connected to a bottom-valved nozzle on the tote (refer to Figure A.14). The diaphraghm pump discharged the clay slurry through the 2-in. hose into the bottom of the tank via the 2-in. bulkhead connection and pipe extension(s). An inline static mixer (Koflo Model 2-40C-4-6-2, 2-in. PVC 6 blade, 19 in. long, maximum working pressure 140 psi, typical flow 9 to 60 gpm, pressure loss 0.25 to 9.25 psi) at the discharge of the diaphragm pump was used for all testing (see Figure A.15).

Figure A.14. Clay Slurry Tote and Diaphragm Pump Configuration.

Figure A.15. Static Inline Mixer Detail (to right of pump discharge valve located in center of picture).

A.1.4.5   Clay Slurry Makeup and Totes

Approximately 3000 gal of clay slurry consisting of ten 300-gal batches was made at PNNL for use in ALC testing. After makeup at another PNNL building, the clay slurry was delivered to APEL on September 22, 2014. Sealed totes were used to store and transport the clay slurry for ALC testing. When clay remained in the test vessel over a period of multiple days, it was covered with a plastic sheet when testing was not ongoing to mitigate water losses by evaporation and maintain a headspace that was more humid than the ambient air.

When clay slurry was pumped out of the ALC test tank at the end of a test sequence, it was routed to totes for storage. As totes were filled and emptied, they were weighed on a floor scale (typically using a forklift) to track the inventory of clay slurry used during testing.

A.1.4.6   Clay Slurry Tank Draining and Wash Down

When clay slurry was removed from the ALC test tank after a test run, it was generally pumped from the top in layers to capture any particles resident in each layer. The method and device used for particle capture during ALC tank pump down with clay slurry is detailed in Section A.2. Pump down of clay slurry using the bottom ports was an alternative method used to drain the tank, and all methods routed the pumped clay slurry to totes.

Final removal of clay from the bottom 2 to 3 in. was done using a squeegee to scrape the remaining clay to a moveable 1-in. lance suction at the bottom of the tank. The tank was then washed down to remove residual clay (if necessary). The initial wash water introduced into the tank was generally exisiting decanted waste water that contained some particulate but allowed the clay slurry to be liquefied and moved. The wash water was used to spray down the sides and bottom to remove remaining clay slurry. Final wash down used clean water and included flushing the side bulkhead fittings where tank fluid had seeped in. Another method used for residual clay slurry cleanout was to let the residual clay slurry "dry" and then strike the flexible poly tank lip and sides with a mallet (or similar) to drop contents to the bottom where they could be swept up and removed; this method generally required an extended drying time of several days.

A.2 Test Setup/Description and Instrumentation

A.2.1   Air Mixing Device Setup and Instrumentation

A.2.1.1   ALCs (Assembly/Installation/Positioning)

The ALCs used in the PNNL testing consisted of a vertical tube and air outlet near the bottom of the tube. The ALCs fabricated for testing were of various sizes, nominally 4, 10, 18, and 25 inches in diameter, and constructed of acrylic, PVC, or steel. ALC tube length was varied by either constructing multiple tube lengths or connecting various shorter ALC sections into longer sections. Where multiple shorter ALC sections were used to construct a longer ALC length, the joints were taped externally to eliminate leakage and make the ALC a continuous length.

The ALC tube was inserted into an adjustable ALC unistrut frame (see Figure A.16), which held the ALC tube diameter on four sides, with a landing unistrut feature on the bottom (feet) to distribute the weight of the ALC assembly on the tank floor and a top unistrut feature to lift and secure the ALC assembly during operation. The ALC was positioned within the ALC unistrut frame to provide the standoff distance from the tank floor required for testing. The ALC unistrut frame was made to accept a variety of ALC diameters up to 25 inches in diameter.

The other element of the ALC assembly was the air line, which was made of PVC or steel. The most typical air tube configuration used for the majority of testing followed the frame down from the surface, ran along the outside of the ALC tube to the bottom, and then wrapped around the bottom to position the air tube in the ALC tube at the bottom in the ALC tube inlet. In this typical configuration, air was expelled into the ALC tube via a multi-hole nozzle (see Figure A.17) that typically extended 3 in. into the ALC tube; later ALC testing used just an open air tube (see Figure A.18) that typically extended 2-1/8 in. into the ALC tube. For all testing, air tube lines and nozzles used 1-in. tube or pipe. The very first ALC testing (BM-01, BM-02 – see Table 3.4) used a diverter nozzle (see Figure A.19), and was the only case where the air tube was routed on the inside of the ALC tube. Some limited testing was done on an ALC hybrid (SP-05p) that used two air lines with an open air tube to provide continuous air and pulsed air to the ALC (see Figure A.20).

The ALC in the unistrut frame was lifted and lowered into the tank using the portable gantry crane and the top unistrut lifting feature. For water operation, radial positioning at the tank bottom was done visually using the ring lines on the bottom of the tank floor as guides. For clay slurry operation, visual radial positioning at the tank bottom was not possible, so instead the unistrut portion of the frame that protruded above the tank fluid level was centered in the tank and checked to make sure the frame was positioned vertically (i.e., not tilted, which would affect the ALC bottom position in the tank). Once the ALC was radially positioned, only the top of the unistrut frame was secured by poly ropes to rigid features on the top of the tank.

Prior to testing, the ALC air line was attached via a union coupling using 1-in. hose that routed from the air source (building air), air source pressure regulator, and air flow manifold assembly. To initiate testing, air was turned on and the desired air flow set at the air flow manifold assembly. At the end of testing, air flow was turned off. During most ALC operations, plastic covers were used to contain fluid in the tank, especially at high flow rates that often created large waves and/or splatter in the PNNL tank.
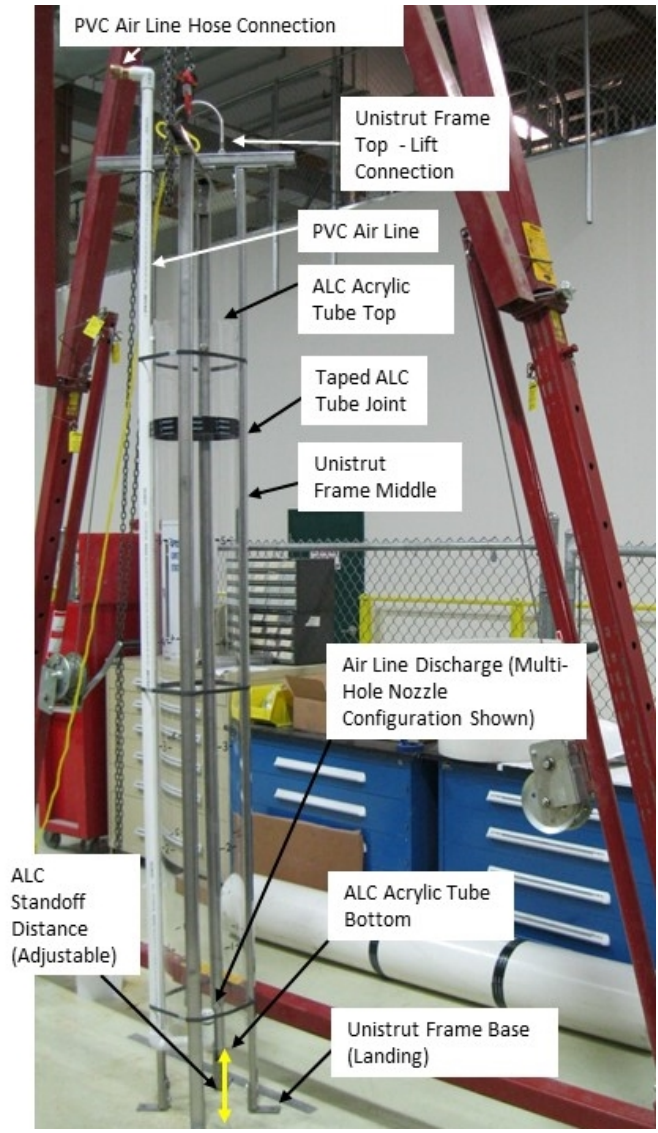
Figure A.16. Typical ALC in Unistrut Frame (shown: 10-in. acrylic tube, 5 ft long).

Figure A.17. ALC Nozzle with Air Line and Positioning Feature in ALC Tube.

Figure A.18. Open Pipe Nozzle – Air Line and Positioning Feature in ALC Tube.
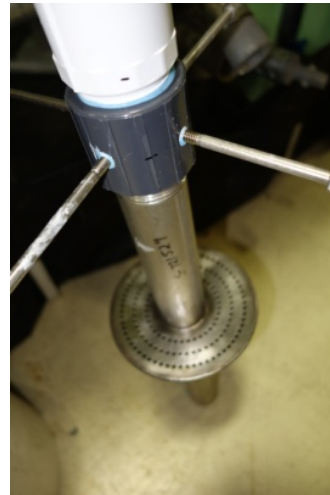
Figure A.19. Diverter Nozzle with Air Line and Positioning Feature in ALC Tube Used in BM-01 Test.

Figure A.20. Open Pipe Nozzle – Hybrid ALC SP-05p with Two Air Lines (normal and pulse modes).

A.2.1.2   Geyser Pump (Assembly/Installation/Positioning)

The Geyser pump was a modified ALC mixing device that included both a typical ALC and a pulse air option. The Geyser pump pulse function consisted of a chamber outside of the ALC tube that was filled with a volume of air and then intermittently released the air in a single slug. The air chamber filling would create buoyancy, so a large concrete ring was added to the bottom to counter this action. The large concrete ring would not allow the ALC unistrut frame to be used; however, the Geyser pump came with lifting eyes that allowed a lifting strap to be used to lower the Geyser pump into the tank. Without the unistrut frame, the Geyser pump could not be tied off at the top as was done for the ALC devices.

The Geyser pump also had two air lines: one for ALC operation and one for pulsing operation. These air lines were independent, allowing ALC only, pulse only, and simultaneous ALC and pulse (hybrid) operation. These air lines were the only thing exiting the surface of the PNNL tank and were tied to the flow metering assembly like the ALC, but used the air flow metering assembly valves to separate the air supply as needed for operation. During Geyser pump operation, sometimes the pump would move a small distance from tank center. When this happened, the Geyser pump was re-centered before testing continued. Geyser pump video taken in water during pulsing mode showed the pump jumping slightly as the large gas volume was released, and this likely contributed to the pump movement off centerline. Typically the Geyser pump is attached to or rigidly braced in the tank to secure the pump at location, but this ALC and poly tank did not make those options viable and it wasn't required for the ALC testing activities.

In water testing, the Geyser pump location on the PNNL tank bottom could be easily positioned because clear water allowed the bottom mark circles to be seen (see Figure A.21). In clay testing, there was no visual reference to the bottom, so positioning was based on the location of the tie-off ropes attached to the Geyser pump lifting eyes. To contain clay in the tank during Geyser pump operation, especially when pulse mode was activated, plastic covers/temporary tent were used to contain the water or clay slurry that was shot up by the pulsing action (see Figure A.22). The tent structure was used to minimize interference with tank fluids during pulsing actions, which may influence tank mixing.
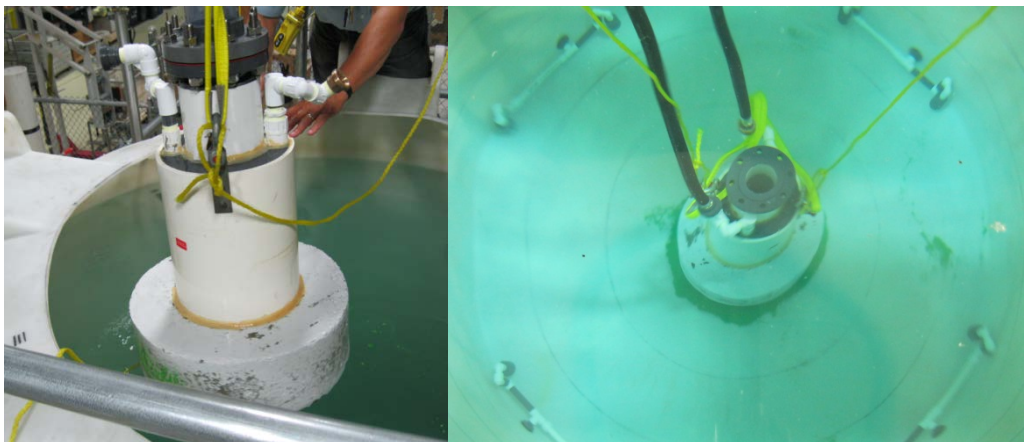
Figure A.21. Geyser Pump Water Configuration: insertion (left), and in-tank (right).

Figure A.22. Geyser Pump Used for Clay Slurry Testing: removal (left) and containment tent (right).

A.2.1.3   PHi Plate Mixer (Assembly/Installation/Positioning)

The Pulsed Hydraulics, Inc. (PHi) plate mixer was an air mixing device that did not use a tube like the ALC and Geyser pump devices. This plate mixer discharged a large gas volume between two 8-in. diameter, 3/16-in. thick plates with a 3/8-in. gap at the bottom of the PNNL tank. The dual plates on this mixer eliminated the vertical force component and there was no in-tank bubble reservoir like the one the Geyser pump used. The air pulse was generated outside the tank via a control box that opened and closed a valve for a short period using pressurized air (nominally 80 psi in PNNL testing). Because higher pressure air than other ALC systems was required to generate the air pulse out of tank, no PVC piping was used and instead stainless steel tubing and hoses with fittings were used to route the air to the PHi mixer discharge plates.

A long, 1-in. diameter stainless steel tube was used to attach to the pipe fitting on the PHi mixer plate. With the PHi air mixer plates sitting on the bottom of the tank, this tube stood above the top of the tank where the hose from the PHi control box was connected.

To stabilize the PHi mixer horizontally in the PNNL tank, three PVC arms were constructed to attach near the PHi plates and rotated to be spaced evenly apart and brace off the tank wall (see Figure A.23). The upper part of the PHi mixer used the air pipe to tie off at the top of the tank in a similar manner used for the ALC unistrut assembly.

Operationally, the PHi mixer used a control box (i.e., controller) to control the pulsed air flow (see Figure A.24). The flow monitoring assembly with rotameters could not be used with this controller, so it was bypassed and the hose from the building air supply was attached directly to the PHi controller. Pressure was regulated first at the building air supply in APEL Room 184 and again downstream in the PHi controller. The PHi controller provided the pulse timing and pulse duration via switches on the controller front panel.

Figure A.23. PHi Mixer PVC In-Tank Horizontal Stabilizers: positioned for insertion (left) and deployed (right).

Figure A.24. PHi Mixer Controller and Front Panel Switches.

A.2.1.4   Air Pressure (Building Air Supply to APEL Room 184)

Air was supplied to the air mixing devices during testing from APEL building air via a 1-in. drop line and pressure regulator/pressure gage in the Room 184 space. APEL building air is supplied by a primary compressor rated at 70.4 standard cubic feet per minute (scfm) at 100 psi and a standby compressor rated at 35.8 scfm at 100 psi. Maximum observed pressure at the APEL Room 184 supply location was around 90 psi with a sustainable air flow of around 30 cfm at the ALC flow meter location. The APEL building air supply is subject to variation due to air supply use in other parts of the APEL building. Larger sustained (more than a few minutes) air flows above 30 cfm would likely have required the addition of an air receiver tank to store additional compressed air volume. The building air pressure gage associated with the Room 184 building air supply and regulator was used as the pressure monitor for all testing of the ALC air mixing device. All hoses used were 1-in. 150 flex hose purchased from McMaster (Figure A.25) with 1-in. brass unions for connection. Approximately 50 ft of hose connected the building air from the regulator/pressure gage to the ALC air flow manifold using a union coupler. The air flow manifold was made of 1-in. tube using 1-in. Swagelok fittings. Hose length from the air flow manifold to the air device union connection at the top of the tank was approximately 10 to 25 ft for all of the ALCs with the exception of the Geyser pump, which had direct hose connections. Typical ALC 1-in. piping/connections from the top of the tank to the air injection point were similar to what is pictured in the left image of Figure A.20. The typical air system schematic is shown in Figure A.26, with the building air connections shown in Figure A.27.

It should be noted that for most testing, PVC tube was used for a portion of the air line that was located in the tank. PVC is not typically recommended for use with air due to possible fragmentation under pressure, but in this case it was deemed safe because it had minimal pressure (open tube/nozzle),

was contained (in the poly tank), and was mostly submerged in the tank fluid. PVC was used because it was inexpensive, easy to route, and could be easily reconfigured.
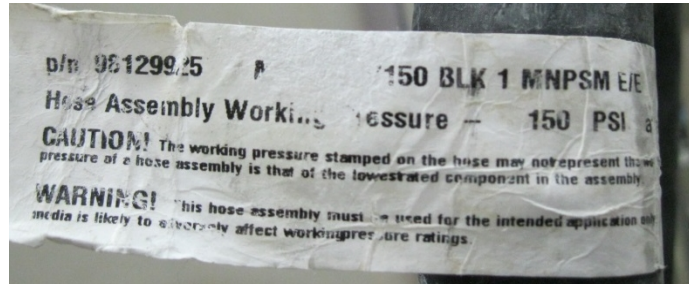
Figure A.25. Hose Details.
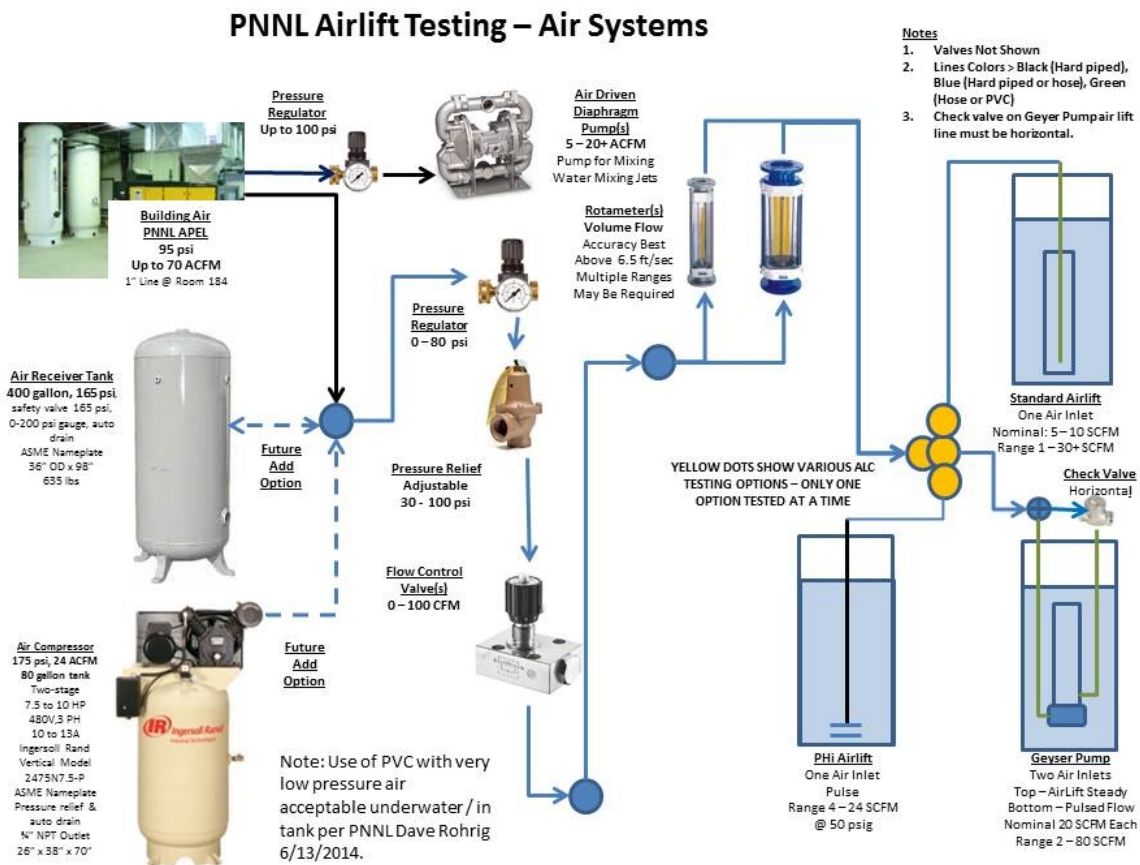
Figure A.26. ALC Testing Air System Schematic.

Figure A.27. APEL Room 184 Building Air Regulator and Pressure Gauge.

A.2.1.5   Air Distribution and Flow (Rotameters - Single and Rack of Five)

Initial ALC testing used a 1000 scfh (equivalent to 16.66 scfm) Dwyer rotameter with an adjustable flow valve (see Figure A.28). This was later upgraded to a flow meter rack with five Dwyer rotameters with adjustable flow valves. This flow meter rack was built out of 1-in. pipe with valving to distribute the air flow to one or two ALC air device inputs (see Figure A.29 and A.30). The Dwyer instruments installed in the flow meter rack were: (1) RMC-121-SSV, 1 to 10 scfm flow meter with stainless steel metering valve and (2) RMC-123-SSV, 4 to 30 scfm flow meter with stainless steel metering valve. The Dwyer flow meters could be changed out to other air flow ranges if needed.

Figure A.28. Original Single Flow Meter System 0 to 1000 scfh Air.
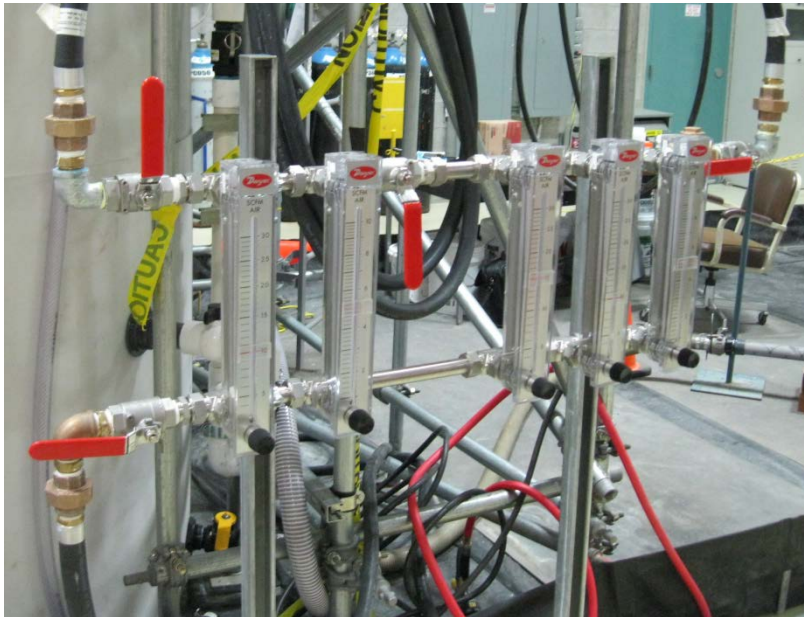
Figure A.29. Flow Meter Rack (five rotameters and valving).

Figure A.30. Flow Meter Rack Details: Left Bank (0 to 30 scfm and 0 to10 scfm) and Right Bank (two 0 to 30 scfm and 0 to 10 scfm).

A.2.2   ALC Instrumentation

A.2.2.1   Tank Fluid Level

Tank fluid level was generally measured each day of testing. For water testing, a tape measure or marked rod was used to measure the fluid level or to fill fluid to a specific level. Initially tank fluid level was measured using a Stanley 25 ft tape measure either off the bottom or from some premeasured reference point like the tank lip. During water testing, various measuring rods were fabricated with markings to indicate the desired fluid level from the tank bottom (see Figure A.31) and used in place of the measuring tape because they were easier to use and more repeatable (being rigid devices instead of flexible).
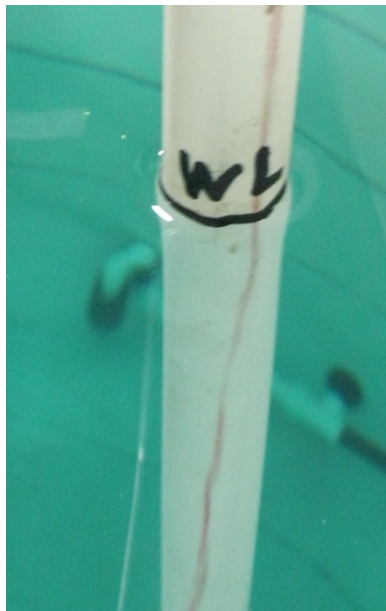
Figure A.31. Typical Water Measuring Rod with Water Level Mark at 105.5 in.

When clay slurry mixing started, a Bosch DLR130 laser range finder was acquired and was used exclusively for tank fluid level. The laser range finder was checked to various reference distances and found to be very accurate and repeatable on the order of ±1/64 in. A bracket was fabricated to attach to the range finder (see Figure A.32) that allowed more accurate repeatability when resting at one of three marked specific points on the tank lid opening (see Figure A.33). The laser range finder worked well with the clay slurry (which has a reflective surface) but was not usable on water (too transparent). The range finder proved to be a very reliable height measurement with the clay slurry and was also used to monitor tank filling and emptying operations. When horizontal layers of clay slurry were removed for particle location determination, the range finder was used to monitor the height of clay slurry removed.

Figure A.32. Laser Range Finder with Bracket and Tank Top Lip Level Locations.
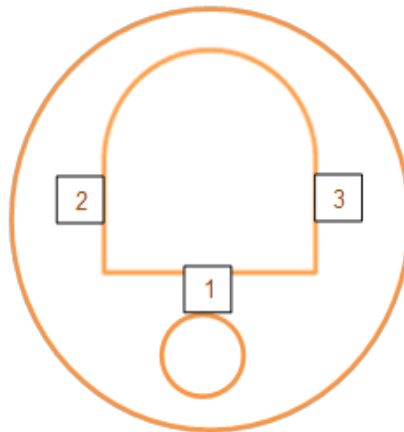
Figure A.33. Range Finder Tank Lip Reference Locations (three locations: 1, 2, 3).

A plumb line was also fabricated to determine the clay slurry surface vertical height location. A key concern was that if a layer of water was on the clay slurry surface, the range finder might be inaccurate. Since no top water layer was ever observed during this PNNL testing sequence, the range finder was found to work much more quickly and accurately, so the plumb line measurement was never used.

It should be noted that the PNNL poly test tank construction was not exact and this affected tank fill level measurements. The tank bottom was wavy with variations on the order 1/2 in. or more. The tank

top lip was cut from a shaped head, so the lip edge from bottom varied. Tagging specific tank lip locations for range finder level measurement (see Figure A.33) established reference distances to the tank bottom and allowed tank fill level measurements to be consistent between all clay slurry (non-Newtonian) testing. Water testing (Newtonian) used the measuring rod marked at 105.5 in. and water was added/removed to reach the desired water fill height.

A.2.2.2   Tank Fluid Temperature

Tank fluid temperature was generally taken each day of testing. The instrument used was a Fluke thermocouple device (Fluke 52II Thermometer, PNNL ID #18527, range 0 to 300 °C, accuracy greater of +/- 2.2 °C or 0.75% of reading); see Figure A.34. The thermocouple device had been calibrated previously but was not recalibrated for this PNNL testing.

The installed probe was a Type K thermocouple. The thermocouple portion of the device was inserted at least 6 in. below the top surface of the fluid and at a distance of at least a 1/4 in. radius away from the tank wall to minimize external temperature influences and measure bulk fluid temperature. The fluid (water and clay) bulk temperature remained very stable over the course of testing due to the large mass of the tank fluid used (on the order of 3000 gal) and being located inside a building that moderated the effects of outside temperature changes.

Figure A.34. Tank Fluid Temperature Device.

A.2.2.3   ALC Air Pressure

For a description, see Section A.2.1.4. The ALC pressure was dictated by hydrostatic head at the submerged ALC air line outlet and not the regulator pressure. Thus, regulator air pressure was not calibrated for PNNL testing but instead was used as installed.

A.2.2.4 ALC Air Flow

For a description, see Section A.2.1.5. The RMC Dwyer flowmeters used had a temperature limit of 130 °F, pressure limit of 100 psi, and accuracy of 2% of full scale and were designed for use in air. Flowmeters were not calibrated for PNNL testing but used as received.

A.2.2.5 Fluid Velocity

For some air mixing testing devices, it was desired to measure the fluid velocity to determine mixing flow and intensity at key locations. The instrument used was a propeller device (Flowatch with wand and remote sensor from JDC Electronic SA, Switzerland; see Figure A.35). This propeller device was built for measuring water flows in canals, streams, and rivers, and used a small plastic propeller either on a 1.5 to 4 ft adjustable hand held wand or remotely weighted to be dropped into the water from the surface with up to 50 ft of submerged cabling available. This velocity probe had a threshold velocity of 0.1 ft/s and did not allow flows lower than 0.1 ft/s to measured (i.e., would read zero). The Flowatch was not calibrated but used as received.

The readout on this device had the ability to provide either instantaneous or average velocities. In the turbulent areas of the air mixing devices, the instantaneous function was not useful as it varied constantly. During PNNL testing, the averaging feature of this device was used. The device was set to perform 1 minute averaging and the system being tested was operated at steady air flow for at least 2 minutes to ensure the averaging had stabilized. Even with the averaging function, there was some small variation in the average velocity measurements, so the most consistent measurement was recorded.

This device worked well in clean water but deployment in clay slurry quickly wore down the propeller shaft bearing surface. The device's design, with a plastic propeller rotating on a metal shaft, was not made to hold up in slurry over long time periods. During clay slurry testing, as the clay slurry movement from the air mixing device was increased, it was apparent when the propeller failed. Upon removal and cleanup of the propeller, slight blowing to spin the propeller would result in a vibration that was not there when the new device was installed. Multiple propellers were used to obtain some of the clay slurry mixing velocity data, as propellers were replaced when they wore out.

It should be noted that this velocity device is one directional. Good measurements were obtained where the fluid flow was generally one directional such as at the exit above the ALC tubes. In areas of multi-directional flow or where the flow direction was not matched with the orientation of the propeller, the measured velocities may not be accurate. Additionally, all of the measured fluid flows were actually two-phase flow consisting of air bubbles from the air mixing device entrained in the fluid (water or clay slurry). Air and fluid have a large density difference so the fluid flow should be the dominant mass flow component.

The hand held wand propeller option was initially used to measure fluid velocities in water. In most cases, the ALC systems did not permit access to the desired measurement locaitons by hand. Later, the remote probe propeller option was used and rigidly fixed in place when aggressive mixing action was being measured (e.g., exit of ALC tubes). Figure A.36 to Figure A.40 show the remote probe rigidly fixed at the exit of various ALC devices in water and clay slurry. During rigid attachment of the remote probe, the cross-sectional profile was kept small to minimize flow interference. The remote probe propeller was positioned below the support structure to minimize fluid flow interference to the propeller.

The remote probe was also attached to a long rod in an attempt to measure low velocities at the bottom and side of the tank as well as at the inlet to the ALC device (see Figure A.39 and Figure A.40). The velocities in these areas were low, with most being below the 0.1 ft/s velocity threshold of this device.

Figure A.35. Flowatch Velocity Probe: Wand and Remote Probe.

(a)

(b)
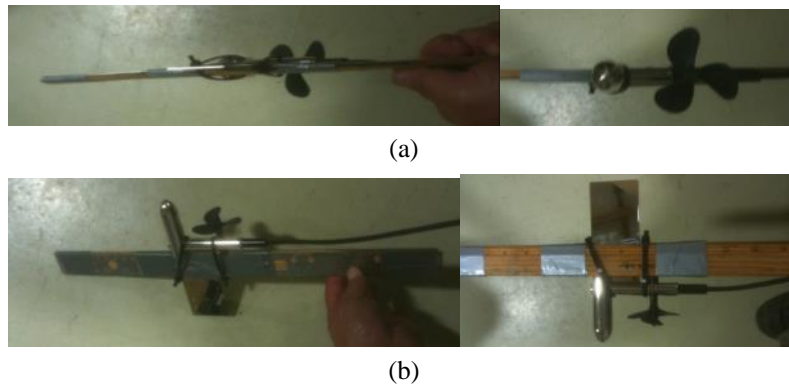
Figure A.36. Remote Velocity Probe Installed in Bar Mount: (a) side view and (b) top and bottom views
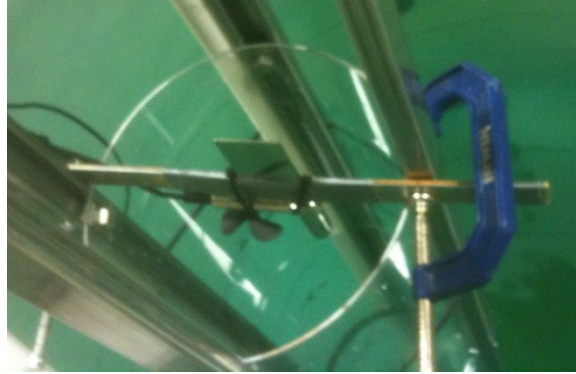
Figure A.37. Remote Velocity Probe Bar Mount Installed at ALC Outlet.

Figure A.38. Remote Velocity Probe Bar Mount in Water (left) and Clay Slurry (right).
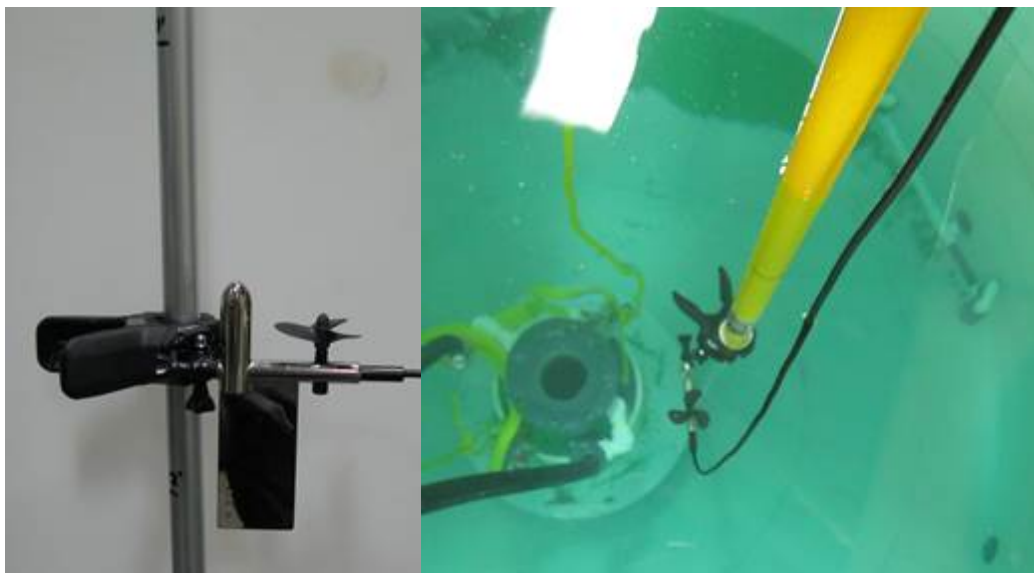
Figure A.39. Remote Velocity Probe Installed on Extension Pole.
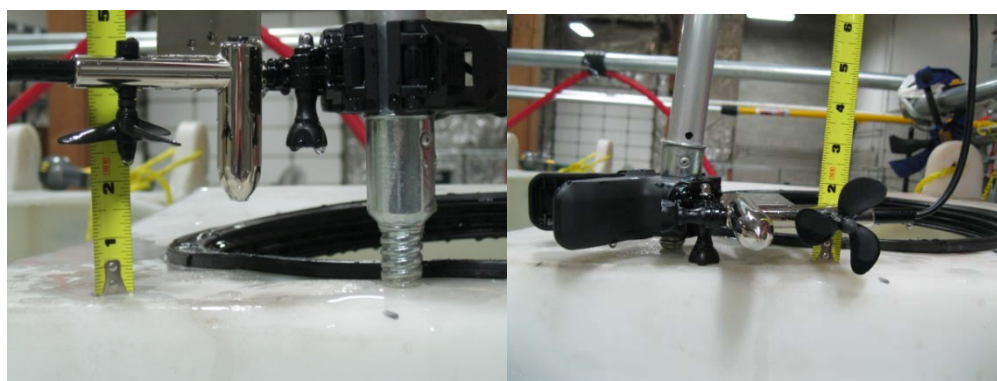
Figure A.40. Remote Velocity Probe on Extension Pole Positioned Two Different Directions.

A.2.2.6   Particle Motion – Water (Newtonian Fluid)

Particle motion in water with ALC mixing devices was observed/measured by various methods and using various particles that were attempted and refined as ALC testing progressed.

Sponges

Initially, small (~1/4 in.) sponges soaked in water (approximately neutrally buoyant) were inserted near the ALC inlet. Sponge motion in the tank was observed visually and with an in-tank GoPro video camera. The sponges were useful for observing whether ALC operation in water was developing a pumping action but did not quantify particle lifting capabilities.

Green 500 to 750-Micron Particles

Green 500 to 750-micron spherical particles were procured to simulate the largest size particles expected in the Waste Treatment and Immobilization Plant (WTP) tank where ALC mixing device application may be used. These green particles were acquired from CER-O-GLASS Technologies, Inc.,

on PNNL order #11841648 with item description as 07070 DB-4502/374S (0.50-0.75MM) Kelly Green Glass Beads shipped June 30, 2014. These green beads were heavier than water (2.5 g/mL) and thus would quickly settle to the bottom of the PNNL tank filled with water. In the beginning, a small quantity (100 to 500 g) of green particles was introduced to the inlet of the ALC mixing device via a tube that extended from the water surface to the entrance of the ALC mixing device. During this operation, the green particles developed momentum as they dropped down the tube in water to approximately 8 ft, and the particle motion affected by the ALC mixing device was observed with an in-tank GoPro video camera. Next, a large quantity of green particles (on the order of 12 lb) was staged below the ALC mixing device on the PNNL tank floor in a ~3-ft radius from ALC mixing device centerline. The ALC mixing device was then operated and the green particle motion was observed with the in-tank GoPro video camera, and then the resulting green particle dispersion across the tank floor was observed after the mixing device was turned off.

Initially, individual 8-in. diameter 100-mesh sieves were placed in the tank at various locations to get an idea of where the ALC device was moving the green particles (see Figure A.41).   Based on this data, it was decided that the green particles in the tank should be collected along a radial horizontal line from the center at various vertical elevations to better characterize mixing action in the PNNL tank as ALC mixing devices were operated over a range of air flow rates. A sieve array was fabricated (see Figure A.42) consisting of three 8-in. diameter, 100-mesh sieves spaced radially from the ALC centerline to capture particles from three equal areas of the tank. Initially the quantity of particles collected in the sieves was visually assessed, but later the volume of particles collected was determined using a graduated cylinder (see Figure A.43).
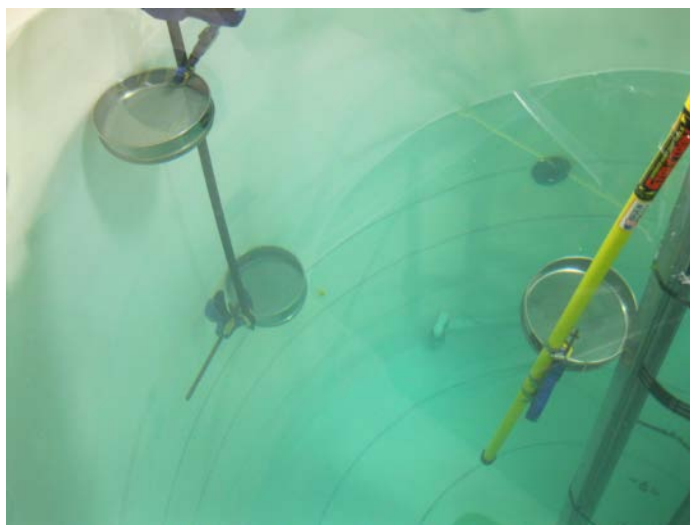
Figure A.41. Individual Sieves In-Tank.
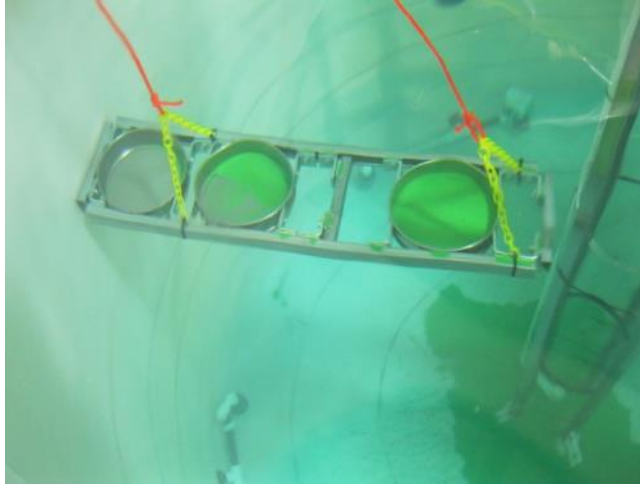
Figure A.42. Sieve Array at One of the Elevations In-Tank with Green Particles Collected.

Figure A.43. Measuring Volume of Green Particles Collected from One Sieve in Sieve Array.

Pea Gravel Particles

Local small pea gravel particles (see Figure A.44) were washed and injected into the ALC mixing device inlet in the same manner described above for the green particles. The goal of this testing was to observe how effective the ALC mixing devices were at moving and lifting particles larger than the green particles. As with the green particles, the visual observations were done with an in-tank GoPro video camera.

Figure A.44. Gravel Particles.

A.2.2.7 Particle Seeding – Clay Slurry (Non-Newtonian Fluid)

Motion in clay slurry motivated by ALC mixing devices was observed/measured using various colors of Airsoft particles (also called beads, BBs, ammo; see Figure A.45) pre-located at various places in the PNNL tank, and then observed/measured after an ALC mixing device operational period. The particle material and associated method developed by PNNL for non-Newtonian mixing flow assessment has not been performed in any previous WTP-associated testing, so some development was required. The Airsoft particles are made in a large variety of colors and the nominal characteristics of the Airsoft particle (mass of 0.12 g, 6-mm diameter) are slightly lighter (densities of 1.037 to 1.225 g/mL) than the clay slurry (density of 1.259 g/mL), i.e., the particles were slightly positively buoyant. A discussion of the rationale for considering the particles as tracers is given in Section 6.1. The Airsoft 6-mm particles are available from a variety of manufacturers, with some variance in actual diameter and associated weight. The PNNL testing used 0.12-g particles with the exception of some slightly heavier red 0.15-g particles that were loaded on the bottom for some testing. Heavier Airsoft 6-mm particles are available from 0.20 to 0.30 g or more, but they were not used in the PNNL testing.

Figure A.45. Examples of Typical 6-mm Airsoft Particles.

The method used for PNNL testing was developed and refined over time. In all cases, the PNNL tank was initially filled with the clay slurry prior to Airsoft particle insertion. Where there were large, open

areas for access, Airsoft particles were inserted using a sieve on a pole to push Airsoft particles deposited on the clay slurry surface to the in-tank radial location and depth (see Figure A.46). Prior to using this placement method, a small test was done using a 5-gal bucket of clay to ensure that particles stayed in the desired location. It was found that if the mesh was pushed down too fast the particles would flow around mesh pocket and if the mesh was pulled straight up some particles would follow. Therefore, a modified mesh insertion/extraction technique was developed that consisted of very slow insertion, "shake and rotate" release, and slow extraction. Most testing also included a layer of Airsoft particles on the clay slurry surface in a rectangle shape orientated along the tank radius (see Figure A.47)

Figure A.46. Airsoft Particle Insertion to Location Using Sieve on a Pole (large access area).

Figure A.47. Airsoft Particles on Clay Slurry Surface.

After the Airsoft particles were placed at set locations in the PNNL tank, the ALC mixing device was operated at a fixed air flow rate for a period of (typically) 0.5 to 1 hr. The ALC mixing device was then turned off and the top ~1 ft of clay slurry surface was swept with nets to collect the particles at that elevation (see Figure A.48). The net used for the surface sweeping (Ranger 12 in. square with 4-in. deep

pocket; see Figure A.49) had a mesh just slightly smaller than the 6-mm particle diameter that allowed clay material to flow through with minimal resistance while still capturing Airsoft particles. The technique developed was to sweep the surface area back and forth several times and periodically lift the net out of the clay slurry against the tank wall to minimize Airsoft particle spill around the net due to highly viscous material. Sweep operations were done twice for each half of the tank to ensure good particle capture in the clay slurry layer. The depth of the net in the clay slurry was not uniform across the clay surface: there were variations in human arm sweeping motions and the net needed to be extended from the scaffolding to get to the far edges of the tank (or to lift the net out at the wall), which often required angling the net. When the net was angled, the depth of the net in the fluid was increased to try to compensate for the difference and maintain the desired 1-ft layer sweep. Coverage of the layer being swept included many repeated and overlapping motions that resulted in good particle capture, and this was verified with the second, repeat sweep where only a few more particles were typically captured.

Figure A.48. Airsoft Particle Sweeping of Top Clay Slurry Layer and Particles Collected.
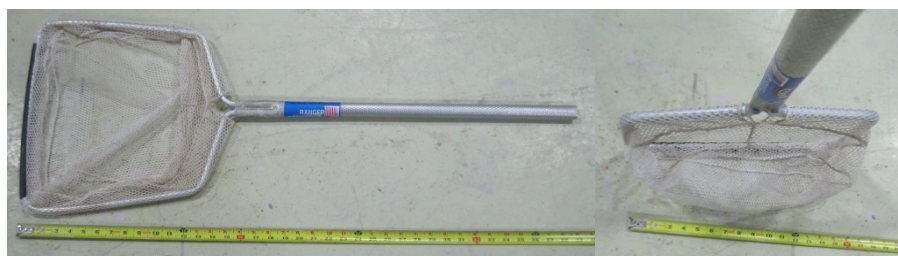
Figure A.49. Range Sweep Net Details.

After particles were collected in the top 1-ft layer on both halves of the PNNL tank, the particles were washed to remove clay and dried on a cloth, the colors were separated, and then the particles were counted/weighed (see Figure A.50). With time, it was found that counting particles was redundant with weighing after a good average particle weight had been established for each color.

Figure A.50. Airsoft Particles Collected and Separated Prior to Weighing/Counting.

After each ALC mixing device test run was completed, some additional particle mixing information could be acquired during tank pump down. When this method was used, pump down would occur from the top surface using a suction hose that was swept in the layer volume being removed and captured in an in-line filter (Banjo LSM300-50 3-in. PP "Y" strainer with 50-mesh stainless steel screen). This method was not exact in removing a layer of fluid but it was adequate, as demonstrated by the retrieval of "unmixed particles" that were found at their insertion depth layer in the tank clay slurry. This pump down layer removal method was not performed after every test. Whether pumped down from the top or not, particles were always captured in filters during tank pump down and cleanout to recover the particle inventory left in the tank and compare it against the inventory swept/netted previously out of the tank.

Particle weighing was done using a high sensitivity scale in APEL Room 107 that had a tare/zero capability. The scale was a Mettler PM2500 DeltaRange scale that had a maximum load capacity of 2100 g and the calibration ID 1113060392 (expiring 02/2016). A weigh tray would be tared and then particles weighed in the tared tray. Particle counting (if performed) was done manually and then checked against expected weight.

A.2.3 ALC Test Record and Observations

A.2.3.1 Recording

Testing activities were recorded in two PNNL laboratory record books (LRBs) with the first designated BNW-61799 (all pages) and second BNW-61859 (pages 1 – 75). Date and time were used to relate the various test activities recorded (e.g., datasheets, visual observations, photos, and video). Key photos and video snapshots were included in the LRBs to document testing activities, with raw photos and video archived to a project computer drive. The date of each photo was captured (at a minimum), with time of day also captured where applicable. Photo/video correlation to testing activities was often documented by taking a picture of a written record of the test activity being performed as well as the included date and time stamping on the media metadata.

A.2.3.2 Visual

Visual observations relevant to testing were recorded in the LRBs. LRBs also included photographs and video stills relevant to record test information and data.

A.2.3.3 Photo

Photographs were taken with a digital camera and occasionally cell phone cameras. Photos were used to record test setup, test conditions, test layout, test progression, and test results. The primary digital camera used for test photography was a Canon PowerShot 3100IS (DOE# WE 18462), but various cell phone cameras and video stills also provided photographs. When lighting was inadequate, supplemental lighting was used. During testing, photos were generally downloaded daily and archived to a computer drive. Each camera picture/image has metadata that includes date and time to allow correlation to the various testing activities. Photo correlations to testing activities were also sometimes documented by taking a picture of the associated written record (e.g., written sticky note, datasheet) of the test activity being performed.

A.2.3.4 Video

Video records were taken by the GoPro video camera, Canon PowerShot 3100IS in video mode, and occasionally cell phone cameras. The main camera used for testing was the GoPro video camera (GoPro Hero3+ Black Edition Adventure) due to its ability to take long duration video, link to an iPad, and be submerged in fluid. The GoPro and other videos have metadata that includes date and time to allow correlation to the various testing activities. Similar to the photos, correlations to testing activities were also sometimes documented by taking a picture of the associated written record (e.g., written sticky note, operator video movement) of the test activity being performed.

Submerged testing with the GoPro was successful in Newtonian water testing but not in non-Newtonian clay mixture testing because the fluid was opaque. When the GoPro was submerged in water during Newtonian testing, the waterproof camera was typically attached to a pole via a clamp and flexible mount that allowed the camera to be positioned. For some GoPro videos taken in water at the bottom of tank, an adjustable attachment at the end of the pole was used to allow the camera to be given a known offset off the tank bottom. Radial positioning of the video camera in the tank was done using the circular line marks on the bottom of the tank or measurement to the tank wall at the top of the tank. During non-Newtonian testing using a clay slurry mix, the GoPro camera was housed in a sealed ammunition box with a viewing window to keep the slurry simulant from contacting the camera; however, this did not provide any useful information because there was no visibility beyond the ammunition box window.

A.3 Air Mixing / Air Lifting Devices Tested

A.3.1 General

Air mixing and air lifting devices operate on the principle that when compressed air mixes with a fluid it becomes a less dense mixture than the surrounding fluid and is displaced upward via a bubble action, passing through the higher density fluid to the fluid surface. A pictorial summary of various air mixing / air lifting devices and their operation is shown in Figure A.51. Testing was performed for all modes of the ALC and for one of the plate mixer modes. For the WTP, the sparger is the current supplemental air mixing device being considered in the design, and numerous test activities and reports on spargers have been completed.
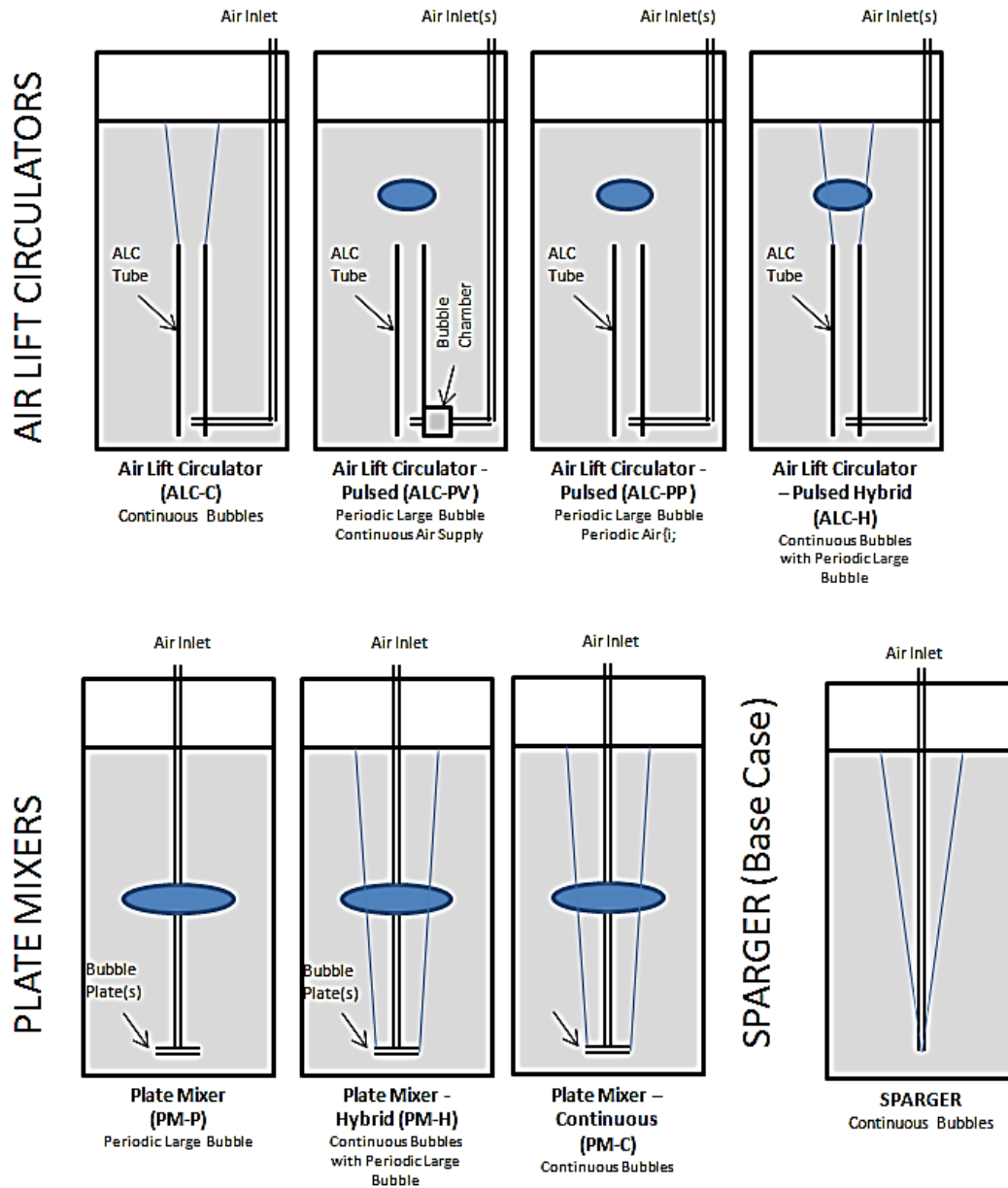
Figure A.51. Various Air Mixing / Air Lifting Devices.

A quick summary of the various air mixing / air lifting devices and air operations is as follows:

- Spargers – The "base case" sparger is an unconstrained air mixer that ejects air out of a tube in the fluid at depth in a tank, and the bubbles rise to the surface around the air tube, causing a localized mixing action. The classic sparger design uses a continuous air flow that is ejected near the bottom of the tank.

- Airlift Circulators – In the simplest terms, an ALC can be considered a "sparger" constrained by a riser tube. ALCs eject air into a riser tube immersed in the tank fluid that constrains the interaction of the air bubbles with the surrounding fluid to a horizontal plane over a vertical length, causing a pumping effect—which is why these devices are also called air pumps in some applications. The

classic airlift design uses a continuous air flow / bubble stream to provide mixing and lifting action with the riser tube located near the bottom of the tank.

- Pulsed Air Flow – Pulsed air flow is also used in airlift devices to enhance mixing/pumping. Pulsed air flow operation in an ALC configuration releases a periodic air volume in the riser tube to provide higher fluid velocities in the riser tube for a period and/or more mixing action.

- Plate Mixers – A device that uses pulsed air flow ejected below a plate to spread the air bubble pulse horizontally is called a plate mixer and is similar to a sparger in that no riser tube is used to constrain the air bubbles as they rise vertically.

- Hybrid Air Flow – Air mixing/lifting devices can be operated in a hybrid mode having both continuous and pulsed air ejection operating either independently or together.

- Special Features – Air mixing devices can have special features like nozzle designs with a single or multiple outlets, mixing enhancers as part of the air mixer / air lifting device, or an external feature like a diverter at the bottom of the tank to rechannel horizontal flow or a top cap to divert vertical flow at the top of the tank.

Various airlift design features are shown in Figure A.52.
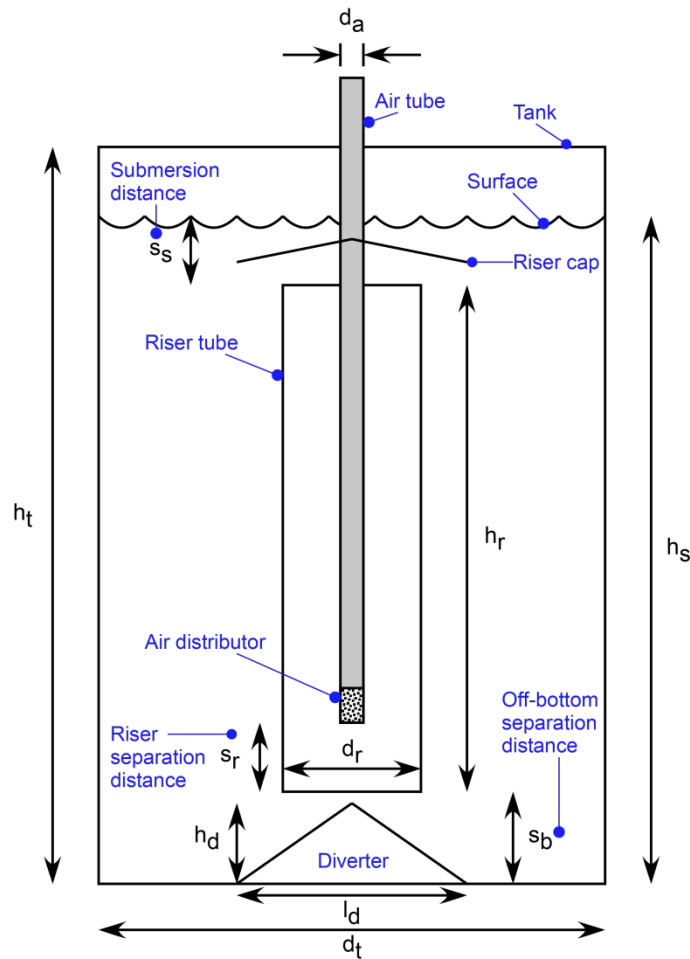
Figure A.52. Airlift Design Features and Relationships.

Airlifts / air mixers are used for a variety of applications, including well water pumps and aquarium pumps/aeration. The airlift / air mixer application that was most applicable to the WTP operations was mixing in aerobic digesters, slug waste, aeration ponds, and large industrial chemical tanks. In many of these applications, long-term mixing with a simple air supply system uses air blowers with high cfm and low pressure, thereby limiting the depth below the fluid surface at which air can be ejected because of hydrostatic forces. The air lifting/mixing devices tested have air ejection points lower than a blower can provide and therefore a compressed air supply is required to overcome the hydrostatic forces and to provide high pressure for air flow, especially with pulsed air operations that use short duration, high cfm air injections.

All air mixing / air lifting devices can be operated continuously or periodically and under changing air supply conditions. Key concerns when using these air systems with Newtonian and/or non-Newtonian fluids include plugging (especially at the air-fluid interface as air tends to "dry" some fluids), aerosol generation (developed when bubbles release at the fluid surface), and interference with other in-tank operating components like pulse jet mixers.

A.3.2 Airlift Circulators – Continuous Air Flow

A.3.2.1 General

The basic ALC design consists of a riser tube and air ejection nozzle located near the bottom of the riser tube where air bubbles are formed. The air ejection nozzle was located in the center of the riser tube for all test cases except for the 4-in. Geyser pump, which had a side ejection. Three sizes of this airlift design were tested using 4-, 10-, and 18-in. nominal riser tubes of various lengths. On the 10-in. airlift, various nozzle configurations were tested. Additional details of each test configuration are given for each airlift size.

Airlifts of this design are available from various vendors, but the simplistic design of this configuration allows a custom unit to be fabricated easily with simple material. Vendor sources include the GasLifter (Walker Process Equipment, Aurora, IL) for a basic airlift and the Geyser Hybrid Pump (GHP) (Geyser Pump Tech, LLC, Seattle, WA) for a hybrid design.

A.3.2.2 4-inch

The 4-in. ALC was a variation of the GHP configuration. For details of the GHP, see Section A.3.4. During testing as a 4-in. ALC, the GHP was operated with the airlift line only; pulse operation mode was off. In the GHP design, the air ejection port is on the side of the riser tube near the bottom instead of at the center of the riser tube as in the 10- and 18-in. ALC configurations. The GHP riser tube minimum length was 3 ft, dictated by the minimum size of the GHP required to also incorporate the hybrid air design features of this device. A 2-ft riser extension was fabricated that extended the GHP airlift riser tube to 5 ft. In the GHP, an air line supplied air via a 1-in. hose to the airlift through a 1.25-in. connection on the side of the GHP. The GHP 3-ft base was fabricated out of standard white PVC Schedule 40 and the 2-ft riser extension was fabricated from a clear blue tinted PVC that allowed flow conditions inside the riser extension to be observed during water testing. The GHP riser tube interior diameter was nominally 3.998 in. based on 4-in. PVC Schedule 40 pipe standards.

A.3.2.3   10-inch

The 10-in. ALC was the initial ALC tested and was used to baseline the system against other available data. Initially the ALC riser tube was fabricated from standard white PVC but later this was changed to clear acrylic that allowed flow in the riser tube to be observed during water testing. The 10-in. riser tube interior dimension was nominally 9.976 in. in diameter based on 10-in. PVC Schedule 40 pipe standards and 10-5/16 in. in diameter based on 10-in. acrylic purchased.

The ALC riser tube length was adjustable by adding sections of tubing taped together at the joints. The ALC riser tube was put in a unistrut frame consisting of four legs with sufficient length for the upper legs to extend to the top of the tank. The ALC was secured in the unistrut frame with bolts that either passed through the ALC riser tube or clamped the riser tube at the ends. A unistrut cross at the top allowed adjustment for various sizes of ALC diameters, attached to the four legs, and also provided a lifting location at the top. After the ALC was located in the unistrut frame with the required riser tube length and bottom standoff distance, the unistrut frame was secured and the unistrut legs were secured against the riser tube by wrapping the legs around the diameter with large tie-wraps or similar banding materials. Figure A.53 and Figure A.54 show a typical test arrangement of the 10-in. ALC.
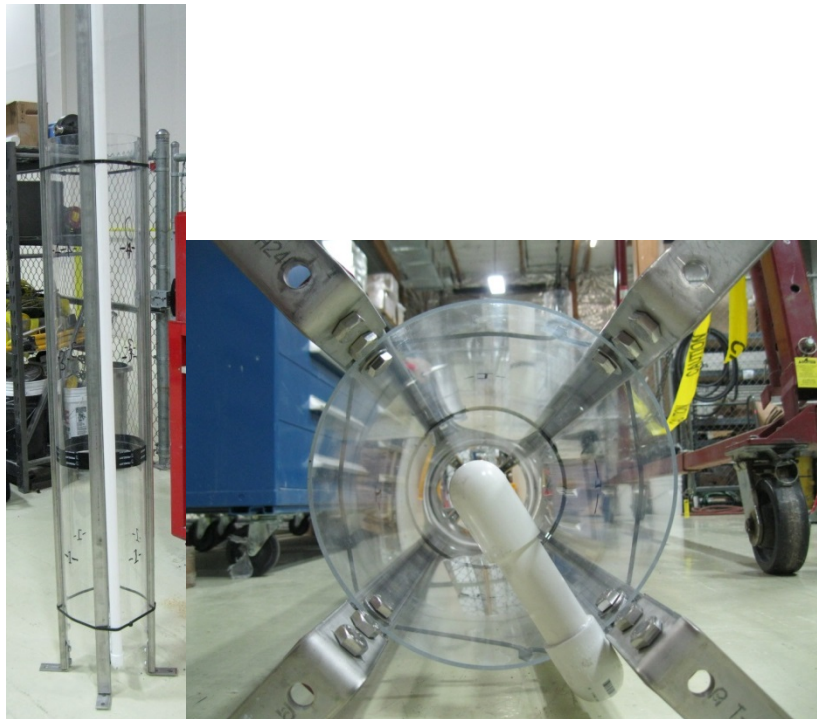
Figure A.53. Overall Setup: ALC 10-in. Diameter, 5 ft Riser Tube, 5 in. Standoff Distance from Bottom (left is vertical configuration as would be installed in the tank, right is a view looking from the tank bottom up the riser tube with the PVC nozzle centered in riser tube).

Figure A.54. Dimension Verification of Tube Length (5 ft), Standoff (5 in.), and Diverter Location (centered).

Nozzles

Testing with the 10-in. ALC used various nozzle configurations (also called air distributors). It was used initially to try various nozzle designs in water and the following designs were tested:

- Sieve plate footpiece (see Figure A.55) fabricated in metal to match the nozzle design described in an available reference during benchmarking of the system (see Figure A.56).

- Open pipe with sieve plate footpiece removed

- PVC 1-in. cap drilled with holes (see Figure A.57) that consisted of eight side holes and eight top holes, all ~1/4 in. in diameter.

- PVC open pipe; PVC cap removed.

The PVC nozzle extended into the riser tube by several inches and was supplied with air using 1-in. PVC Schedule 40 tube and then transitioning to 1-in. hose to the air metering device(s).
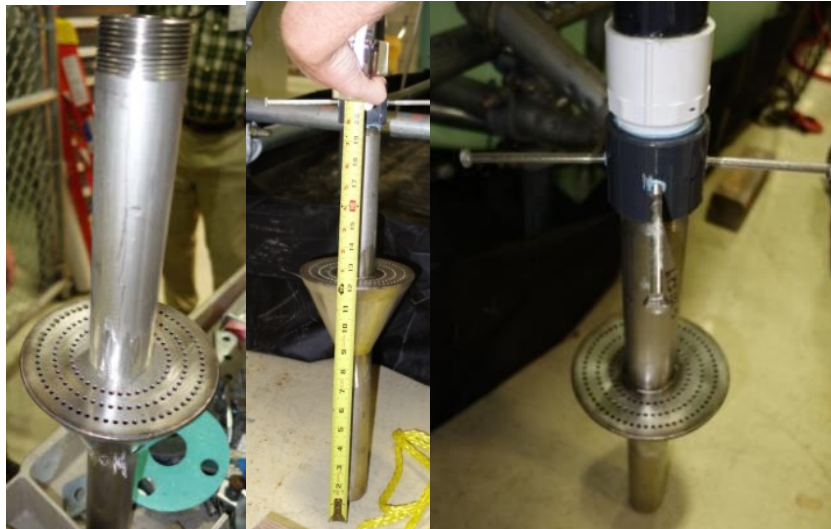
Figure A.55. Sieve Plate Footpiece Nozzle
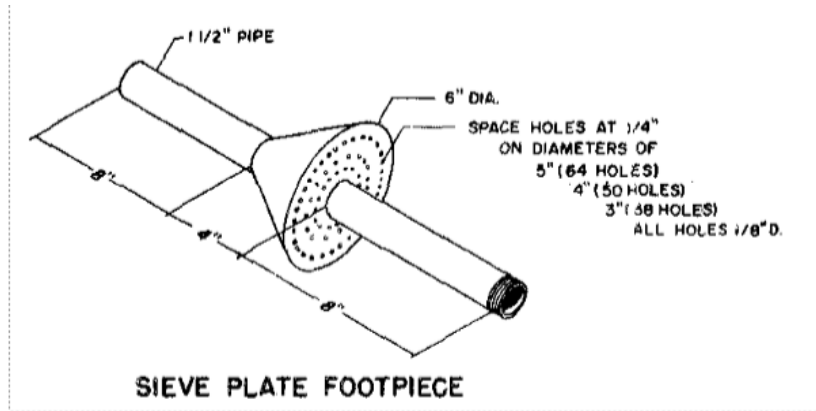
All parts are stainless steel.

Figure A.56. Sieve Plate Footpiece Nozzle – Design Information.

Figure A.57. PVC Cap Nozzle (drilled holes).

Diverter

A diverter was fabricated (see Figure A.58) as a possible accessory to be placed under an ALC to help divert fluid flow up the ALC.   The concept of a diverter is to direct bottom-sweeping flow (mainly from the bulkhead nozzles in the case of the PNNL testing, but provided by pulse jet mixers in a WTP vessel) up the ALC tube.   However, only some initial operation observations were made with an ALC device and the diverter was not used in the PNNL testing activities that collected any mixing data.

C:\Users\boer684\Documents\Projects\Air Lift\140519pyramid.dwg, 3/13/2
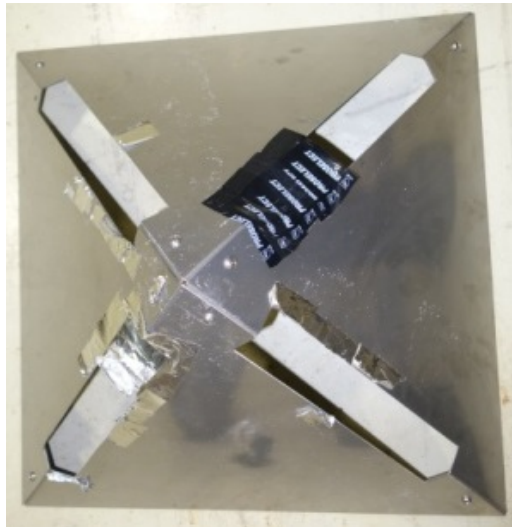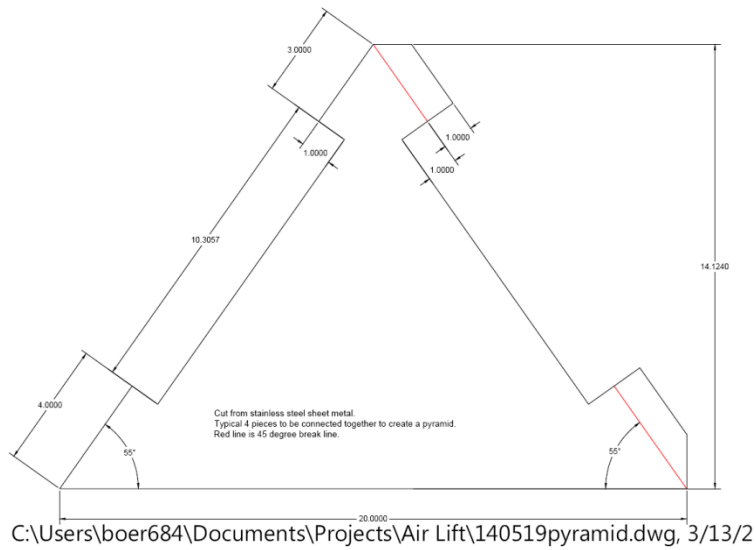
Figure A.58. Diverter Plate (intended to be mounted at tank center under ALC riser tube).

A.3.2.4   18-inch

The 18-in. ALC was configured and assembled in the same manner as the 10-in. ALC except 18-in. Schedule 40 PVC pipe was used, yielding a riser tube interior dimension that was nominally 17.4 in., and the nozzle pipe was extended to locate the nozzle outlet in the center of the riser tube. The configuration of the 18-in. ALC is shown in Figure A.59.

Figure A.59. 18-in. ALC Configuration (shown with and without nozzle cap).

A.3.2.5   25-inch

A 25-in. diameter, 5 ft long ALC was fabricated from stainless steel in anticipation of scale-up testing; however, this testing was not performed.

A.3.3   Airlift Circulators – Periodic Air Flow

A.3.3.1   General

The ALC design with periodic air flow releases a large cfm, short duration air pulse near the bottom of the riser tube. Per vendor descriptions of this type of ALC, the large quantity of air released is designed to create a slug of air that fills the full section of the riser tube with air, creating slug flow conditions; this slug flow increases suction and fluid velocity in the riser tube. Periodic air release in these ALC devices is accomplished by one of two ways:

- A bubble chamber at the bottom of the ALC is filled with air that periodically releases a large air bubble when the in-tank bubble chamber is full. For this type of system, a change in air flow only changes the frequency of the release, as the bubble size is fixed by the bubble chamber size. The GHP testing used this method (see Figure A.60 for a schematic of the process).

- An out-of-tank air controller using valving, timing, and pressure regulation releases an air charge in the air supply lines to the riser tube nozzle. In this case, the size of the bubble being released can be changed by varying the air pressure and air release duration. Because the path is longer from the bubble release on this device compared with the previous bubble chamber device, some delay between air release valve actuation and bubble release in the riser tube may have to be accounted for.

Two sizes of this airlift design were tested using nominally 4- and 18-in. diameter riser tubes of various lengths. Additional details of each test configuration are given for each airlift size.

Airlifts of this design are available from various vendors. Vendor sources for the in-tank bubble chamber design include the GHP or Geyser Air-Pulse Mixer (Geyser Pump Tech, LLC, Seattle, WA) and Cannon Mixer (Infilco Degremont, Richmond, VA). No vendor was found that specifically had an air charge ALC system, but two vendors were found that had the required air charging system typically used for a plate mixer system; these were PHi (Pulsed Hydraulics, Inc., Oroville, WA) and Pulsair (Pulsair Systems, Inc., Bellevue, WA).

A.3.3.2   4-inch

The 4-in. ALC large periodic bubbler was a variation of the GHP configuration. For details of the GHP, see Section A.3.4.2. In this variant, the GHP was operated with the pulse mode only; airlift mode was off. In the GHP design, a large air bubble is generated periodically in-tank with a bubble ejection port that is on the side of the riser tube near the bottom (see Figure A.60). No test data is reported from this configuration.
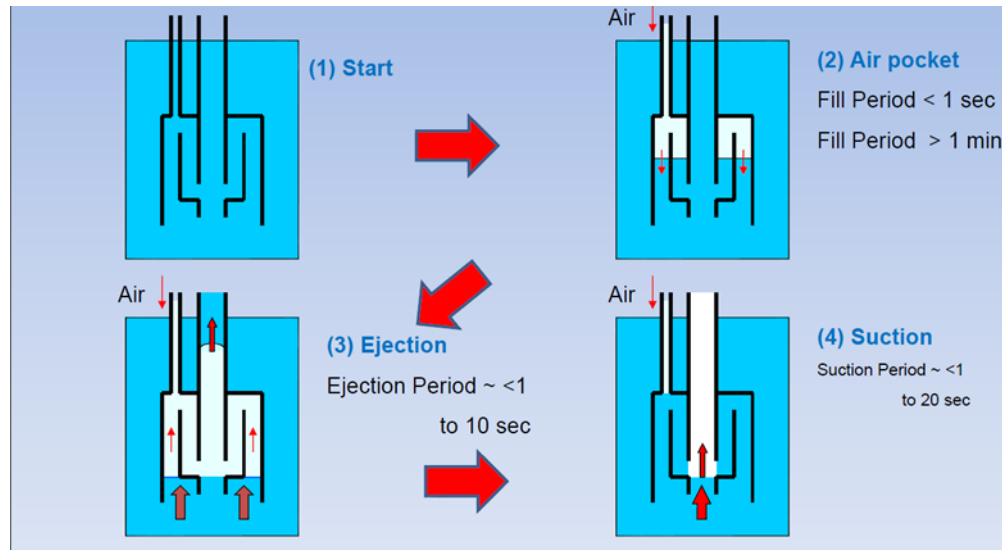
Figure A.60. GHP Operation Schematic, Pulsed Air Flow Generation Only (vendor literature).

A.3.3.3   10-inch

The 10-in. ALC large periodic bubbler was a variation of the 10-in. ALC hybrid configuration. For details of the 10-in. ALC, see Section A.3.4.3. In this variant, the 10-in. ALC was operated with only a pulse line nozzle; the separate (continuous) airlift line nozzle was not operating. The PHi pulse mode controller was used to supply the air pulse through a 1-in. hose to 1-in. metal pipe with connections that exited from an open 1-in. pipe nozzle located at the base of the riser tube. The 10-in. ALC riser tube was set at 5 ft for this periodic air flow testing. No test data is reported from this configuration.

A.3.4   Airlift Circulators – Hybrid

A.3.4.1   General

The ALC hybrid design uses both a normal airlift with continuous air flow and a periodic large air release and is only considered a hybrid system when both systems are operating together (most common configuration) or alternating (where one mode is off while the other mode is running). Per vendor descriptions, operation in hybrid mode allows a large suction force to be generated in the riser tube during the periodic air pulsing, which is useful for lifting heavy solids, and the continuous air flow keeps any solids moving up the riser tube between the air pulses. Hybrid mode is the most effective and efficient ALC operation with regards to air usage and moving heavy solids and/or higher intensity mixing. The ALC hybrid systems can be tuned by varying both the air flow to the continuous ALC mode and varying the air pressure and air release duration to the pulsed ALC mode.

An ALC hybrid system operating exclusively in only one mode, continuous or pulsed, is not considered a hybrid system. Operation in these single modes is described under either Section A.3.2 or Section A.3.3 depending on the operating mode activated.

Two sizes of this ALC hybrid design were tested using 4- and 18-in. nominal riser tubes of various lengths. Additional details of each test configuration are given for each airlift size.

Airlifts of this hybrid design are available from at least one vendor source, the Geyser Hybrid Pump (Geyser Pump Tech, LLC Seattle, WA), which uses an in-tank bubble chamber for gas pulse formation and activation. Geyser Pump Tech can supply the technology in a variety of sizes (including the 4-in. size used in this ALC testing) and materials (PVC and metal materials including thin-walled stainless steel, powder-coated carbon steel). No vendor was identified that uses an "out of tank" air charging system to generate a periodic gas release for this type of ALC hybrid system.

A.3.4.2   4-inch Geyser Hybrid Pump

The 4-in. GHP is a commercial ALC hybrid product that uses both a conventional airlift (ALC – continuous bubble) and a pulsed airlift (ALC – periodic air flow). The GHP product is unique in that continuous air is supplied through two air lines to the in-tank unit and the periodic releases occur in-tank without a valve actuation air pulsing system. Key features of the GHP pump are its ability to generate more suction and velocity in the riser tube compared to a regular airlift (see Figure A.61, Figure A.62, and Figure A.63) and the fact that these pumps have no moving parts.
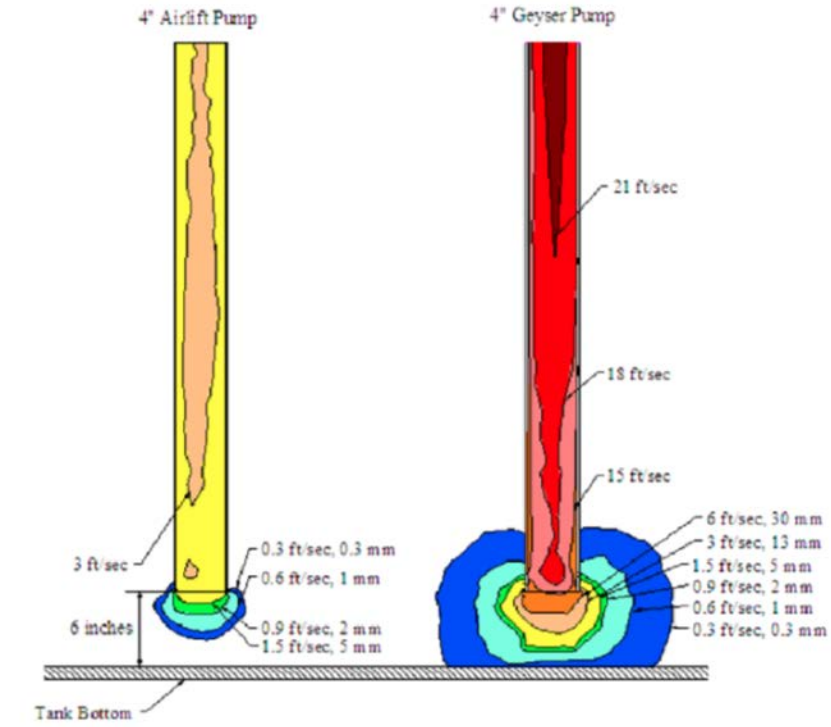
Figure A.61. GHP Velocity Increase over Conventional Airlift (vendor literature).
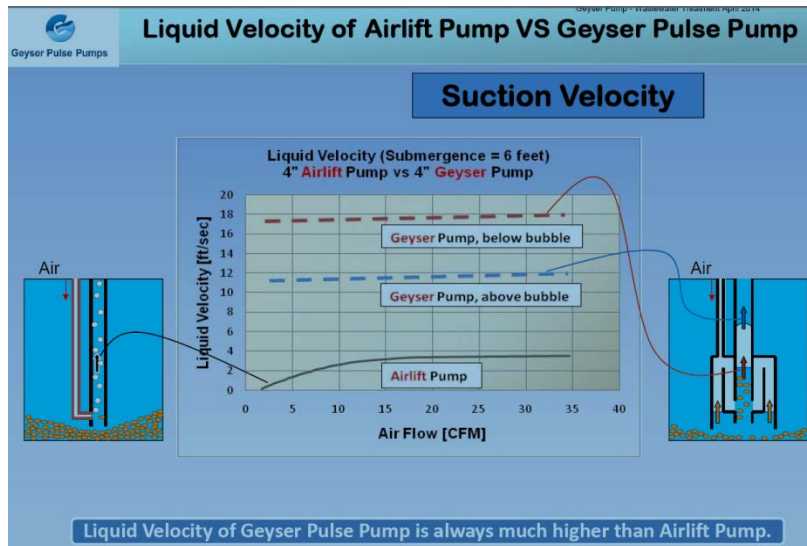
Figure A.62. GHP Velocity Increase over Conventional Airlift (vendor literature).

A.45
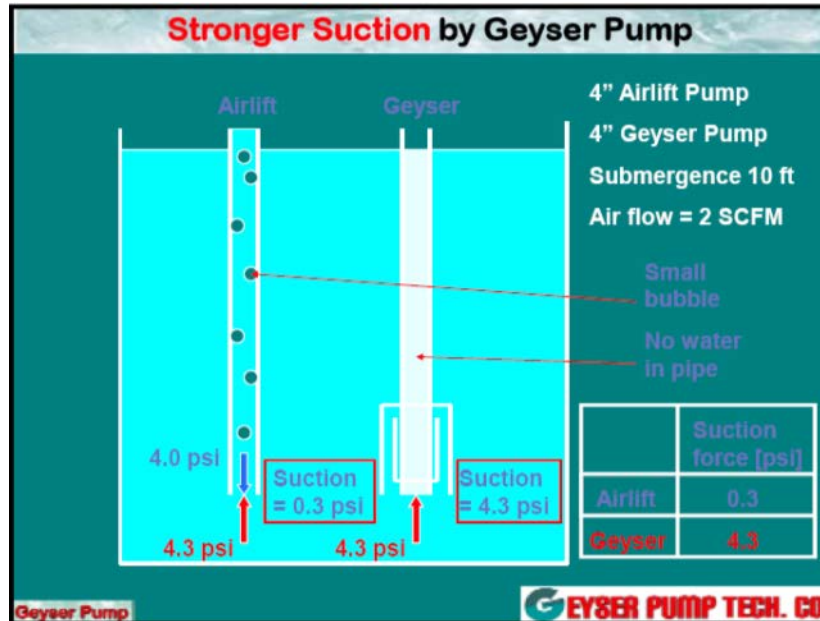
Figure A.63. GHP Suction Increase over Conventional Airlift (vendor literature).

A GHP pump was purchased from Geyser Pump after consultation with the vendor regarding the best design for use in mixing a ~ 3000-gal tank with a capability to provide lifting/pumping or solid particulate motivation in the >1000-micron range. The GHP selected for this application was a 4-in. GHP (from an available range of 2 to 12 in., see Figure A.64) made from PVC. Since fluid mixing was being done in-tank, a GHP with an open bottom design was selected. Although available, no cleanout ports of the GHP bubble chamber were delivered with the purchased unit. A large concrete doughnut was also provided with the GHP that is used to counteract the buoyancy forces as the GHP bubble chamber is filled. Per vendor information (Figure A.65), the bubble volume released from the 4-in. GHP is approximately 0.52 ft^3 per pulse. The top of the GHP has a standard flange connection with an o-ring seal to allow extension of the riser tube. The bottom of the GHP has adjustable feet to allow variable "off tank bottom" spacing in the range of 2 to 5 in. The GHP test pump was procured from Geyser Pump Tech, LLC[1] and delivered in July 2014 with serial number GHP-14-4-201.

Specifications (GHP)

	2″	3″	4″	12″
Discharge pipe diameter				
Overall height	1′ 10″	2′10″	3′2″	3′11″
Overall diameter (does not include intake screens)	10″	12″	16″	2′6″
Weight (lb)	30	40	50	100
Air supply (3)	1/2″	1″	1 1/4″	2″
Typical pumping rate (gpm)	28	64	86	1,200

Materials: PVC standard (Max. operational pressure 40 psig), Powder coated mild steel and stainless steel

*(note) Proper pumping rate selected based on submergence, lift, application and gpm required.

Figure A.64. GHP Available Sizes (vendor literature).

---

[1] Contact: P.O. Box 20025, Seattle WA 98102 U.S.A., web: http://www.geyser-pump.com/, phone: (614) 398-0960.

Geyser Hybrid Pump (GHP)
Low Cost, Low Energy for Grit Removal (Patent Pending)

Operating pressure = [Submergence (ft) + GEP height (ft)] x 0.43 (psi/ft)]

Air flow [DCFM] = # [pulses/min] x Delivered air volume to GEP [ft3/pulse]

Air flow [SCFM] = [Operating pressure (psi) + 14.7 (psi)]/14.7 (psi) x Air flow [DCFM]

Flow rate: # pulses/min x gallon/pulse = flow (gpm)

Delivered Air Flow to GHP [ft3 / pulse]

2"GHP	3"GHP	4"GHP	12"GHP
0.13	0.35	0.52	6.12

Delivered Liquid and Grit to GHP [gallon / pulse]

2"GHP	3"GHP	4"GHP	12"GHP
1.1	2.4	4.3	38.9

Figure A.65. GHP Operating Information (vendor literature).

The 4-in. GHP as configured for ALC testing was lowered into the ALC test tank and rested on the bottom of the tank on its adjustable feet, which were preset for testing at an offset of around 3 in. from tank bottom. The GHP was not secured to the tank bottom, but was supported by multiple ropes tied to the pump and to the top of the tank. These ropes generally held the GHP in position in the center of the tank, and this was checked and adjusted after each run if required.

Setup of the GHP air lines required a check valve in a horizontal position on the airlift line, and this was installed on the air supply exit on the Dwyer rotameter rack. The check valve in the air line prevents tank fluid from being pushed further back in the airlift line when the GHP periodic bubble chamber releases a bubble. Refer to Figure A.66 for the check valve configuration as recommended by the vendor.
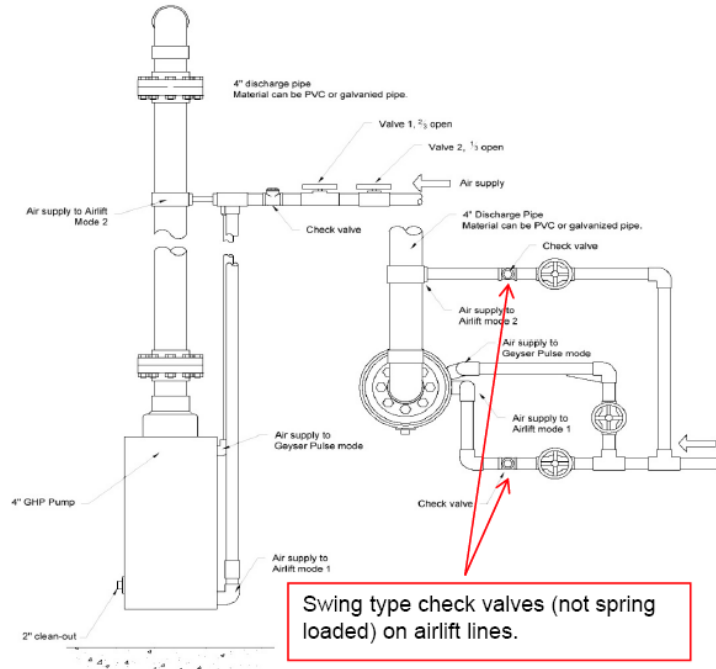
Figure A.66. GHP Installation Configuration (vendor literature).

Much of the preceding information and Figures A.67 to A.70 are from vendor provided reports, literature, or communications.
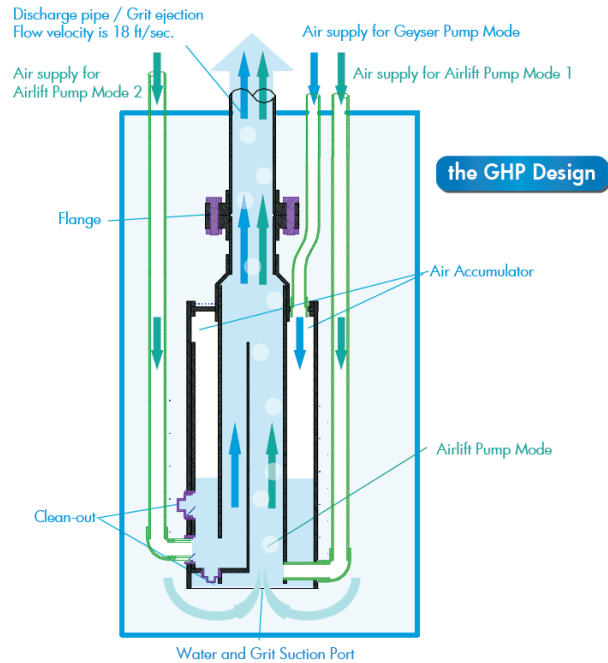
Figure A.67. Geyser Hybrid Pump (ALC tested by PNNL did not have airlift Mode 2 or cleanout options) (vendor literature).
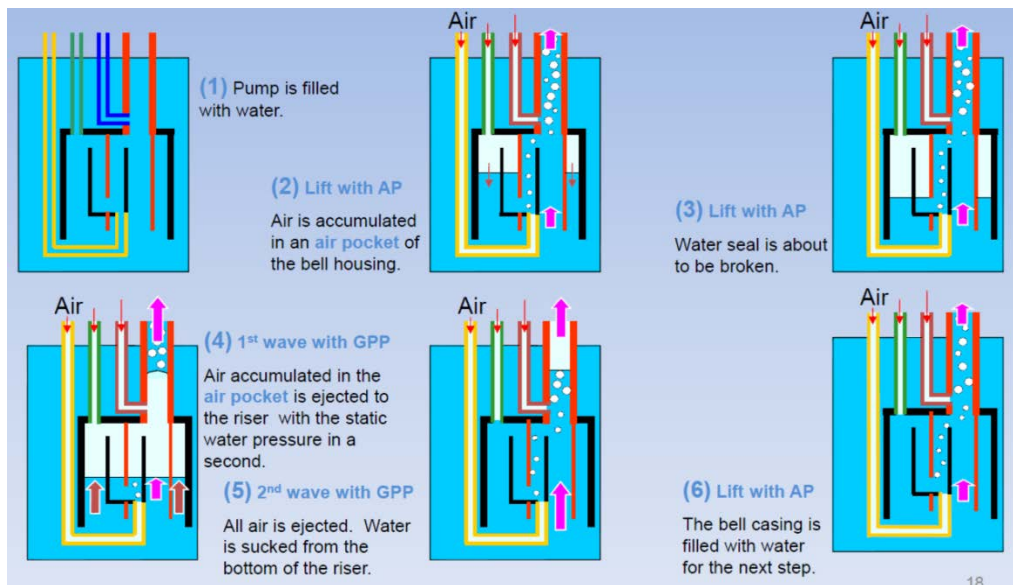
Figure A.68. Geyser Hybrid Pump Operation Schematic – Hybrid Mode (vendor literature).[1]

---

[1] The GHP configuration shown in the figure includes the option of a second continuous bubble ALC as part of the bubble chamber that enters closest to the bottom. This option was not included in the GHP pump purchased for this ALC testing. The GHP purchased included only one continuous bubble ALC that ejected air directly into the riser tube near the bottom of the riser tube and not above the bubble chamber release point as shown in the figure.
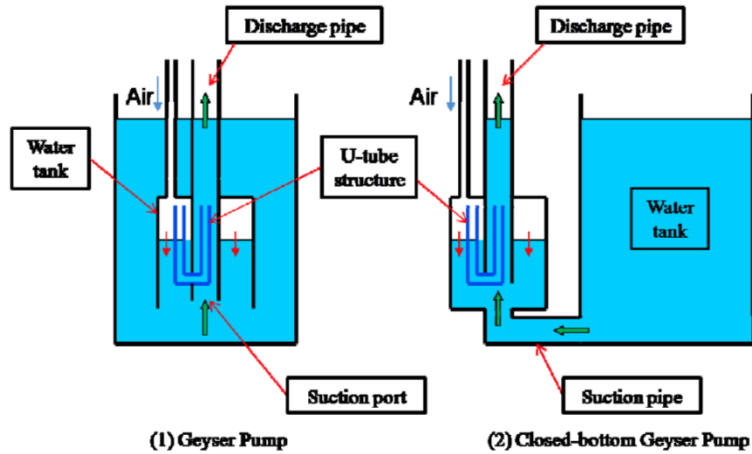
Figure A.69. Basic Structure of the Geyser Pump (ALC hybrid test used closed bottom design) (vendor literature).
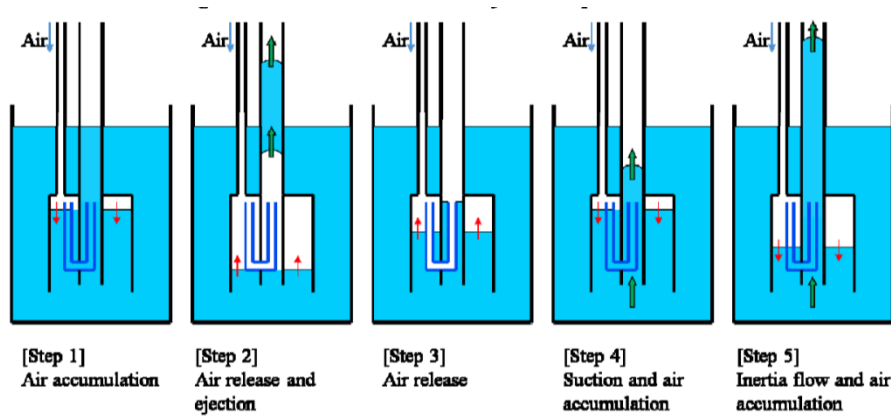
Figure A.70. Sequence of the Geyser Pump Phenomenon (ALC only pulsed/periodic mode shown) (vendor literature).

The following several pages contain pictures of the GHP procured for ALC testing in Figures A.71 through A.75.

Figure A.71. 4-in. GHP Details as Configured for ALC Testing (1 of 2).

Airlift Outlet Near Bottom
of Geyser Pump

Bubble Outlet Above
Vertical Center of Geyser
Pump

Geyser 4-inch
Extension Tube Above
Flange Connection

Geyser Hybrid Pump
Top View Looking Down Inside 4-inch Outlet Pipe
(Fluid Enters Geyser Pump At Bottom and Air
Enters Partway Up Geyser Outlet. Wood pallet can
be seen at bottom of Geyser pump fluid inlet.)
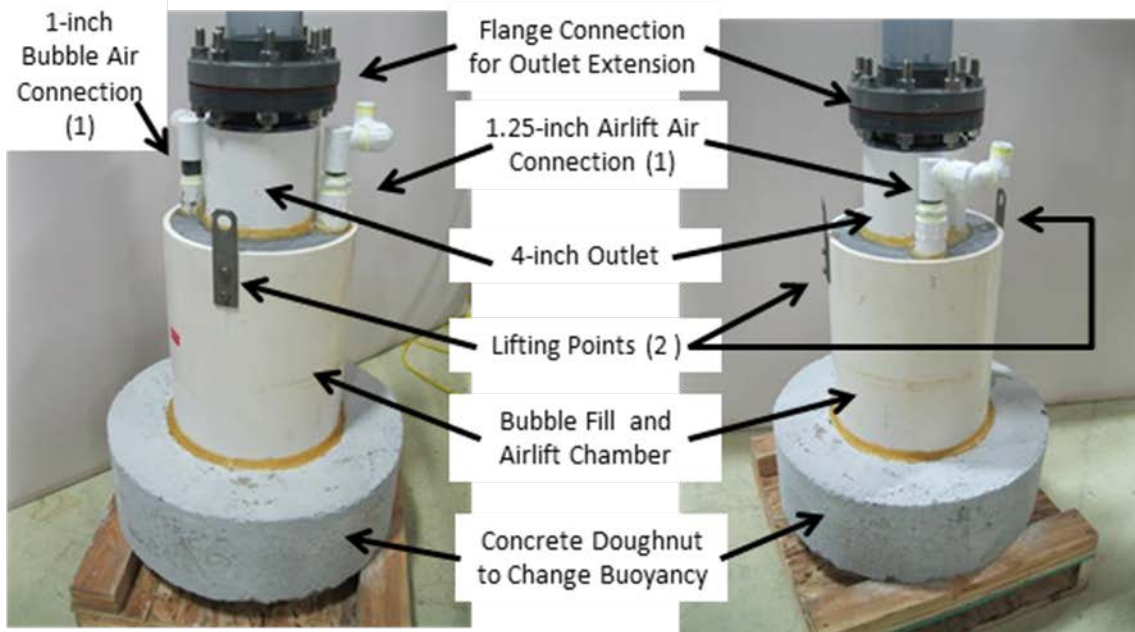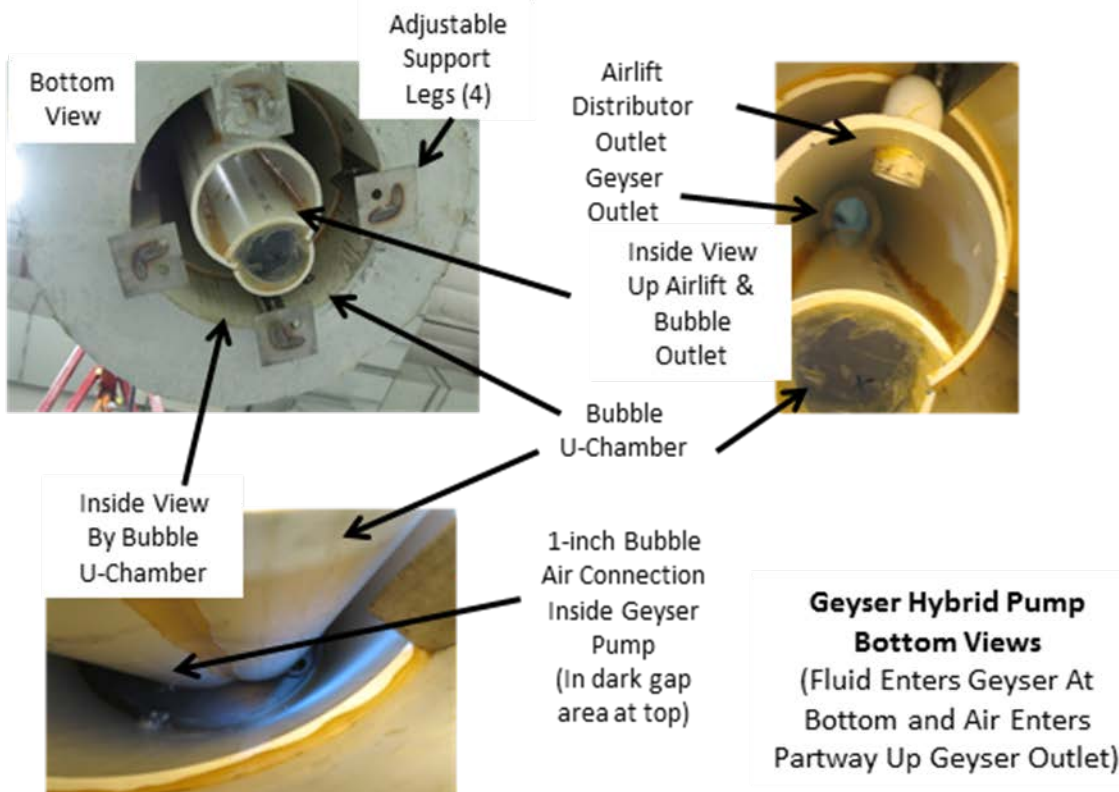
Geyser Hybrid Pump
Bottom View Showing Support Legs
(Four adjustable steel legs with foot pads)

Figure A.71. 4-in. GHP Details as Configured for ALC Testing (2 of 2).
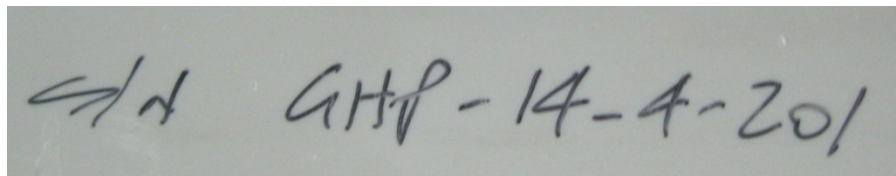
Figure A.72. 4-in. GHP Name Plate and Serial Number (GHP-14-4-201)
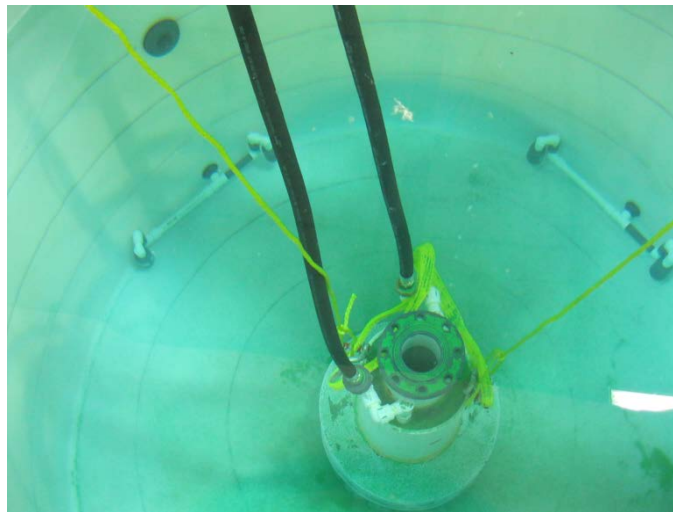
Figure A.73. GHP Installation in ALC Tank Filled with Water.
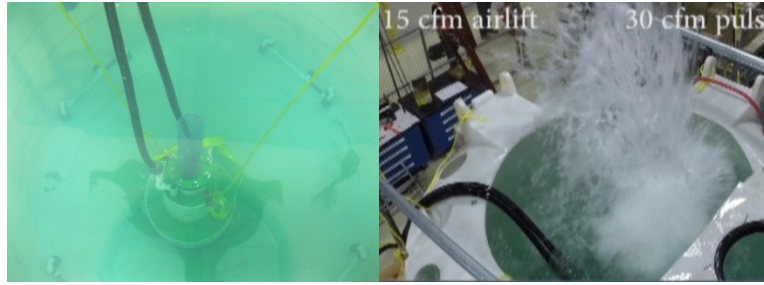
Figure A.74. GHP Operation in ALC Tank Filled with Water, Large Water Spout

Figure A.75. GHP with Riser Tube Extension (two views rotated 90°).

A.3.4.3   18-inch Hybrid ALC

The 18-in. hybrid ALC was a PNNL-fabricated device that added a second air line to the existing conventional ALC to generate periodic air releases (see Figure A.76). A PHi air charging system was used to provide pulsed air (see Figure A.77 and A.81). This device operated in the same manner as the conventional 18-in. ALC except for the addition of the periodic large air volume.

Figure A.76. Second Connection for Large, Periodic Air Volume Addition (right view looking down ALC pipe to see nozzle locations).

Figure A.77. PHi Air Controller (regulator shown).

A.3.5   Plate Mixer – Periodic Air Flow

A.3.5.1   General

The plate mixer uses periodic pulses of compressed air that are ejected under the center of a flat plate close to the floor, forming a bubble that sweeps radially outward under the plate and initially displaces fluid in the horizontal direction. The bubble (or gas volume) then breaks around the edges of the plate, where it accumulates and rises to the tank fluid surface, creating vertical fluid motion. The generation of a large bubble that motivates fluid in first the horizontal and then the vertical direction causes significant circulation of the surrounding fluid and solids (if present) in the tank. The plate mixer systems can be tuned by varying air pressure and air release duration. Typically a plate mixer uses two horizontal flat plates where the air is ejected between the plates to counter the reactionary forces of the downward bubble formation and minimize erosion on the bottom of the tank.

Air plate mixers are available from two vendors, PHi (Pulsed Hydraulics, Inc. in Oroville, WA) and Pulsair (Pulsair Systems, Inc. in Bellevue, WA). The plate mixer from PHi was the device acquired and used in ALC testing. The PHi device uses an 8-in. diameter plate whereas the Pulsair system was a 12-in. plate.

A.3.5.2   PHi

The PHi device is a plate mixer operating on compressed air and consists of three components: compressed air supply, the air pulse generator, and the bubble forming plates. Compressed air is generally supplied by a compressor. The air pulse generator controls bubble formation by regulating the air to the forming plates by pressure (intensity), duration, and time between pulses. The forming plates are typically metal but materials can vary depending on the specific application.

Compressed air is pulsed through a forming plate installed on the bottom of the tank, creating a fluid pulse wave that captures sediment from the bottom and starts the mixing process. The forming plate's design causes the air to form into a bubble-mass above the forming plate, pulling liquid and sediment from the bottom of the tank. As the PHi literature states, when the bubble begins its ascent, it presses liquids and solids above it upward, and draws liquid and sediment along from beneath. As the bubble continues to rise, liquid and solids in its path are put into motion upward. When the bubble breaks on the surface, the liquid and solids move tangentially to the surface, producing a surface mixing motion that moves to the tank wall and then down the sides to the bottom, completing the mixing cycle. The operation of the forming (or accumulator) plates is shown in Figure A.78, Figure A.79, and Figure A.80.
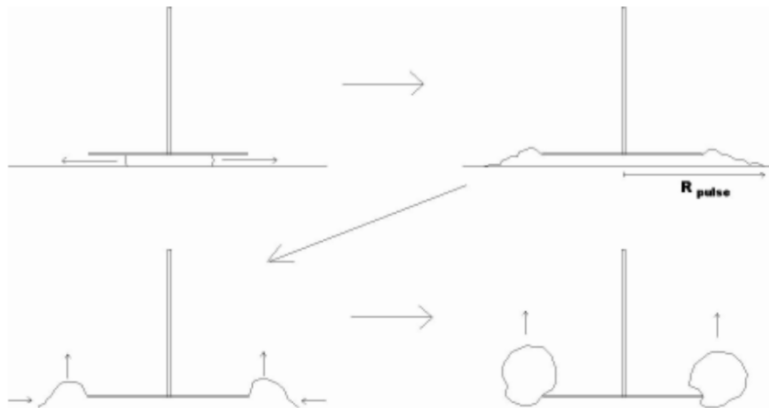
Figure A.78. Plate Mixer Bubble Formation (Reference: DOE/EM-0462[1]).
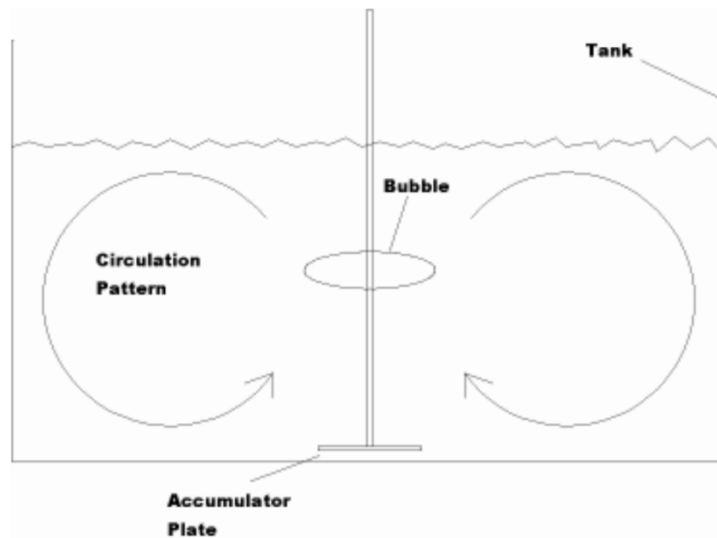
Figure A.79. Plate Mixer Mixing Action (Reference: DOE/EM-0462[1]).

---

[1] DOE/EM-0462. 1999. Innovative Technology Summary Report: *Pulsed Air Mixer*. Tanks Focus Area, U.S. Department of Energy, Washington D.C.

Figure A.80. Plate Mixer Bubble Release (vendor literature).

The PHi mixing system used for PNNL testing was bought on October 24, 2014 on PHi Invoice # 14-068-01 and consisted of the following:

- One controller (PHi 300-101SS1) in a NEMA-4X enclosure (18 in. × 16 in. × 8 in.), with IDEC smart relay controller, on/off switch, low/med/high pulse selection switch, air filter-regulator, stainless steel internal piping, 1-in. Ross Poppet valve. See Figure A.81.

- One forming plate consisting of two 8-in. diameter plates spaced 3/8 in. apart, all made of 316 stainless steel. See Figure A.82.

  PHi operating parameters include the following:

- Power – 110 VAC at 60 Hz, consumption <100 watts

- Operating temperature – 32°F to 110°F

- Air consumption: 4 to 24 cfm at 50 psig (operator adjustable)

- Front mixing rate switch – Adjustable pulse rate via three settings (low/med/high)

Additional options from PHi beyond those in the unit purchased for PNNL testing include a heater and additional insulation for cold weather operation, second valve for mixing multi zones/tanks, and PLC control that can include touchscreen controls and direct plant interface.

Figure A.81. PHi Mixing System Controller (outside and inside shown).
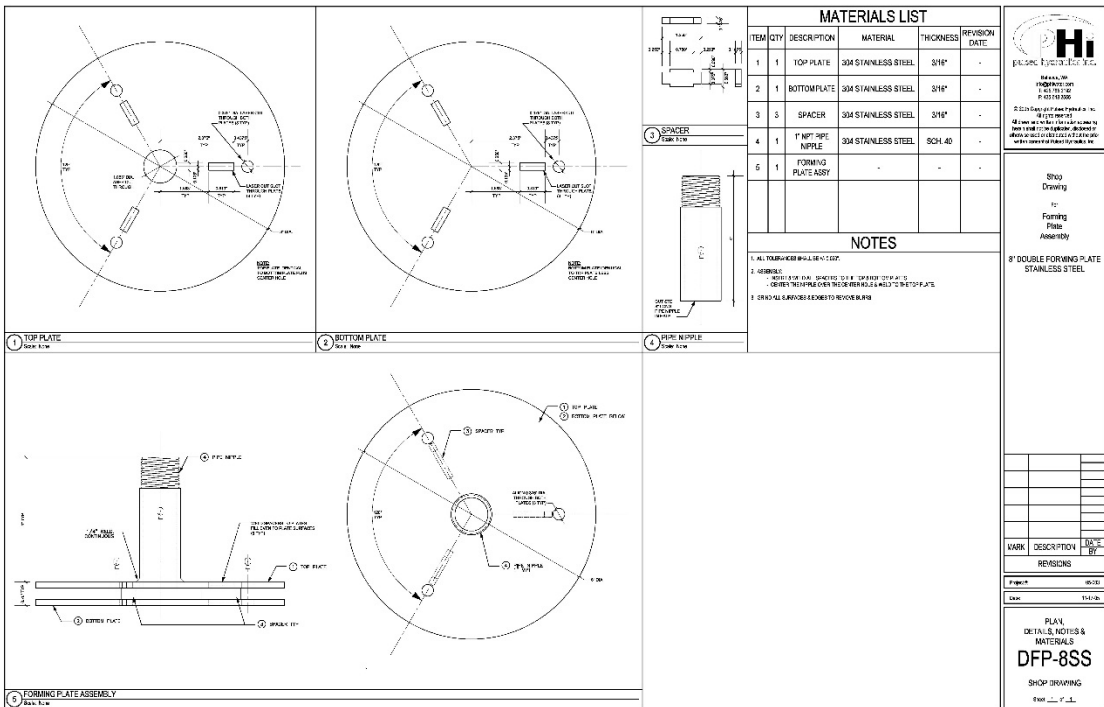
Figure A.82. PHi Forming Plate (top, side, and drawing shown).

The following information is primarily from PHi literature with relevant information inserted related to PNNL testing.

- **Typical PHi-300 Applications** – Used in wastewater treatment plants to mix sludge holding tanks, aerobic digesters, lift stations, chemical tanks, polishing basins, anoxic basins and aeration basins to enhance the oxygen transfer, and any other liquid vessel that requires mixing. It is also used to mix potable water tanks of any size or shape. Complete mixing is accomplished in minutes. The system can mix almost any liquid and is used in wine blending, oil storage tanks, drilling mud, inks, paint, and distilled spirits.

- **PHi Mixing Design Information**

  – Mixing Zones – When mixing requires solids to be suspended, as found in wastewater treatment plants, the effective mixing area is a 1:1.2 ratio. This means for each foot of water depth the effective mixing zone is a 1.2-ft radius from the center of the forming plate. Thus, a forming plate in 10 ft of water will have a radius of influence of 12 ft (24 ft in diameter). The practical placement of the forming plates is at a 1:1 ratio. When mixing potable water without solids, each plate has a 60-ft radius of influence. Therefore, typically one plate will mix a 120-ft diameter water tank. By comparison, the PNNL tank was 7.5-ft in diameter with the forming plate submerged approximately 8 ft., and thus was "oversized" for the application, but the plate that was used is the smallest plate mixer PHi offers.

  – Mixing Cycles – The number of mixing cycles per day is determined by lift station loading. Mixing cycles can be initiated by a timer function in the control relay or by contact inputs from the lift station pump relays that are linked with level sensing devices in the wet well. Any liquid that can be stored in a vented vessel can be mixed with by a PHi mixing system. Bulk storage tanks come in all shapes and sizes. If the sludge can be pumped, it can be mixed by the PHi-300. The location and number of plates and the number of valves are determined by the size of the sludge tanks and the minimum mixing level required. PNNL testing did not use any mixing cycles but instead operated a single mixing cycle per test, consisting of multiple air pulses.

- **PHi-300 Series Mixer System Description** – The PHi-300 mixer system is unique in that it uses large air bubbles that are sequentially injected in a liquid to create powerful mixing currents. The system controller is contained in an 18-in. × 16-in. × 8-1/2-in. NEMA-4X enclosure and consists of three major components:

  – An electro-pneumatic valve that has a high CV value, allowing it to open and close in milliseconds, which creates a well-formed bubble.

  – A pressure regulator/filter, with auto-drain, that controls the pressure of the mixing air (typically set at 50 psi).

  – A three-position switch that sets the mixing at low, medium, or high settings. The position used is based on the viscosity of the liquid being mixed.

The PHi-300 system controller has three parameters that control mixing efficiency:

  – Air pressure

  – Pulse duration

  – Pulse frequency

The system is shipped preset with the air regulator at 50 psi, pulse duration at 0.5 seconds, and pulse frequency at four pulses per minute. Increasing the pulse size (bubble) will lift more liquid to the top; this is done by increasing the air pressure but should not exceed 80 psi. The control relay has two adjustments to control mixing. Pulse duration (milliseconds) controls the duration of the pulse adding more air mass to the bubble. For effective mixing, the duration should not exceed 1 second. Pulse delay (seconds) controls the number of valve firings per minute; the maximum rate should allow one pulse of air to exit the liquid before a second pulse is created. PNNL testing used the factory settings but varied the pulse delay between 2 (low), 4 (medium), and 6 (high).

PHi measured air flow at factory setting is 2.88 cubic feet per pulse. Because valves vary in opening and closing times, the flow rate could be slightly higher or lower. The key to its effective mixing is proper sequencing of very large air bubbles. Each bubble contains 2 to 4 cubic feet of air and requires approximately 1/2 to 1 hp of energy. Depending on the application, the system will generate 2 to 6 bubbles per minute. The air pulse is approximately 1/2 second in duration and is injected through the forming plate.

- **Forming Plate** – The only equipment installed in the vessel is the forming plate and piping. Piping is run from the enclosure and connected to the forming plate. The electro-pneumatic valve delivers the compressed air through the piping to the forming plates, where it is squished between the two plates, creating a large, relatively flat bubble. The mixing is created by the bubble rising to the top of the vessel, forcing a wave action to the sides of the vessel down the walls of the vessel, and back to the forming plate. PNNL used stainless steel forming plates. The forming plate distributes the air equally around its circumference, creating a large, flat bubble mass that rises at a rate of approximately 4 ft per second in a waste water treatment application. This rapid rise of the large bubble mass pulls liquid and solids up behind it as it rises.

- **Forming Plate Mounting** – Many tanks have top access ports and hatches that allow the 1-in. diameter air delivery lines that PHi uses to enter the tank. These air lines can be anchored to the tank at the access point, eliminating the need to anchor the plate(s) to the tank floor. Plates can also be mounted to the tank floor. Plates must be kept horizontal, so leveling may be required on a non-flat tank attachment surface. PNNL testing used a flat bottom tank with the weight of the forming plate to hold vertical position (no anchors) and three horizontal PVC pipe restraints braced off the tank walls to hold horizontal position. See Figure A.83 for images of the forming plate and restraints.
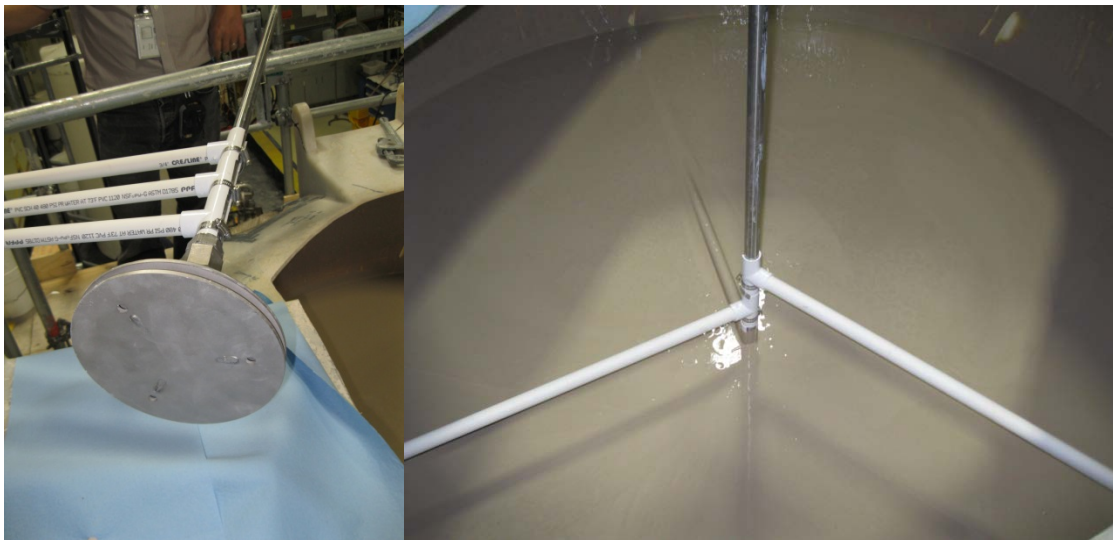
Figure A.83. PHi Forming Plate with PVC Pipe Horizontal Restraints.

- **Piping** – Piping is sized to meet the required air flow and will always be at least 1 in. PNNL testing used all 1-in. piping/hose. The forming plate was attached to approximately 10 ft of 1-in. stainless steel piping using a Swagelok connection.

- **Air Supply** – A compressor rated at 120 psi is required to provide the air that creates the bubbles. The compressed air is plumbed to the electro-pneumatic valve. Basic rule of thumb for sizing the compressors is each valve will require up to 4 hp of air. Add 2 hp if using a reciprocating compressor. Add 10% if using a rotary screw compressor. PNNL testing utilized APEL building air supply that could provide up to 30 cfm at 60+ psi to the Controller.

- **PHi Contact Information** – Pulsed Hydraulics, Inc., 15 Oro Beach Dr., Oroville, WA 98844. Website: www.phiwater.com. Email: info@phiwater.com. Phone: (800) 641-1726.

Appendix B

Non-Newtonian Seeding Experimental Data

Appendix B

Non-Newtonian Particle Seeding Experimental Data

The non-Newtonian particle seeding tests were conducted as described in Section 6.1. This appendix presents the measured mass of colored particles collected in each configuration tested. Each table of data contains the particle colors used, the original location and mass of each particle color, and the amount recovered after each run of the configuration being assessed. The runs are numerically identified and the conditions of the run (air flow rate, duration) are given in parentheses. Note that the colored particles were also manually counted during testing, but this data is not tabulated in this appendix. It can be reconstructed accurately using the mass data and the information in Table 3.3. The configurations tested were SP-03 (Table B.1), GP-02 (Table B.2), SP-05 (Table B.3), SP-05p (Table B.4), and PPM (Table B.5). Testing with configuration SP-03 was repeated after all the other configurations were tested (see Table B.6). The order of the tables is chronological with respect to the tests except for the initial SP-03 and the GP-02 tests, which are reversed.

The other significant data obtained during particle seeding tests was the distribution of colored particles remaining in the tank after a configuration was tested. This was assessed by pumping the tank out from the top in 1-ft layers. The masses of particles recovered from each layer are also presented in this appendix. The tables describing this data contain the layer number, approximate mean elevation of the layer, and the mass of each particle color recovered from that layer. Pumping the tank down in layers was conducted following testing with configurations SP-03 (Table B.7), GP-02 (Table B.8), and SP-05 (Table B.9). A final pump down was performed after proof-of-principle testing with configurations SP-05p and PPM and the SP-03 repeat test (see Table B.10).

The rest of the appendix contains the tables referenced in the two preceding paragraphs.

Table B.1. Particle Masses Collected During Initial SP-03 Testing with Non-Newtonian Slurry.

Particle Color	Approximate Original Location[a]	Original Mass (g)[b]	Particle Mass Recovered from Top 12 in. of Slurry (g)					
			Run 1 (15 scfm, 1 hr)	Run 2 (15 scfm, 1 hr)	Run 3 (15 scfm, 1 hr)	Run 4 (20 scfm, 1 hr)	Run 5 (25 scfm, 0.3 hr)	Run 6 (30 scfm, 0.5 hr)
Yellow	Surface[c]	319 .6	98.43	40.52	29.98	33.58	26.04	24.71
Brown	24 in. below surface at R/2	100.1	21.33	15.05	10.68	13.39	10.54	8.54
Green	48 in. below surface at R/2	97.2	21.18	16.32	11.29	15.19	9.04	5.75
White	72 in. below surface at R/2	100.0	19.10	14.07	13.04	12.59	9.33	10.42
Red	96 in. below surface at R/2	100.1	8.14	6.61	5.73	5.57	3.47	1.67
Orange	24 in. below surface at 0.91R	100.0	1.63	1.52	1.42	1.51	0.81	0.70
Blue	48 in. below surface at 0.91R	100.0	0.11	0.45	--	--	0.11	--
Grey	72 in. below surface at 0.91R	100.1	--	0.12	--	--	--	--

(a) The locations are approximate and subject to the following considerations:
  - Depths are ± 1 in., with an approximate slurry level of ~96 in.
  - R refers to the tank radius, which was 45 in.
  - The radial location refers to the center of the loaded particles, which were installed using an 8-in. diameter sieve. For example, 0.91R is 41 in., indicating that some of the particles were against the tank wall.

(b) The target mass for all non-yellow particles was 100 g. Amounts different from ~100 g were achieved when particles were hung up on equipment during loading and were removed from the tank. These particles were weighed and subtracted from the original pre-weighed mass.

(c) The particles were loaded randomly in a rectangle of approximate dimensions 18 in. (width) × 45 in. (length) that extended from the tank wall to the tank center.

Table B.2. Particle Masses Collected During GP-02 Testing with Non-Newtonian Slurry.

Particle Color	Approximate Original Location[a]	Original Mass (g)[b]	Particle Mass Recovered from Top 12 in. of Slurry (g)					
			Run 1	Run 2	Run 3	Run 4	Run 5	Run 6
			All runs at 5 scfm (airlift) / 10 scfm (pulsed) for 1 hr					
Yellow	Surface[c]	319 .2	12.87	12.09	9.00	8.55	8.07	6.39
Brown	24 in. below surface at R/2	99.9	16.34	15.42	10.80	7.95	6.88	7.35
Green	48 in. below surface at R/2	98.3	15.20	13.25	10.61	9.60	7.63	6.15
White	72 in. below surface at R/2	98.2	14.28	14.63	11.48	9.67	7.20	7.66
Red	96 in. below surface at R/2	92.0	17.12	12.89	10.57	9.08	10.10	7.22
Orange	24 in. below surface at 0.91R	99.7	18.43	12.83	11.78	6.82	6.53	6.53
Blue	48 in. below surface at 0.91R	99.9	13.30	10.56	10.35	7.49	6.59	3.75
Grey	72 in. below surface at 0.91R	99.9	0.47	0.24	--	0.23	0.12	0.24

(a) The locations are approximate and subject to the following considerations:
   - Depths are ± 1 in., with an approximate slurry level of ~96 in.
   - R refers to the tank radius, which was 45 in.
   - The radial location refers to the center of the loaded particles, which were installed using an 8-in. diameter sieve. For example, 0.91R is 41 in., indicating that some of the particles were against the tank wall.

(b) The target mass for all non-yellow particles was 100 g. Amounts different from ~100 g were achieved when particles were hung up on equipment during loading and were removed from the tank. These particles were weighed and subtracted from the original pre-weighed mass.

(c) The particles were loaded randomly in a rectangle of approximate dimensions 18 in. (width) × 45 in. (length) that extended from the tank wall to the tank center.

Table B.3. Particle Masses Collected During SP-05 Testing with Non-Newtonian Slurry.

Particle Color	Approximate Original Location[a]	Original Mass (g)[b]	Particle Mass Recovered from Top 12 in. of Slurry (g)				
			Run 1 (15 scfm, 1 hr)	Run 2 (15 scfm, 1 hr)	Run 3 (20 scfm, 1 hr)	Run 4 (25 scfm, 1 hr)	Run 5 (30 scfm, 1 hr)
Yellow	Surface[c]	319.5	69.69	53.78	60.87	42.63	32.88
Brown	24 in. below surface at R/2	100.0	22.06	16.49	18.72	13.63	11.98
Green	48 in. below surface at R/2	100.0	21.50	17.40	18.22	13.08	9.57
White	72 in. below surface at R/2	100.0	18.88	18.12	19.66	11.84	10.85
Red	96 in. below surface at R/2	100.0	0.30	0.30	13.35	7.27	4.75
Orange	24 in. below surface at 0.91R	100.0	19.47	18.17	18.18	14.30	11.89
Blue	48 in. below surface at 0.91R	98.7	0.57	--	0.23	0.11	0.45
Grey	72 in. below surface at 0.91R	99.8	0.12	0.12	--	0.12	--

(a) The locations are approximate and subject to the following considerations:
  - Depths are ± 1 in., with an approximate slurry level of ~96 in.
  - R refers to the tank radius, which was 45 in.
  - The radial location refers to the center of the loaded particles, which were installed using an 8-in. diameter sieve. For example, 0.91R is 41 in., indicating that some of the particles were against the tank wall.

(b) The target mass for all non-yellow particles was 100 g. Amounts different from ~100 g were achieved when particles were hung up on equipment during loading and were removed from the tank. These particles were weighed and subtracted from the original pre-weighed mass.

(c) The particles were loaded randomly in a rectangle of approximate dimensions 18 in. (width) × 45 in. (length) that extended from the tank wall to the tank center.

Table B.4. Particle Masses Collected During SP-05p Testing with Non-Newtonian Slurry.

Particle Color	Approximate Original Location[a]	Original Mass (g)[b]	Particle Mass Recovered from Top 12 in. of Slurry (g)			
			Run 1 (5 scfm with pulse every ~10 s, 1 hr)	Run 2 (5 scfm with pulse every ~15 s, 1 hr)	Run 3 (Only pulse every ~10 s, 1 hr)	Run 4 (Only pulse every ~10 s, 0.25 hr)
Green	48 in. below surface at 0.91R	99.7	19.97	12.85	9.48	9.94
White	72 in. below surface at 0.91R	95.0	12.53	12.59	11.04	9.26

(a) The locations are approximate and subject to the following considerations:
- Depths are ± 1 in., with an approximate slurry level of ~96 in.
- R refers to the tank radius, which was 45 in.
- The radial location refers to the center of the loaded particles, which were installed using an 8-in. diameter sieve. For example, 0.91R is 41 in., indicating that some of the particles were against the tank wall.

(b) The target mass for these particles was 100 g. Amounts different from ~100 g were achieved when particles were hung up on equipment during loading and were removed from the tank. These particles were weighed and subtracted from the original pre-weighed mass.

Table B.5. Particle Masses Collected During PPM Testing with Non-Newtonian Slurry.

Particle Color[a]	Approximate Original Location[b]	Original Mass (g)[c]	Particle Mass Recovered from Top 12 in. of Slurry (g)			
			Run 1 (Pulse every ~10 s, 1 hr)	Run 2 (Pulse every ~10 s, 1 hr)	Run 3 (Pulse every ~30 s, 1 hr)	Run 4 (Pulse every ~30 s, 0.25 hr)
Orange	48 in. below surface at 0.91R	100.0	19.35	16.06	12.12	8.59
Brown	72 in. below surface at 0.91R	100.0	17.66	15.34	12.09	8.92

(a) Particles shown in Table B.4 remained in the vessel during this test. They were collected during testing and weighed but the data is not indicative of mobilization from a particular region and is not provided.

(b) The locations are approximate and subject to the following considerations:
- Depths are ± 1 in., with an approximate slurry level of ~96 in.
- R refers to the tank radius, which was 45 in.
- The radial location refers to the center of the loaded particles, which were installed using an 8-in. diameter sieve. For example, 0.91R is 41 in., indicating that some of the particles were against the tank wall.

(c) The target mass for these particles was 100 g. Amounts different from ~100 g were achieved when particles were hung up on equipment during loading and were removed from the tank. These particles were weighed and subtracted from the original pre-weighed mass.

Table B.6. Particle Masses Collected During SP-03 Testing (Repeated) with Non-Newtonian Slurry.

Particle Color[a]	Approximate Original Location[b]	Original Mass (g)[c]	Particle Mass Recovered from Top 12 in. of Slurry (g)		
			Run 1 (15 scfm, 1 hr)	Run 2 (15 scfm, 1 hr)	Run 3 (15 scfm, 1 hr)
Yellow	Surface[d]	319.7	101.18	24.94	24.73
Trans. Red	24 in. below surface at R/2	100.0	21.15	21.23	14.90
Trans. Green	48 in. below surface at R/2	100.0	19.99	21.19	14.43
Trans. Orange	72 in. below surface at R/2	100.0	17.43	15.98	13.64
Red	96 in. below surface at R/2	100.0	23.13	15.42	17.65
Bright Orange	24 in. below surface at 0.91R	99.9	15.86	13.03	11.99
Blue	48 in. below surface at 0.91R	100.0	14.07	11.91	12.27
Grey	72 in. below surface at 0.91R	98.3	8.40	8.41	9.24

(a) Particles shown in Table B.4 and Table B.5 remained in the vessel during this test. They were collected during testing and weighed but the data is not indicative of mobilization from a particular region and is not provided.

(b) The locations are approximate and subject to the following considerations:
- Depths are ± 1 in., with an approximate slurry level of ~96 in.
- R refers to the tank radius, which was 45 in.
- The radial location refers to the center of the loaded particles, which were installed using an 8-in. diameter sieve. For example, 0.91R is 41 in., indicating that some of the particles were against the tank wall.

(c) The target mass for all non-yellow particles was 100 g. Amounts different from ~100 g were achieved when particles were hung up on equipment during loading and were removed from the tank. These particles were weighed and subtracted from the original pre-weighed mass.

(d) The particles were loaded randomly in a rectangle of approximate dimensions 18 in. (width) × 45 in. (length) that extended from the tank wall to the tank center.

Table B.7. Masses of Colored Particles in 1-ft Layers of Slurry Collected During Pump Down of the Tank After SP-03 Testing.

Layer No.	Mean Layer Height (ft)	Mass of Colored Particles (g) in Layer							
		Yellow	Brown	Green	White	Red	Orange	Blue	Grey
1	7.5	13.73	4.63	4.22	4.51	0.76	0.35	--	--
2	6.5	16.63	3.8	4.19	5.06	1.5	0.93	--	--
3	5.5	11.09	2.85	2.49	2.48	0.3	80.67	--	--
4	4.5	6.41	3.08	2.11	2.59	0.3	6.3	94.44	--
5	3.5	4.66	2.13	1.82	2.37	0.3	2.33	2.84	--
6	2.5	6.26	2.61	2.11	2.59	0.91	1.52	1.49	--
7	1.5	4.45	1.19	0.91	1.58	1.21	0.58	0.46	79.68
8	0.5	1.59	0.48	0.53	0.56	62.66	0.23	--	19.64
TOTAL		64.82	20.77	18.38	21.74	67.94	92.91	99.23	99.32

Table B.8. Masses of Colored Particles in 1-ft Layers of Slurry Collected During Pump Down of the Tank After GP-02 Testing.

Layer No.	Mean Layer Height (ft)	Mass of Colored Particles (g) in Layer							
		Yellow	Brown	Green	White	Red	Orange	Blue	Grey
1	7.5	2.65	6.16	4.6	3.49	5.56	5.01	3.52	0.24
2	6.5	4.44	5.45	4.97	3.83	4.36	5.14	3.85	--
3	5.5	56.11	4.98	5.22	4.28	3.77	4.43	3.98	--
4	4.5	18.07	2.84	3.93	3.04	1.35	2.78	3.07	--
5	3.5	14.79	5.93	4.98	5.62	3.47	5.13	24.2	0.12
6	2.5	40.86	3.32	5.39	5.4	3.45	5.25	3.63	6.03
7	1.5	54.32	3.56	5.12	3.83	2.55	5.37	3.41	88.66
8	0.5	9.69	2.37	1.3	2.92	0.75	3.28	2.04	2.36
TOTAL		200.93	34.61	35.51	32.41	25.26	36.39	47.70	97.41

Table B.9. Masses of Colored Particles in 1-ft Layers of Slurry Collected During Pump Down of the Tank After SP-05 Testing.

Layer No.	Mean Layer Height (ft)	Mass of Colored Particles (g) in Layer							
		Yellow	Brown	Green	White	Red	Orange	Blue	Grey
1	7.5	1.7	0.35	0.39	0.45	0.29	0.47	--	--
2	6.5	0.97	0.24	--	0.67	--	0.23	--	--
3	5.5	19.97	4.63	6.55	6.81	4.3	5.72	0.34	--
4	4.5	5	1.54	2.63	2.81	1.79	1.99	20.84	--
5	3.5	5.6	2.49	1.7	3.02	0.74	1.51	30.03	--
6	2.5	9.45	3.08	3.39	3.23	2.08	3.39	30.26	50.13
7	1.5	4.39	0.83	0.4	0.78	0.29	0.93	5.01	13.49
8	0.5	11.79	3.55	4.72	2.69	60.01	3.49	10.59	34.67
TOTAL		58.87	16.71	19.78	20.46	69.50	17.73	97.07	98.29

Table B.10. Masses of Colored Particles in 1-ft Layers of Slurry Collected During Pump Down of the Tank After SP-03 Repeat Testing.

Layer No.	Mean Layer Height (ft)	Mass of Colored Particles (g) in Layer											
		Yellow	Brown[b]	Green[b]	White[b]	Red	Orange[b]	Blue	Grey	Trans. Red	Trans. Green	Trans. Orange	Bright Orange
1[a]	7.5	24.73	3.70	3.27	2.62	17.65	5.64	12.27	9.24	14.90	14.43	13.64	11.99
2	6.5	6.59	0.83	0.13	0.58	2.52	1.05	1.82	1.06	1.22	1.22	1.90	1.59
3	5.5	20.81	3.08	2.22	1.00	8.30	2.67	7.26	4.14	5.33	6.22	5.59	7.44
4	4.5	8.85	1.30	0.27	0.78	0.59	2.22	5.35	2.60	3.90	4.66	5.59	4.01
5	3.5	35.45	5.33	2.75	1.68	12.46	5.16	14.30	8.28	9.34	10.43	10.85	13.40
6	2.5	14.48	2.96	1.05	0.67	6.67	0.94	3.06	10.06	2.45	1.89	2.90	3.78
7	1.5	63.84	14.03	4.85	4.03	9.64	11.89	22.65	37.27	12.70	13.10	18.10	20.33
8	0.5	17.65	6.64	1.57	3.02	3.41	5.12	7.05	8.64	7.80	6.33	7.71	8.12
TOTAL		192.40	37.88	16.11	14.37	61.25	34.69	73.76	81.29	57.65	58.27	66.28	70.66

(a) Note that Layer 1 was removed by sweeping the top foot of the tank with a net, i.e., the procedure performed after test runs, and so the data presented here is the same as data appearing in the Run 3 column of Table B.6, with the exception that other opportunistic colored particles are included in this table (brown, green, white, and orange).

(b) These colors were remnants from previous configurations that were tested (see Table B.4 and Table B.5). However, all particles were collected during pump out and thus all masses are reported for completeness.

Distribution

ONSITE

4	**DOE Office of River Protection**	
	DH Alexander	H6-60
	LK Holton	H6-60
	BR Eccleston	H6-60
	IA Bolanos	H6-60
	JJ Davis	H6-60

7	**Pacific Northwest National Laboratory**	
	PP Schonewill	K6-28
	EJ Berglin	K5-22
	GK Boeringa	K6-28
	WC Buchmiller	K6-24
	CB Burns	K4-18
	MJ Minette	K7-15
	SD Rassat	K6-28
	Information Release (PDF)	

Pacific Northwest
NATIONAL LABORATORY

Proudly Operated by **Battelle** *Since 1965*

902 Battelle Boulevard
P.O. Box 999
Richland, WA 99352
1-888-375-PNNL (7665)

U.S. DEPARTMENT OF
ENERGY

www.pnnl.gov